UC Berkeley
Research Reports

Title
Emergency Vehicle Maneuvers and Control Laws for Automated Highway Systems

Permalink
https://escholarship.org/uc/item/67j758c3

Authors
Toy, Charmaine
Leung, Kevin
Alvarez, Luis
et al.

Publication Date
2001-08-01

eScholarship.org Powered by the California Digital Library
University of California

CALIFORNIA PATH PROGRAM
INSTITUTE OF TRANSPORTATION STUDIES
UNIVERSITY OF CALIFORNIA, BERKELEY

Emergency Vehicle Maneuvers and Control Laws for Automated Highway Systems

Charmaine Toy, Kevin Leung,
Luis Alvarez, Roberto Horowitz
University of California, Berkeley

California PATH Research Report
UCB-ITS-PRR-2001-17

This work was performed as part of the California PATH Program of the University of California, in cooperation with the State of California Business, Transportation, and Housing Agency, Department of Transportation; and the United States Department of Transportation, Federal Highway Administration.

The contents of this report reflect the views of the authors who are responsible for the facts and the accuracy of the data presented herein. The contents do not necessarily reflect the official views or policies of the State of California. This report does not constitute a standard, specification, or regulation.

Report for MOU 311

August 2001

ISSN 1055-1425

Emergency Vehicle Maneuvers and Control Laws for Automated Highway Systems*

Charmaine Toy†, Kevin Leung ‡, Luis Alvarez §and Roberto Horowitz¶

Department of Mechanical Engineering
University of California at Berkeley

Instituto de Ingeniería
Universidad Nacional Autónoma de México

*Research supported by UCB-ITS PATH grant MOU311.
†Graduate Student; charm@calalumni.org.
‡Graduate Student
§Professor; *alvar@pumas.iingen.unam.mx.*
¶Professor. Author for correspondence; *horowitz@me.berkeley.edu.*

Abstract

In this report control laws and maneuvers for high priority emergency vehicle transit on automated highways are presented. The work presented is specifically designed for use with the Partners for Automated Transit and Highways (PATH) hierarchical control architecture. The types of control laws that are needed for the different hierarchical layers are examined, and specific maneuvers for the coordination and link layers are presented. Simulations using SmartCAP (a mesoscopic traffic simulator) and SmartAHS (a microscopic traffic simulator) demonstrate the maneuvers' functionality.

Keywords

Automated Highway Systems, emergency vehicles, coordination layer, link layer, SmartCAP, SmartAHS, traffic simulation.

Acknowledgements

The researchers would like to thank the SmartCAP and SmartAHS software development teams for their support of this project.

Executive Summary

This report consists of two parts, written by Kevin Leung and Charmaine Toy. Luis Alvarez and Roberto Horowitz provided feedback and guidance for the material.

The first part, written by Kevin Leung, focuses on the development of coordination layer maneuvers for emergency vehicles (EVs) on automated highways (AHS). These maneuvers provide the decision logic for the cooperation of a group of vehicles to facilitate high priority EV transit. Different maneuvers are required for varying traffic conditions. The Vortex maneuver facilitates EV travel faster than the nominal flow in free flowing traffic conditions. The Zig-Zag and Part-and-Go maneuvers are designed to move stopped vehicles out of the way so that an EV can reach an accident site. The Reverse-and-Merge maneuver enables vehicles in a stopped lane to back away from an accident and merge into a neighboring free flowing lane; the maneuver can be used by both EVs and normal AHS vehicles. It is assumed that all highway vehicles are fully automated and can respond to commands from the EV or roadside controllers. Each maneuver is verified to be deadlock free using the finite state machine software, COSPAN.

The second part, written by Charmaine Toy, focuses on the development of emergency vehicle maneuvers for free flowing traffic conditions. Two different link layer maneuvers, the Bubble and Volcano, are developed for low and high traffic density scenarios, respectively. To accomodate the Volcano maneuvers, the link layer stabilizing control laws must be modified while the EV is located in that area of highway. The link layer maneuvers and stabilizing control laws are evaluated using the SmartCAP mesoscopic traffic simulator. The Vortex maneuver, presented in the first part, is also explored and evaluated using the microscopic traffic simulation, SmartAHS. Improvements are incorporated into the design of the Vortex2 maneuver, which is also demonstrated in computer simulation.

Part I

Emergency Vehicle Maneuvers for an Automated Highway System

By

Kevin Ji Leung

B.S. (University of California, Berkeley) 1992

A Master of Science final project report submitted in partial satisfaction of the requirements for the degree of Master of Science

in

Engineering? Mechanical

in the

GRADUATE DIVISION

of the

UNIVERSITY of CALIFORNIA at BERKELEY

Committee in charge:

Professor Roberto Horowitz
Professor Karl Hedrick

Spring 1998

Abstract

"Emergency Vehicle Maneuvers for an Automated Highway System"

By

Kevin Ji Leung

Master of Science in Engineering ? Mechanical Engineering

University of California at Berkeley

Professor Roberto Horowitz, Chair

Emergency vehicle maneuvers for an automated highway system (AHS) is presented. The AHS control architecture consists of five hierarchical layers: Network, Link, Coordination, Regulation, and Physical. The Network layer manages the routing of vehicles through the highway network; the Link layer controls the highway density on a microscopic scale; the Coordination layer handles the inter-vehicle communications; the Regulation layer executes maneuvers by providing feedback-based control inputs to the vehicle actuators; and the Physical layer contains the vehicle dynamics. This paper reports on the Coordination layer maneuvers designed to ensure rapid travel of emergency vehicles (EV) through an automated highway system (AHS) and to enable EV transit through a stagnant AHS. Four EV maneuvers? Vortex, Part-and-Go, Zigzag and Reverse-and-Merge? were developed. The Vortex maneuver circulates local traffic around the EV such that the EV can travel through the normal-operating AHS faster. The Part-and-Go and Zigzag maneuvers were designed to enable EV transit through a completely stopped AHS. The Reverse-and-Merge maneuver allows vehicles stuck in a single-lane pile-up to merge into the freely flowing, adjacent lane. As necessitated by these maneuvers, three assisting maneuvers? Platoon-Lane-Change, Stationary-Backward-Join and Stationary-Forward-Join? were also designed. The Coordination layer maneuvers were modeled with finite-state-machines and verified using the software tool COSPAN.

TABLE OF CONTENTS

LIST OF FIGURES

Figure Page

Chapter

1 Introduction

Two main objectives in the development of an automated highway system (AHS) are to increase highway capacity and enhance traffic safety. To sustain the high capacity of traffic that a fully automated AHS is expected to achieve, the system must be able to recover from degraded or faulty conditions of operation as quickly as possible. Less severe faults (e.g., a radar failure) can be handled within the system such that these faults can be removed from the system with minimal disturbance. Such fault handling will involve the caution and assistance of neighboring automated vehicles (Godbole et al., 1995). However, fatal faults, such as the occurrence of a vehicle collision and large debris barriers, will inevitably stop the flow of an AHS.

These fatal faults require the intervention of emergency vehicles (EV), such as tow trucks and police vehicles. To utilize the service of an EV, the AHS must be able to allow it to transit through the stagnant lanes so that it can rectify the situation. Moreover, another scenario to consider is the use of the AHS to facilitate and expedite EV transit through a freely flowing system. For instance, an EV often has to transit in an AHS in order to respond to an emergency service call outside of the system (i.e., fire engines responding to a 911 call from a remote area). In this case, the AHS must grant greater access and resources to the EV so that the EV's travel time is minimized.

This report* studies the control laws and maneuvers that an EV can execute to achieve the following two goals: 1) rapid EV transit within the AHS is ensured, and 2) EV transit to reach an accident site within the system through a completely stopped AHS traffic is possible. The automated highway control system being considered is based on the California Partners for Advanced Transit and Highways (PATH) multi-layer architecture described in (Varaiya, 1993; Varaiya and Schladover, 1991). Specifically this architecture has five hierarchical layers: Network, Link, Coordination, Regulation, and Physical. This report concentrates mainly on the vehicle coordination maneuvers within the Coordination layer.

To begin in Chapter 2, the modeling and verification process used in the design of the EV maneuvers, along with the software tool, COSPAN (Har'El and Kurshan, 1997), are introduced. In Chapter 3, the completed EV Coordination layer maneuvers, Vortex, Part-and-Go, Zigzag and Reverse-and-Merge, are described. Summarily the Vortex maneuver allows the EV to transit through a freely flowing AHS faster than normal traffic; the Part-

* Research supported by UCB-ITS PATH grants MOU-287 and MOU-311.

and-Go and Zigzag maneuvers enable the EV to travel through a completely stagnant system; and the Reverse-and-Merge maneuver, although not pertaining to the EV, helps vehicles stuck in a single-lane pile-up to merge into the freely flowing, adjacent lane. Furthermore, the development of the three complementary maneuvers, Platoon-Lane-Change, Stationary-Forward-Join and Stationary-Backward-Join that are necessitated by these EV maneuvers, will also discussed. Finally, concluding remarks and suggestions for future works are presented in Chapter 4, but first the PATH AHS architecture is now described.

1.1 PATH AHS Architecture

The design done in this report was based on the automated highway system (AHS) control architecture proposed in (Varaiya, 1993; Varaiya and Shladover, 1991). In this architecture, traffic is organized into platoons of closely packed vehicles (i.e. intraplatoon distance of 1?2m). On the contrary, the interplatoon distance is arranged to be very large (i.e., 60m) so that the trailing platoon has enough time to react and safely stop when the front platoon brakes abruptly. The use of this scheme achieves the objective of increasing highway capacity and safety (Ren and Green, 1994). The design of this architecture consists of five hierarchical layers: Network, Link, Coordination, Regulation, and Physical (Figure 1.1). The first two layers are roadside control systems, and the last three are

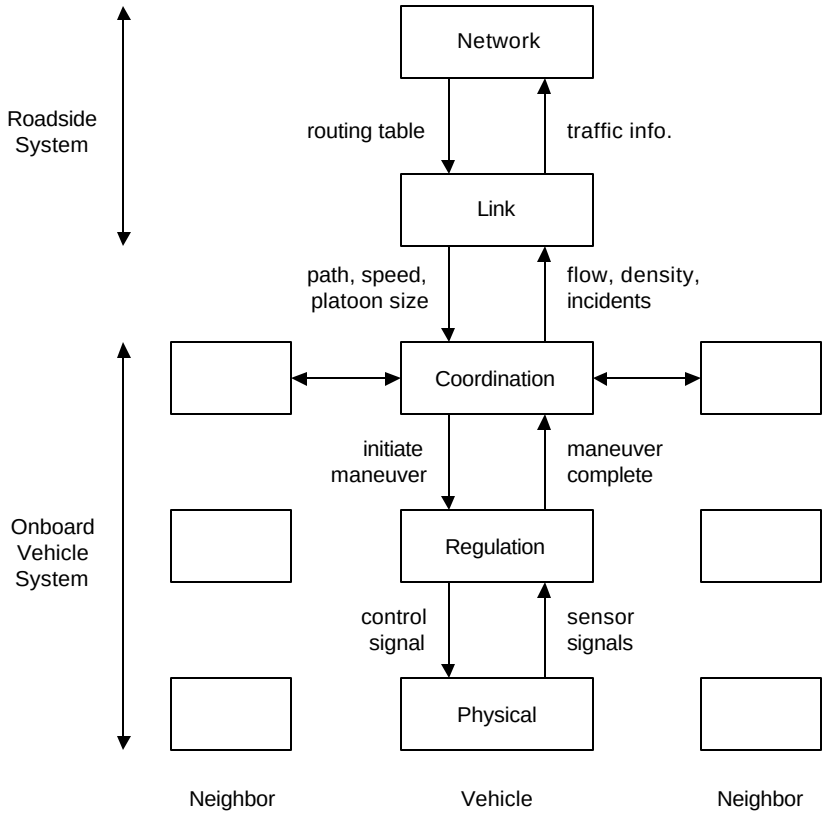

Figure 1.1: PATH AHS architecture

installed on each vehicle. Starting from the top, each layer will be summarized below.

One Network layer exists for the entire automated highway network. It is responsible for assigning a specific route to the vehicles based on the vehicle destinations. The Network layer controller minimizes the travel time of vehicles by prescribing a specific route to each individual vehicle through the use of a routing table. Control is exerted by specifying activities at highway junctions to the Link layer controller.

An AHS network is divided into distinct links, or sections, that can vary from hundred of meters to a few kilometers. A single Link layer controller controls one or moe links. Normally the Link layer does not identify individual vehicles, but rather specifies general parameters such as velocities and platoon size. However, as will be discussed later, the interaction of the Link layer with individual vehicles is necessary in performing certain emergency vehicle maneuvers. Moreover, roadside sensors provide density information for the different types of vehicles on each link. Control commands from the Link layer are passed to the Coordination layer (Horowitz, 1997; Alvarez and Horowitz, 1996; Rao and Varaiya, 1993).

Receiving commands from the Link layer, the Coordination layer is a supervisory controller that determines what maneuvers to perform, manages inter-vehicle communications, and coordinates the movement of the vehicle with neighboring cars. The choice of maneuvers and when to execute them depend on safety, the vehicle's route, commands from the Link layer, and local traffic conditions (Horowitz, 1997; Eskafi, 1995).

The Regulation layer is essentially a continuous-time, feedback-based controller that implements and executes the maneuver directed from the Coordination layer. The control laws at this layer provide the appropriate inputs (e.g., jerk and acceleration values) to the vehicle's actuators in order to perform a particular maneuver.

The lowest in the hierarchy is the Physical layer. Although it is not a controller, it contains all the vehicle's dynamics data and information, receiving steering, throttle, and brake actuator commands from the Regulation layer and returning information such as vehicle speed, acceleration, and engine state.

Chapter

2 Modeling and Verification

As discussed previously, the emergency vehicle (EV) maneuvers in this report were developed mainly within the Coordination layer. The Coordination layer is essentially a discrete-event supervisory controller. Finite-state-machines (FSM), which are finite automata with outputs, were used to model the designed controlled maneuvers within this layer. The verification was performed with the aid of the software tool COSPAN (Coordination-Specification-Analysis).

2.1 Finite-State-Machines (FSM)

The finite-state-machine (FSM) is a generalization of the finite automaton, which is a mathematical description of system with discrete inputs and outputs (Farokh, 1996). The status of the system is described by an internal configuration, or *state*, which is dependent on all past events as well as the input. A FSM can be characterize by:

- Q: finite set of states
- q_0: an initial state
- Σ: set of inputs
- λ: $Q \times \Sigma \rightarrow Q$: the transition function
- Δ: set of outputs
- γ: $Q \rightarrow \Delta$ or γ: $Q \times \Delta \rightarrow \Delta$: the output generating function

Thus, the six-tuple $(Q, q_0, \Sigma, \lambda, \Delta, \gamma)$ will completely define a FSM. The function λ takes as input the pair $(q, \sigma) \in Q \times \Sigma$ and outputs the next state $q' \in Q$. Two distinct approaches to specifying the function γ exist: 1) If the argument of γ is the state alone, the FSM is called a *Moore* machine. 2) If the argument is the pair $(q, \sigma) \in Q \times \Sigma$, the FSM is called a *Mealy* machine. The Mealy model was used for the Coordination layer maneuvers.

The behavior of a Mealy FSM is defined by the states that it crosses and the outputs that it generates. Thus, the verification can be performed by analyzing the FSM and tracing its states and outputs. Assuming the actual behavior of the system is described by the set S and the desired behavior by set D, the verification process can be achieved by comparing S to D. If $S \subset D$, the actual system behavior is *desirable* and in other words, verified.

2.2 System Modeling and Verification

Using the language of the Mealy FSM, the developed Coordination layer maneuvers were specified. However, in addition to the actual supervisory control algorithm, sensors and different processes must also be modeled. For instance, the queue-busy machine was consistently used in all the maneuver verifications (Figure 2.1). It was necessary because it

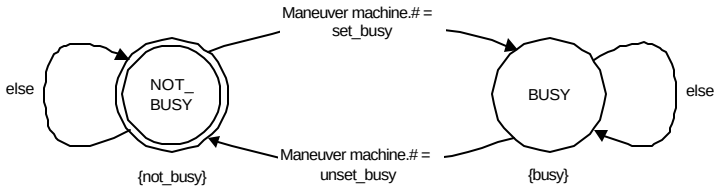

Figure 2.1: A queue-busy FSM

showed whether a vehicle was busy or not, hence indicating the possibility of performing a maneuver. The states were simply *BUSY* and *NOT_BUSY*, where the selection depended on the maneuver machine. Furthermore, because the Coordination layer must be informed of the status of the Regulation layer maneuver (i.e., maneuver aborted and maneuver complete) before it can conclude its maneuver, the Regulation layer maneuvers must also be specified with a Mealy machine in each case. The Regulation layer machine for the merge maneuver is illustrated in Figure 2.2. Although the FSM model contains only

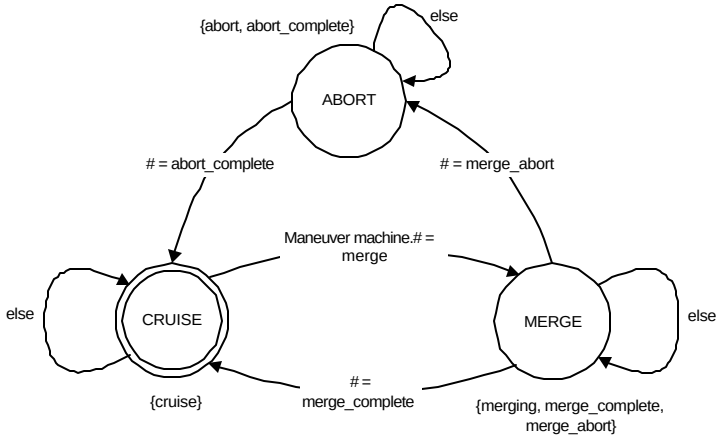

Figure 2.2: Regulation layer merge maneuver response FSM

discrete states, they represent continuous-time movements. For instance, in the *CRUISE* state, the actual vehicle is supposedly cruising at a relatively constant velocity; and in the *MERGE* state, the vehicle is performing the Join. The maneuver initiation is triggered by the maneuver machine, but subsequent selections are determined randomly.

Another crucial element was the specification of binary sensors, necessary in the supervisory selection process in all Coordination layer maneuvers. A sample is shown in

Figure 2.3? it is a front longitudinal sensor machine containing the states *NO_FRONT_CAR* and *FRONT_CAR*, where the selection process is alternating*.

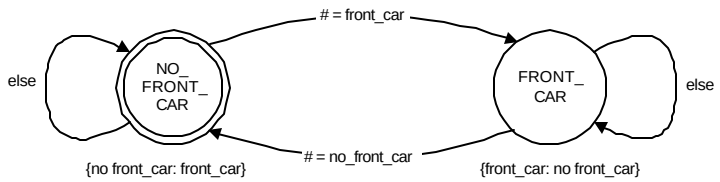

Figure 2.3: Front longitudinal sensor FSM

Upon specifying the needed elements in the syntax of a Mealy FSM, each completed maneuver with its various elemetn models was coded into COSPAN. Next, a *monitor* (the automaton specified to define those sequences of state/event pairs produced by the FSM algorithm which constitute the performance of the stated task) representative of the set *D* described in section 2.1 was specified. Using the monitor as the controlling factor, the maneuvers were correspondingly verified.

* The selection process can be made random as well.

Chapter

3 Emergency Vehicle Maneuvers

In the design of the emergency vehicle (EV) maneuvers, two categories of EV were considered:

1. *Fully automated EV*: EV that operates in the fully automated mode? no driver assistance is necessary. The Link layer and Coordination layer will be responsible to issue the commands, both to the automated vehicles in the AHS and to the EV.
2. *Manually driven EV*: EV that can be driven manually while traveling on the automated lanes. The responsibility of the Link layer and Coordination layer is to control the EV's fully automated neighbors to provide the best possible highway conditions for the EV to transit. The assistance of the EV driver is necessary in maneuvering the vehicle as well as negotiating certain communication protocols.

Furthermore, the criteria for the design were:

1. To design a set of maneuvers and control strategies which are as unobtrusive to the overall AHS architecture as possible.
2. To minimize the travel time of the EV on a freely flowing AHS by giving the EV greater access and resources to the system.
3. To allow EV travel on a stagnant AHS such that it can reach an accident site in the system and rectify the problem.
4. To eliminate the need of additional infrastructure such as dedicated shoulder lanes and entrances. In addition, only two lanes were assumed to exist in the system.

Additionally the EV maneuvers were designed within the degraded mode of operation. This was necessary because the EV needs the authority to instruct neighboring vehicles in the normal mode of operation to abort their maneuvers and respond immediately to the EV maneuvers. Consequently, the EV will have greater access to the system, achieving the goal of the design. Note that this is merely a conceptual change and does not represent any modification in the current design of the Coordination layer.

The maneuvers to be described were designed for the Coordination layer. Four complete EV maneuvers? the Vortex, Part-and-Go, Zigzag and Reverse-and-Merge? were developed. Moreover, as required by these maneuvers, three complementary

maneuvers? Platoon-Lane-Change, Stationary-Forward-Join and Stationary-Backward-Join? were also designed.

3.1 Vortex Maneuver

The context of the Vortex maneuver is to circulate traffic around the emergency vehicle (EV) to allow it to travel faster than the normal traffic flow and causing minimal local disturbance to the *freely flowing* AHS. This is a fully automated maneuver. The goal is to assist the EV (e.g., an ambulance) to respond to a service call and transit within the AHS to reach its destination as quickly as possible. The name of the maneuver was adopted because its execution produces a traffic pattern that resembles a vortex in a fluid. Figure 3.1 illustrates the general vortex maneuver.

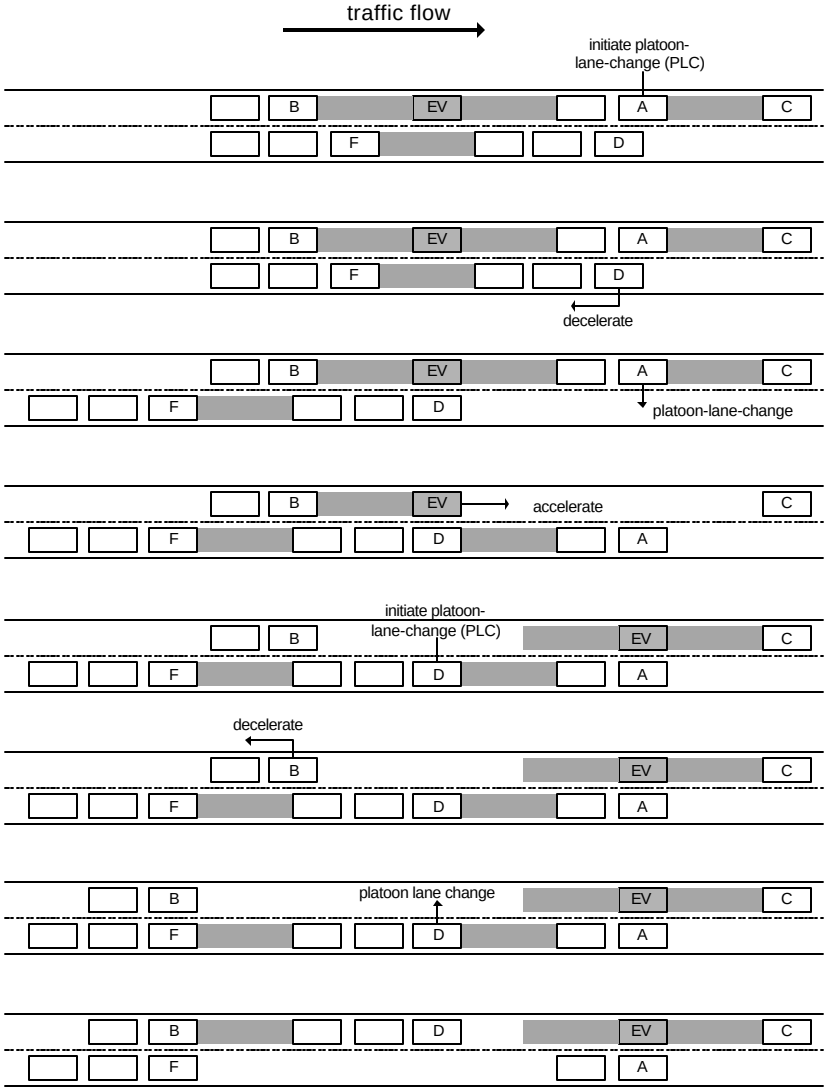

Note: normal interplatoon distance is indicated by the hash marks (not drawn to scale)

Figure 3.1: Vortex maneuvers

The emergency vehicle is denoted by EV and its five neighboring platoons are denoted by A, B, C, D and F. The flow diagram for this maneuver is shown in Figure 3.2.

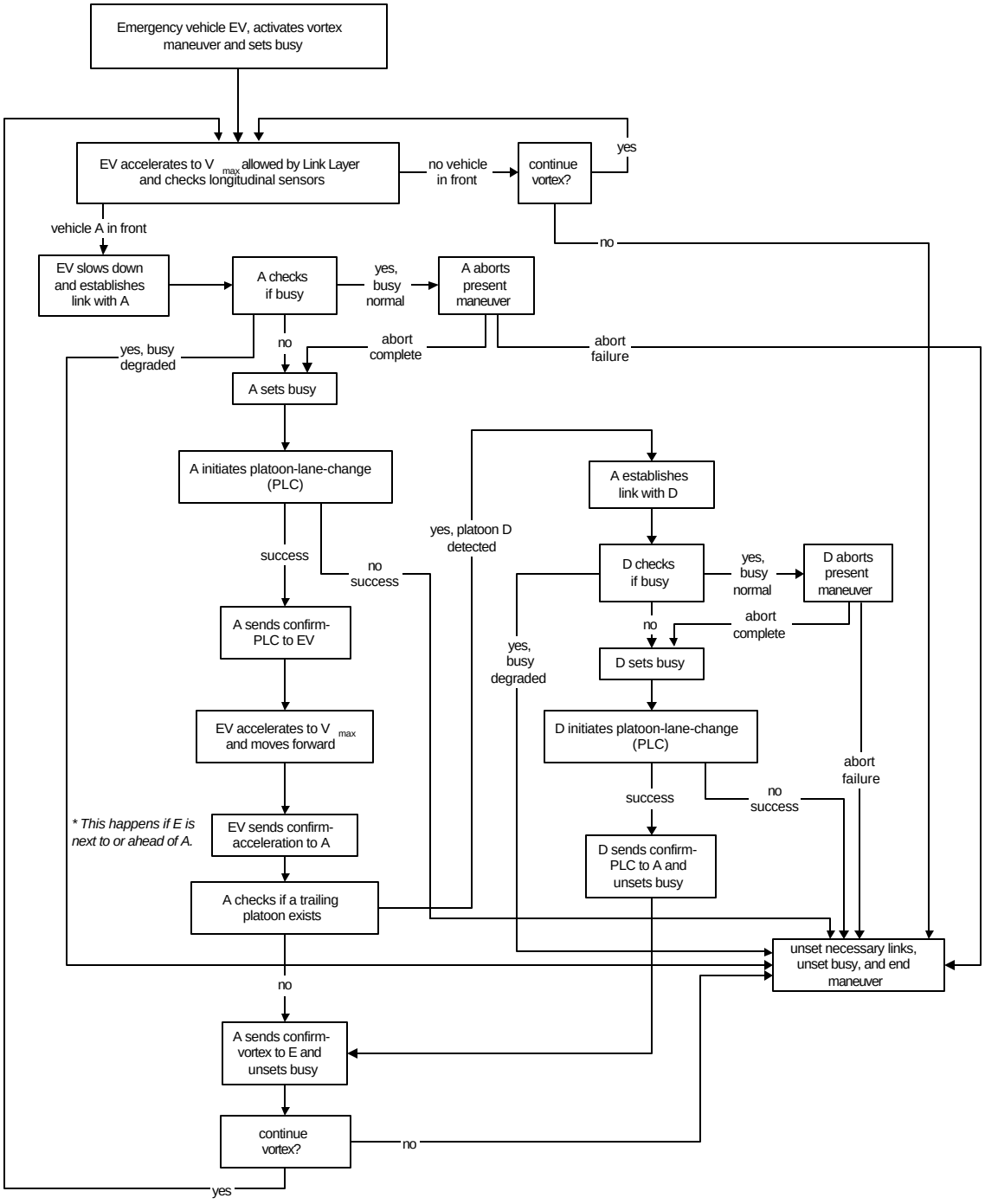

Figure 3.2: Vortex maneuvers flow diagram

When the EV initiates the Vortex maneuver, it will travel at V_{max}, the maximum velocity that the Link layer allows it to travel when no traffic is ahead. Note that this V_{max} value is larger than the maximum velocity the normal vehicles can travel and is determined based on the highway's traffic density, flow pattern, and other safety factors. When the EV encounters a platoon (responder #1? marked A in Figure 3.1) in front, it slows to the normal traffic speed and requests A to execute a Platoon-Lane-Change (PLC) maneuver. Platoon A then negotiates independently with its lateral neighbor, platoon D (responder #2), to perform the maneuver. If necessary, D will have to decelerate to create space for A. Note that if platoon D does not exist, A will simply perform the lane change on its own.

Upon completion of the PLC, A sends a *PLC-complete* message to the EV, which then accelerates to reach its V_{max} again. Note that during this time, the platoons A and D are still linked in communication. When the EV arrives at the neighboring position of the leader of A, it sends *move-complete* to A. A then requests D to perform a PLC to move into the adjacent lane on which A was traveling. Regardless of the success of the PLC by D, it tells A of its completion (*abort-complete* or *PLC-complete*). When the completion message is received, A unlinks from D and informs EV of the conclusion. At this point, responder A's part of the Vortex maneuver is finished, and it unlinks from EV. If the supervisor of the EV chooses to continue the Vortex maneuver, it will again travel at V_{max} until a front platoon is detected, and then the Vortex maneuver recycles[?]. The FSMs for the maneuver initiator (EV) and the two responders are shown in Figure 3.3, Figure 3.4 and Figure 3.5. The maneuver was verified using COSPAN.

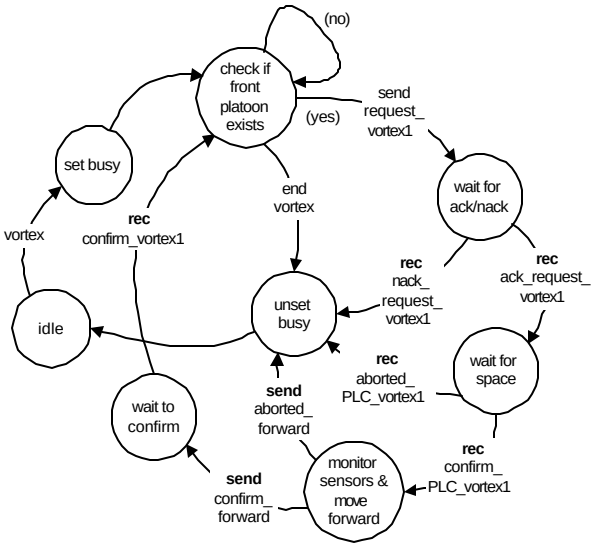

Figure 3.3: Vortex maneuver initiator's (EV) FSM

[?] Platoon C takes the place of A, and platoon A plays the role of D, assuming a resultant configuration as shown in Figure 3.1.

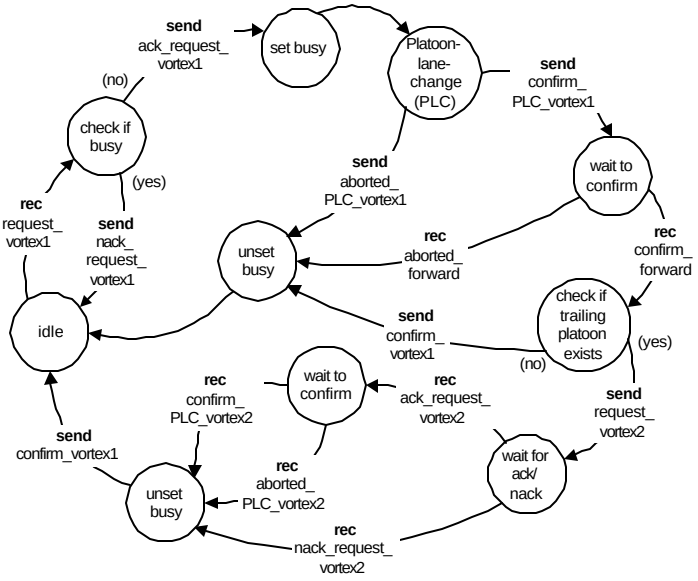

Figure 3.4: Vortex maneuver responder #1's FSM

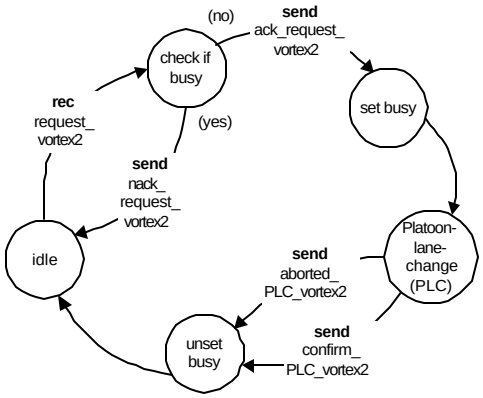

Figure 3.5: Vortex maneuver responder #2's FSM

3.2 Platoon-Lane-Change Maneuver

The design and verification of the Vortex maneuver assumed the existence of the Platoon-Lane-Change (PLC) maneuver. Thus, the PLC maneuver must be designed to enable the Vortex maneuver as well as other degraded mode situations described in (Lygeros et al., 1996). The existing normal mode lane-change maneuver was designed for free agents only. It will not be useful in the Vortex maneuver (or other degraded mode maneuvers) where time is crucial because a complete lane-change for a platoon would require numerous, time-consuming single splits and lane-changes.

The PLC maneuver is a degraded mode maneuver and consists of three options that are illustrated in Figure 3.6. Three platoons? A, B and C? are shown in the figure. The

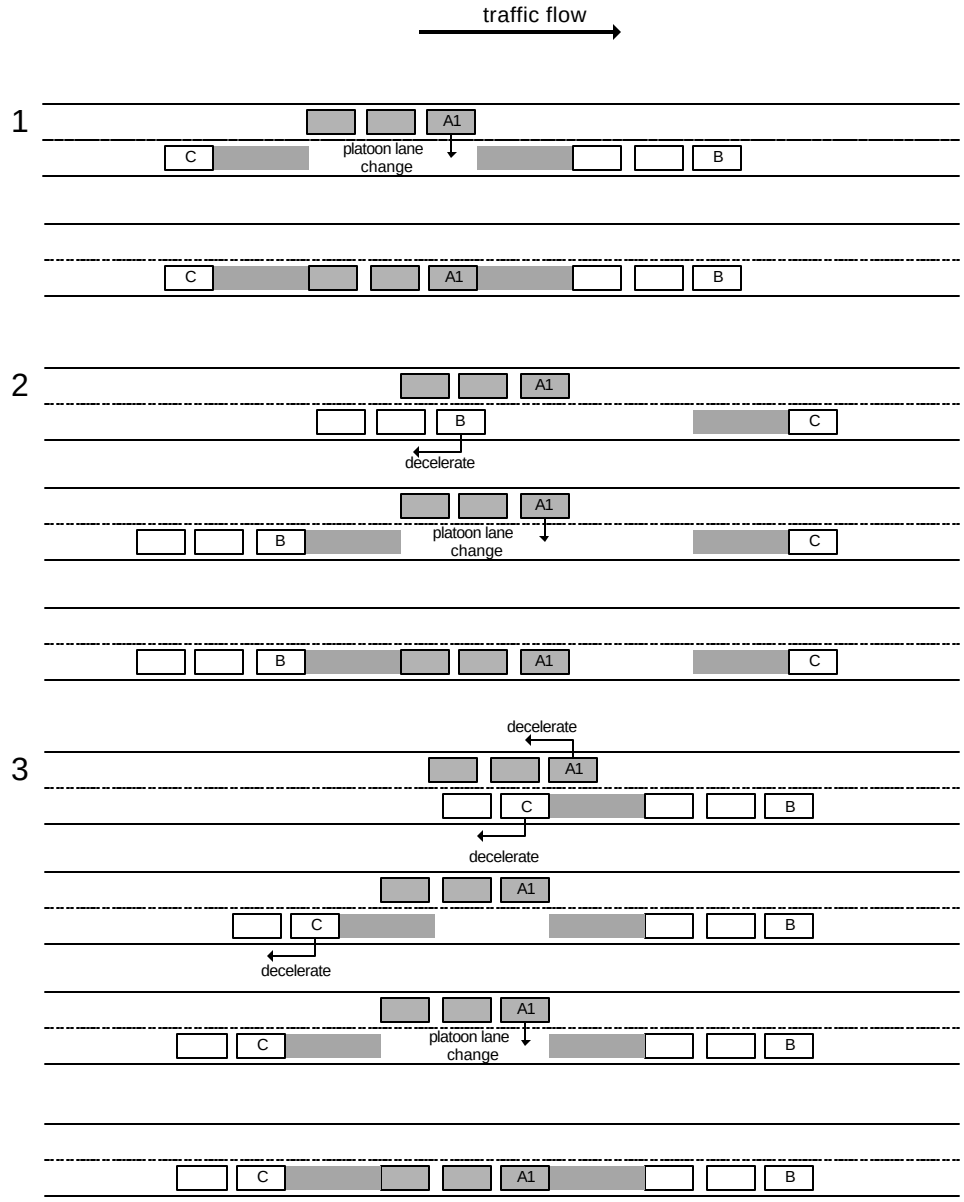

Note: normal interplatoon distance is indicated by the hash marks (not drawn to scale)

Figure 3.6: Platoon-Lane-Change maneuver

leader of platoon A that is initiating the maneuver is denoted as A_1. The full description of the Platoon-Lane-Change maneuver can be found in the flow diagram of Figure 3.7. Note that the design was generalized for a multilane system? A_1 must keep track of the two lanes in the direction of its lane-change, and note also that Figure 3.6 ignores the third lane.

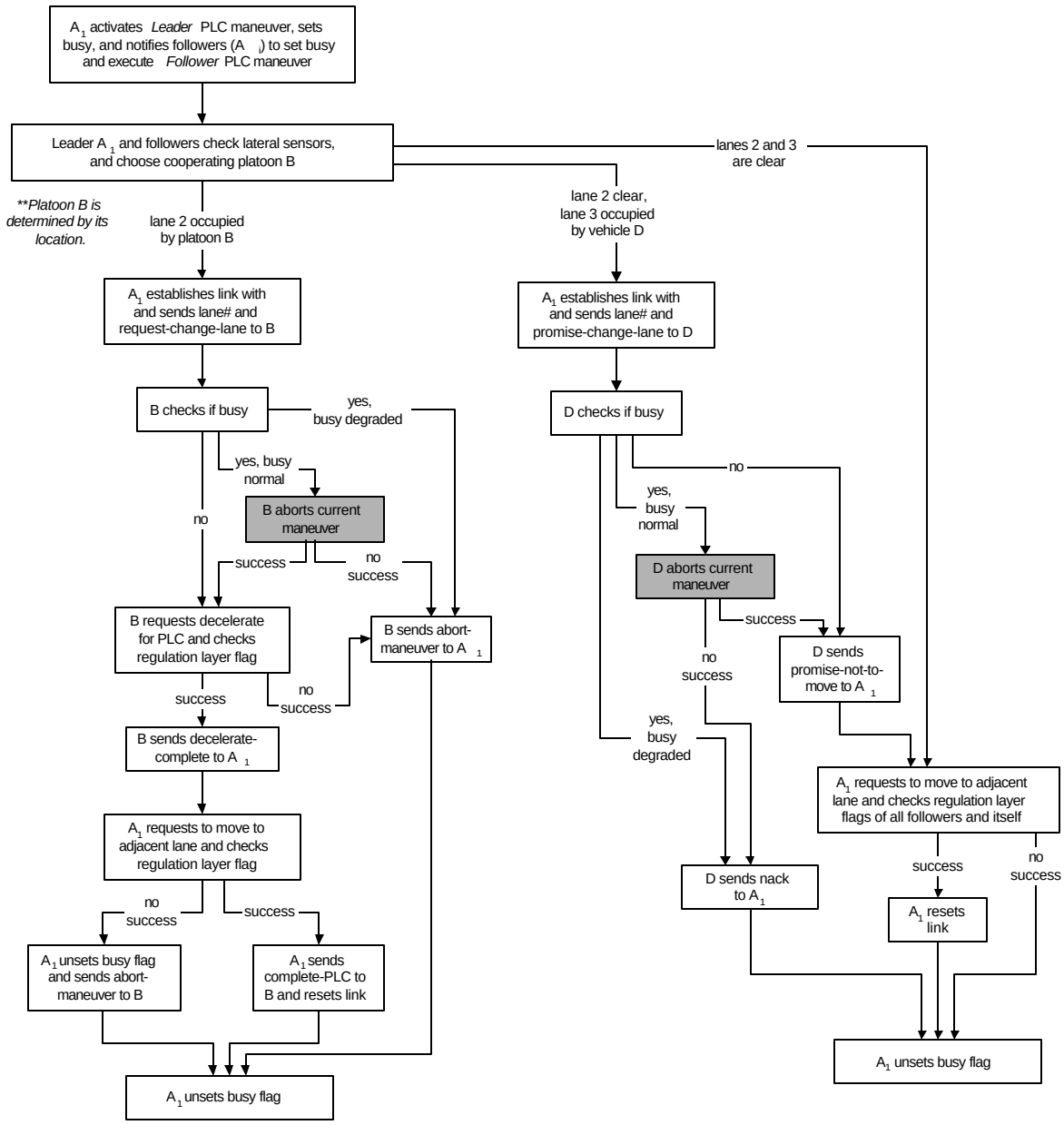

Figure 3.7: Platoon-Lane-Change maneuver flow diagram

When platoon leader A_1 decides to perform a PLC, it checks its lateral sensors for neighboring platoons in the immediately adjacent lane #2 and distant lane #3. Note that platoons are considered to be neighbors if they overlap within one interplatoon distance. For instance, in option #2 of Figure 3.6, platoon A has only one neighboring platoon, while in option #3, it has two. Different possibilities for the PLC maneuver are now discussed in detail:

1. If no platoon is detected in any of the two lanes, A_1 commands its Regulation layer to move to the adjacent lane.

2. If A_1 detects a platoon D in the distant lane #3 but no vehicle in lane #2, it establishes link with D and asks it to *promise-not-to-move*. If D replies with such an acknowledgement, A_1 then changes lane with its entire platoon. This communication exchange is necessary in preventing platoons A and D from changing lane at the same time and colliding.

3. Regardless of the status of lane #3, if lane #2 is occupied by a platoon B (option #2 in Figure 3.6), A_1 requests B to decelerate for PLC. When the space is successfully created, B notifies A_1, and A_1 moves over to the adjacent lane.

4. The most complex scenario is illustrated by option #3 in Figure 3.6 when platoon A is large enough to border two platoons B and C. At the onset of the PLC maneuver, A_1's regulation layer PLC controller (similar to the leader law) will automatically maintain one interplatoon distance away from platoon B. At the same time, A_1 requests platoon C to decelerate for PLC. Subsequent to the successful decelerations, platoon A can then perform the lane-change.

The FSMs for the Platoon-Lane-Change maneuver are shown in Figure 3.8 and Figure 3.9.

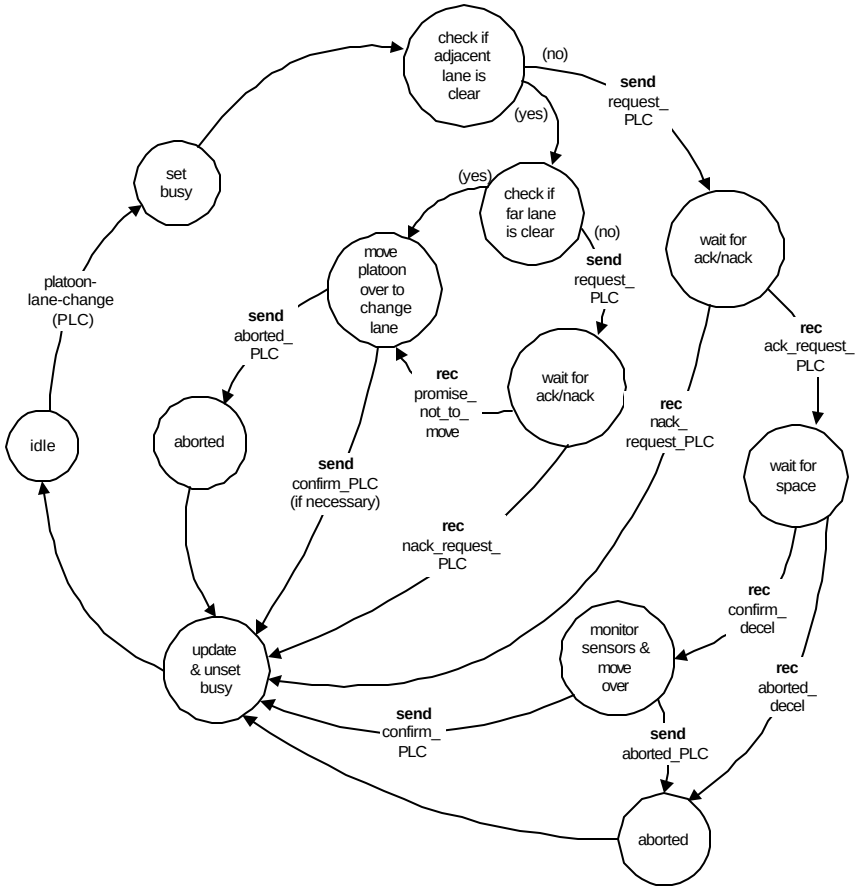

Figure 3.8: Platoon-Lane-Change maneuver initiator's FSM

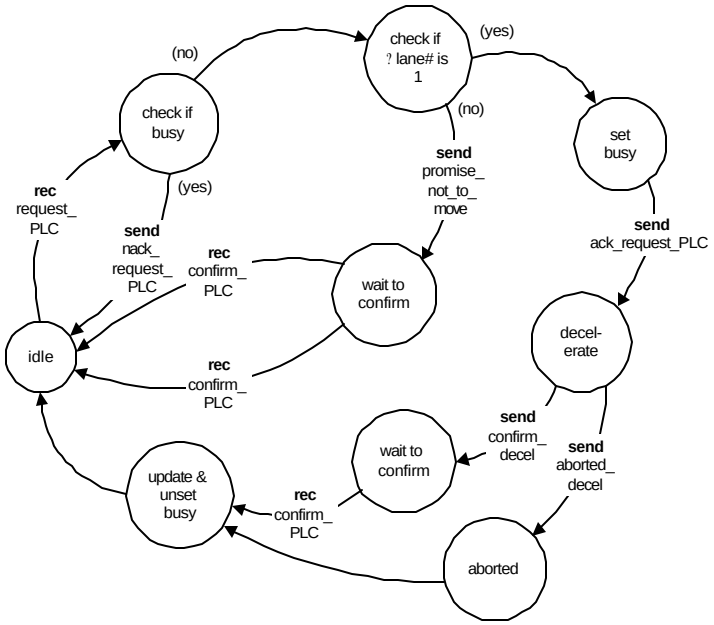

Figure 3.9: Platoon-Lane-Change maneuver responder's FSM

As completion of the PLC maneuver, the Regulation layer control laws need to be developed in the future. The PLC combines both lateral and longitudinal control and requires coordination from all vehicles in the platoon. Two options exist for the PLC, series or parallel.

?? **Series**: All vehicles in the platoon follows a prescribed "S" trajectory in the lane-change process (**Error! Reference source not found.**).

?? **Parallel**: All vehicles change lane simultaneously ().

Clearly, each has its own pros and cons. For instance, the series PLC is simpler to control but takes more time to complete; the parallel PLC is more complex (especially in lateral coordination), but takes less time to complete. Other Regulation layer parameters and safety factors must also be considered.

3.3 Part-and-Go Maneuver

Contrary to the Vortex maneuver, the Part-and-Go maneuver is designed to bring the EV to an accident site through a completely stagnant AHS and rectify the situation (i.e., remove the debris or tow away the collided vehicles). Note that the scenario considers that all lanes of the AHS (in this case two lanes) are stopped. Because vehicles are completely stopped on the AHS, backward vehicle motion is necessary in achieving this maneuver. The Part-and-Go maneuver creates travel spacing for the EV by merging in sequence all existing platoons on both AHS lanes, essentially eliminating all interplatoon distances and using them for travel headway. Figure 3.10 and Figure 3.11 depict the operation of this maneuver.

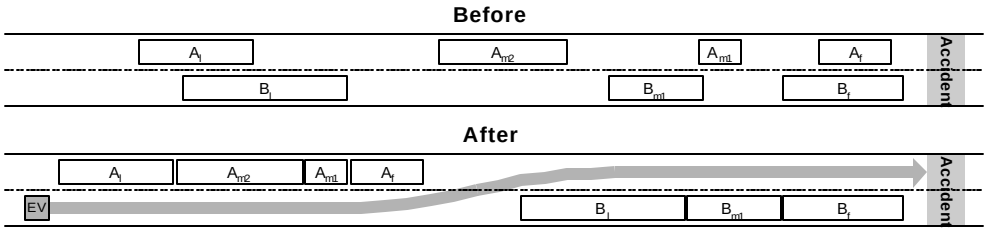

Figure 3.10: Part-and-Go maneuver

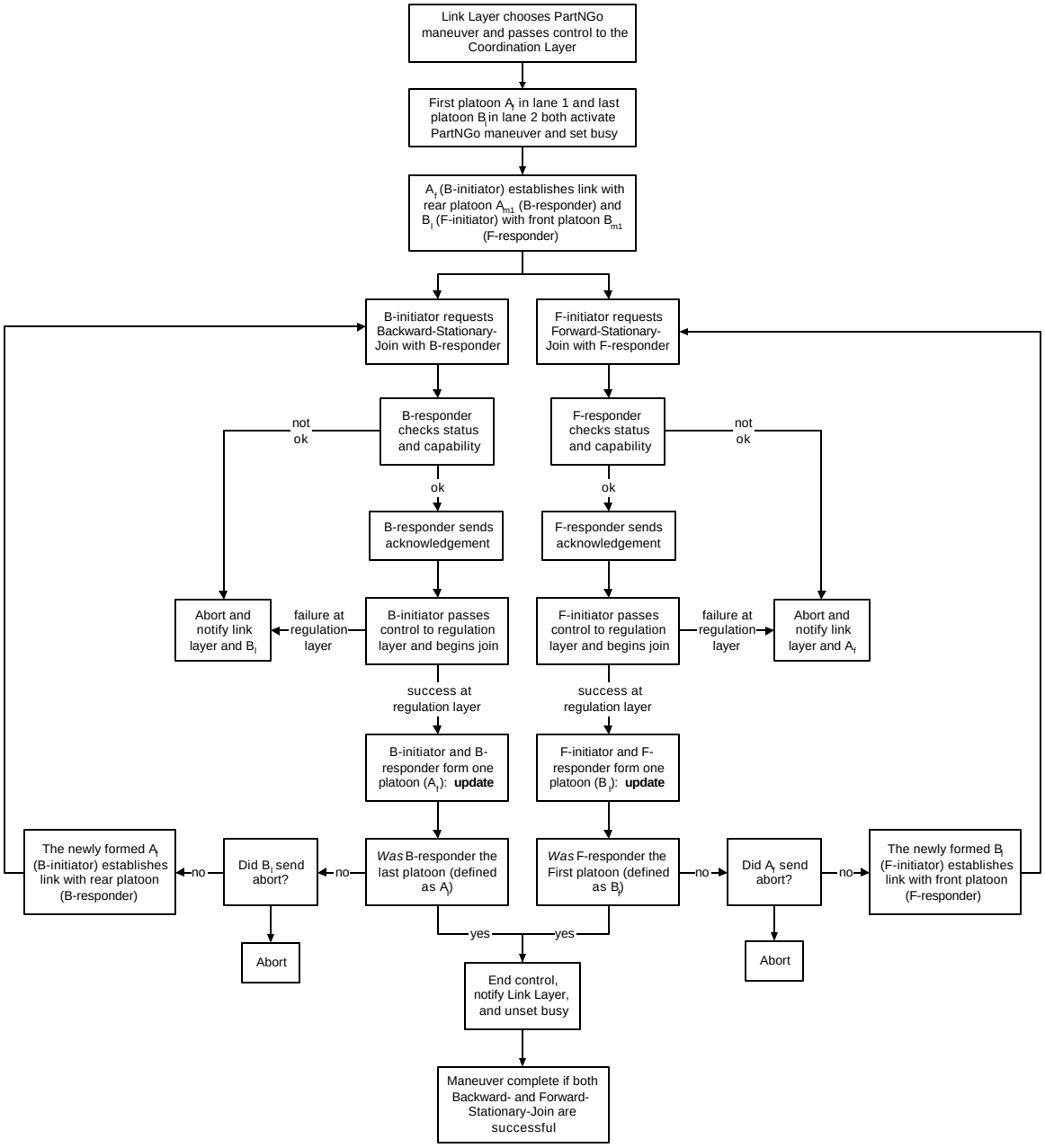

Figure 3.11: Part-and-Go maneuver flow diagram

Once the maneuver is initiated, the first platoon A_f on the left lane begins to backup and joins with its rear platoon, while the last platoon B_l on the right moves forward and joins with its front platoon. The Regulation layer maneuvers employed in this joining procedure are the Stationary-Backward-Join and Stationary-Forward-Join. They are very similar to the normal mode Join maneuver and will be discussed in section 3.4. When a join is completed, the two platoons (e.g., A_f and A_{ml}) update themselves via radio communications and form one logical platoon. The sequence of joins continues until only a single platoon is left on each lane and at opposite ends of the AHS. As a result, headway is created for the EV to travel, as conveyed by Figure 3.10.

Although this maneuver is mainly controlled by the Coordination layer, it is initiated and supervised by the Link layer, which possesses the traffic information (i.e., total vehicle lengths and total interplatoon distances) that is essential in determining the possibility of this maneuver. This maneuver is designed for a manually driven EV (can applied toward an automated EV also), in that the EV driver controls the vehicle as it moves through the headway and changes lane. However, most of the maneuver steps are performed by the normal, automated vehicles.

3.3.1. Applicability of the Part-and-Go maneuver

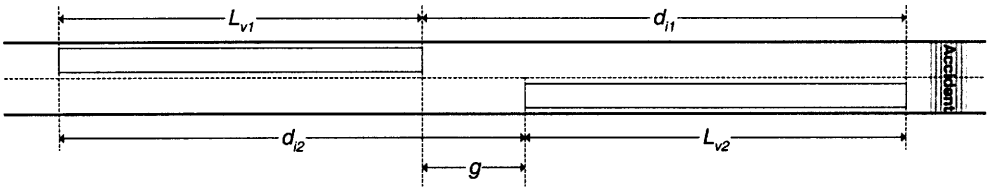

Figure 3.12: Highway variable definitions for Part-and-Go maneuver

The Part-and-Go maneuver will work only if the gap g is big enough for the EV to change from one lane to the other. We define the following quantities (refer to Figure 3.12):

- L_{vi} is the total vehicle length on lane i including intraplatoon distances
- d_{Ii} is the total interplatoon distance on lane i

For the EV to change lane safely, g is required to be at least twice the total EV length L_{ev},

$$\frac{d_{I1} + d_{I2} - L_{v1} - L_{v2}}{4} \geq L_{ev} \tag{3.1}$$

However, if $g < L_{ev}$, the final A platoon (after all the merges are completed) can move backward further to increase g until relation 3.1 holds true, assuming this rear space cushion exists. As another implementation option, this required space can be actively generated by the Link layer by creating a break (ΔB) between the upstream traffic and the piled-up vehicles (Figure 3.13).

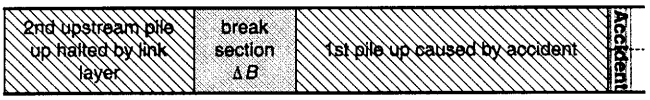

Figure 3.13: Creating a break section

The needed ΔB can be calculated as follows:

$$\Delta B = L_{ev} + \frac{N(L_p - L_i) + L_i}{2} \tag{3.2}$$

where

$L_p \equiv$ average platoon length
$L_i \equiv$ average interplatoon spacing
$N \equiv$ average number of platoons on the AHS section

If we assume a section length of 1000m and an EV length of 8m, we obtain the result depicted in Figure 3.14. The estimated average platoon length and interplatoon distance

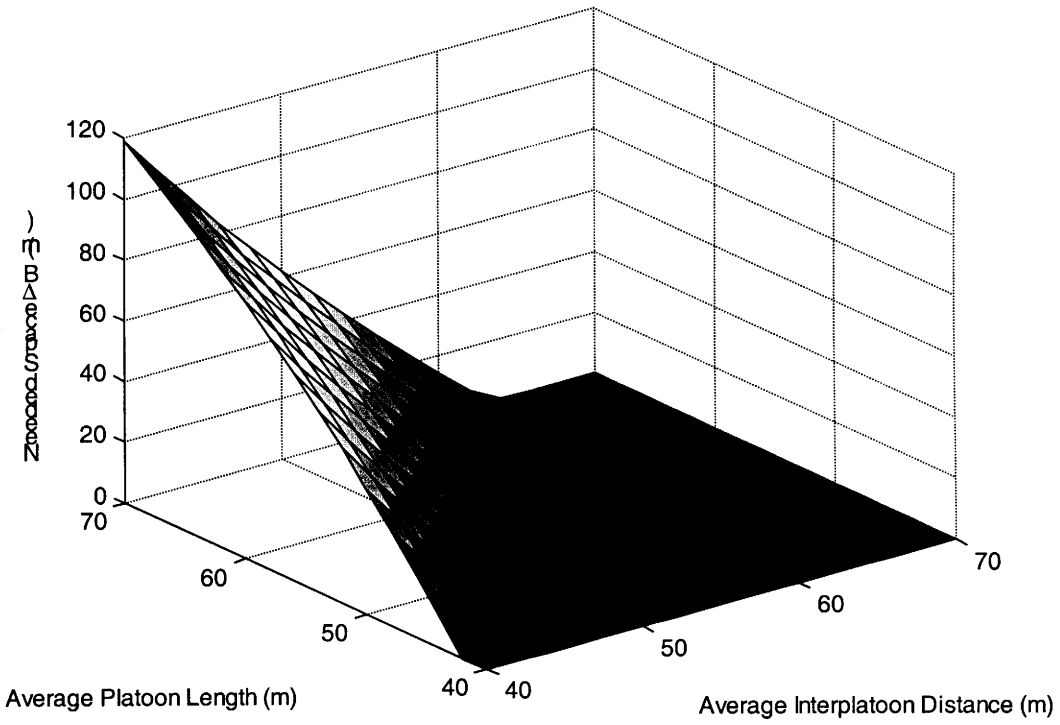

Figure 3.14: Needed space ΔB for Part-and-Go maneuver

are 50m and 60m, respectively. If the actual traffic condition does not exceed these two quantities, the Part-and-Go maneuver will not require the extra space $?B$ and will always be applicable in allowing the transit of an EV through the stagnant AHS. The FSMs for the Link layer initiator and only the responders on the left lane (A_i) are shown in Figure 3.15, Figure 3.16 and Figure 3.17. Besides the forward movement, the FSMs for the right lane responders are almost identical to those of the left lane, and thus, are left out. The maneuver was verified with COSPAN.

The Part-and-Go maneuver is very useful and efficient. The *parting* procedure in generating the headway for the EV can be performed prior the arrival of the EV. Thus, once the EV arrives, it can travel through the system with no delay.

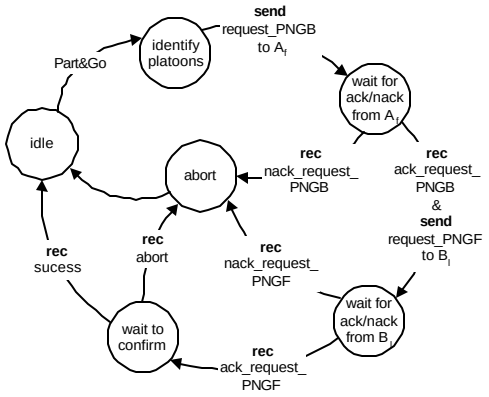

Figure 3.15: Link layer Part-and-Go maneuver initiator's FSM

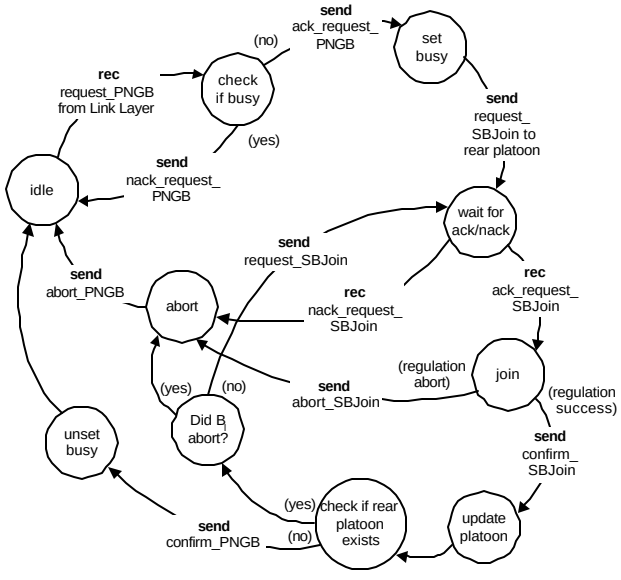

Figure 3.16: Coordination layer Part-and-Go maneuver responder #1's (A_f) FSM

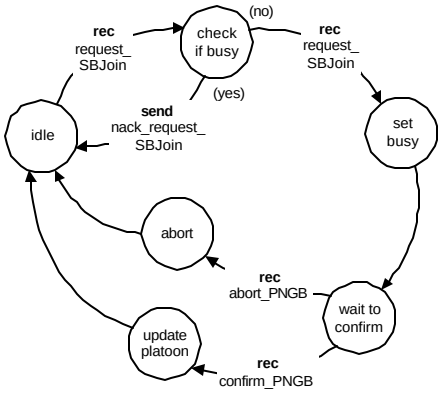

Figure 3.17: Coordination layer Part-and-Go maneuver responder #2's (A_{mi}) FSM

3.4 Stationary Join Maneuvers

The usefulness of the Part-and-Go maneuver depends on the assisting Stationary-Backward-Join (SBJ) and Stationary-Forward-Join (SFJ) maneuvers. They are very similar to the normal mode Join maneuver in the communication protocols; the differences are 1) the responding platoon remains stationary while the initiator performs the joining and 2) the SBJ maneuver involves backward motion. Because the SFJ maneuver is almost identical to the SBJ maneuver, only the SBJ maneuver will be described below.

The SBJ maneuver is illustrated in Figure 3.18. The maneuver is initiated by the

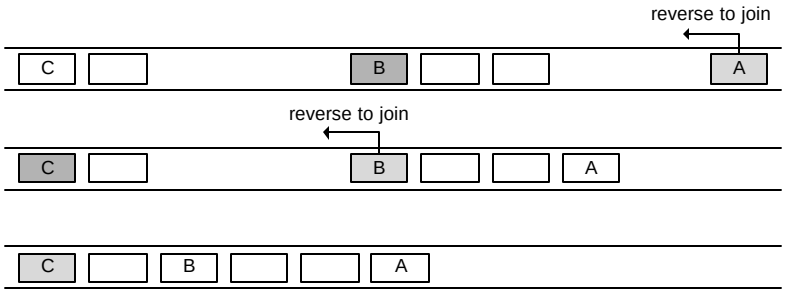

Note: Solid shade?responder, hash shade?leader and initiator

Figure 3.18: Stationary-Backward-Join maneuver

last vehicle, which is the *leader* for this maneuver*. The initiator checks with its rear platoon prior to commanding the Regulation layer to perform the actual joining. Once joined as one platoon, the vehicles in each platoon update themselves and become one

* Note that in the Stationary-Forward-Join maneuver, the leader remains as the first vehicle of the platoon.

logical platoon, and the role of the leader is relayed to the last vehicle. The FSMs for the initiator and responder are shown in Figure 3.19 and Figure 3.20, respectively.

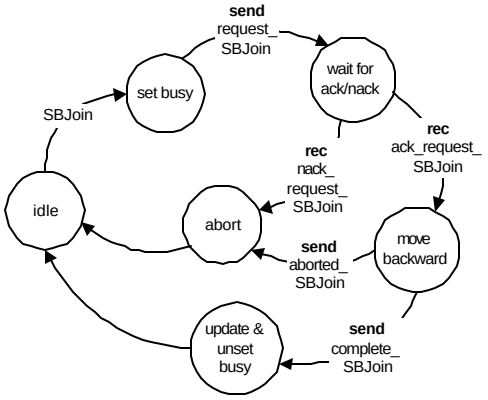

Figure 3.19: Stationary-Backward-Join initiator's FSM

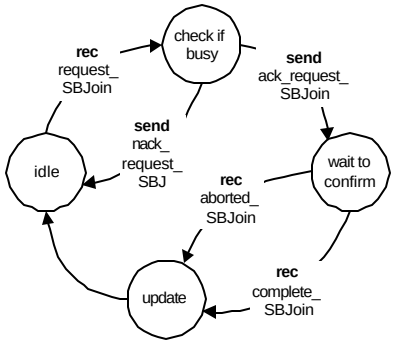

Figure 3.20: Stationary-Backward-Join responder's FSM

Because the protocol or the structure of the FSMs are identical to those of that of the standard Join maneuver, verification was not necessary as the Join maneuver was previously verified.

In completing these stationary join maneuvers, Regulation layer control laws must be designed. One of the biggest changes to the PATH architecture necessitated by the SBJ maneuver is the requirement of backward motion by the vehicles and platoons. Backward travel by a vehicle is known to be unstable at high speeds. Thus backward vehicle dynamics must be extensively researched. A backward speed limit must be found based on the highway's topology and other safety considerations. Furthermore, relevant Regulation layer parameters must be investigated and adjusted; a completely different Regulation layer for backward motion may need to be designed.

3.5 Zigzag Maneuver

Similar to the Part-and-Go maneuver, the Zigzag maneuver also serves the purpose of allowing the EV to transit through a completely stopped AHS. Compare to the Part-and-Go maneuver, it is much less efficient and requires significantly more time in bringing the EV to its destination. However, this maneuver becomes necessary when the applicability conditions of the Part-and-Go maneuver (section 3.3.1) does not hold. In other words, the Zigzag maneuver is an alternative to the Part-and-Go maneuver.

Nonetheless, the Zigzag maneuver also has an applicability criterion. The initial available space must be *at least* the length of the EV plus its headway tolerance distance (e.g., length of the EV) plus the length of the *longest* vehicle on the highway (Figure 3.21).

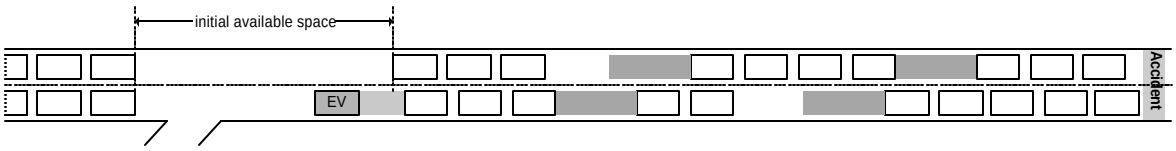

Figure 3.21: Initial available space

This criterion guarantees that the EV has sufficient headway (minimum of one vehicle) for travel and space for changing lanes without having to consider individual vehicle lengths. Note that the EV always starts the Zigzag maneuver on the shorter pile-up lane and the initial available space is the distance from the end of the longer pile-up lane to the beginning of the downstream pile-up. Note that this is not a restrictive criterion because Stationary-Forward-Join maneuvers can be performed to create the initial space. Furthermore, because this small initial space will almost always exist resulting from the existing interplatoon distances, the Zigzag maneuver can almost always be applied.

The format of the Zigzag maneuver is illustrated in Figure 3.23, and its flow diagram is shown in Figure 3.24. As the maneuver begins, the EV establishes link with the leader of the adjacent platoon (L1) and determines if the initial available space criterion is satisfied. If the initial available space is too small, the EV requests L1 to make space by performing one or more Stationary-Forward-Join maneuvers. Once the space requirement is met, L1 will decide which of its followers (F1) or itself will be the responder in the maneuver. This responder is determined as the *farthest* vehicle ahead that is within the EV tolerance distance (Figure 3.22).

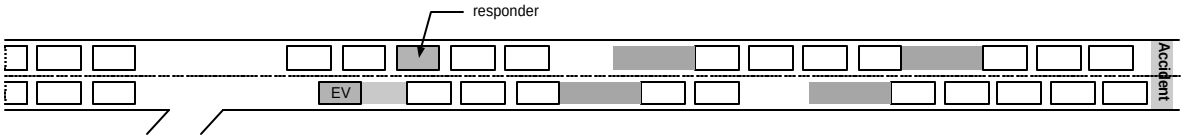

**EV tolerance distance is indicated by the vertical marks in front of the EV*

Figure 3.22: Determination of the Zigzag maneuver responder

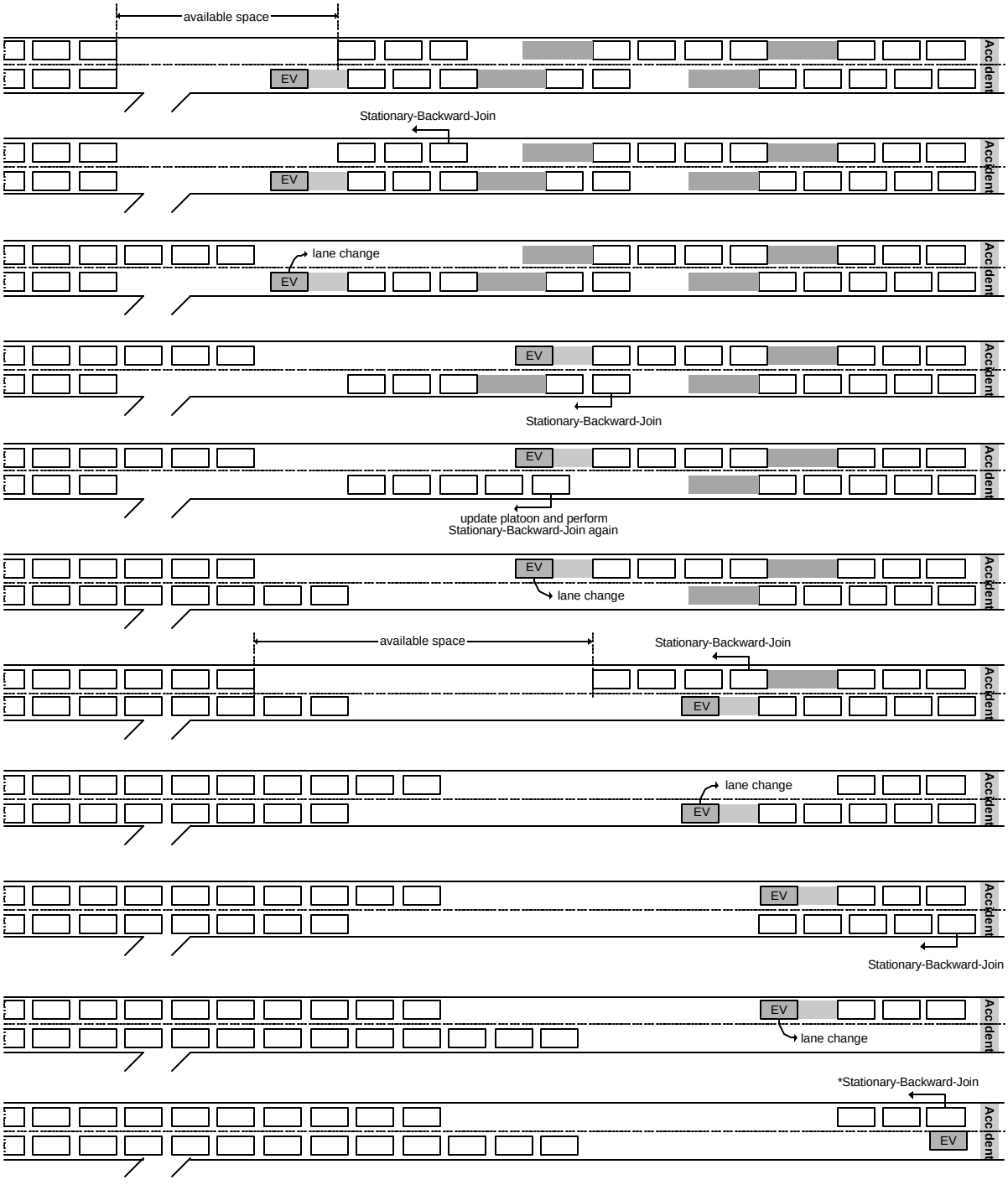

Figure 3.23: Zigzag maneuver

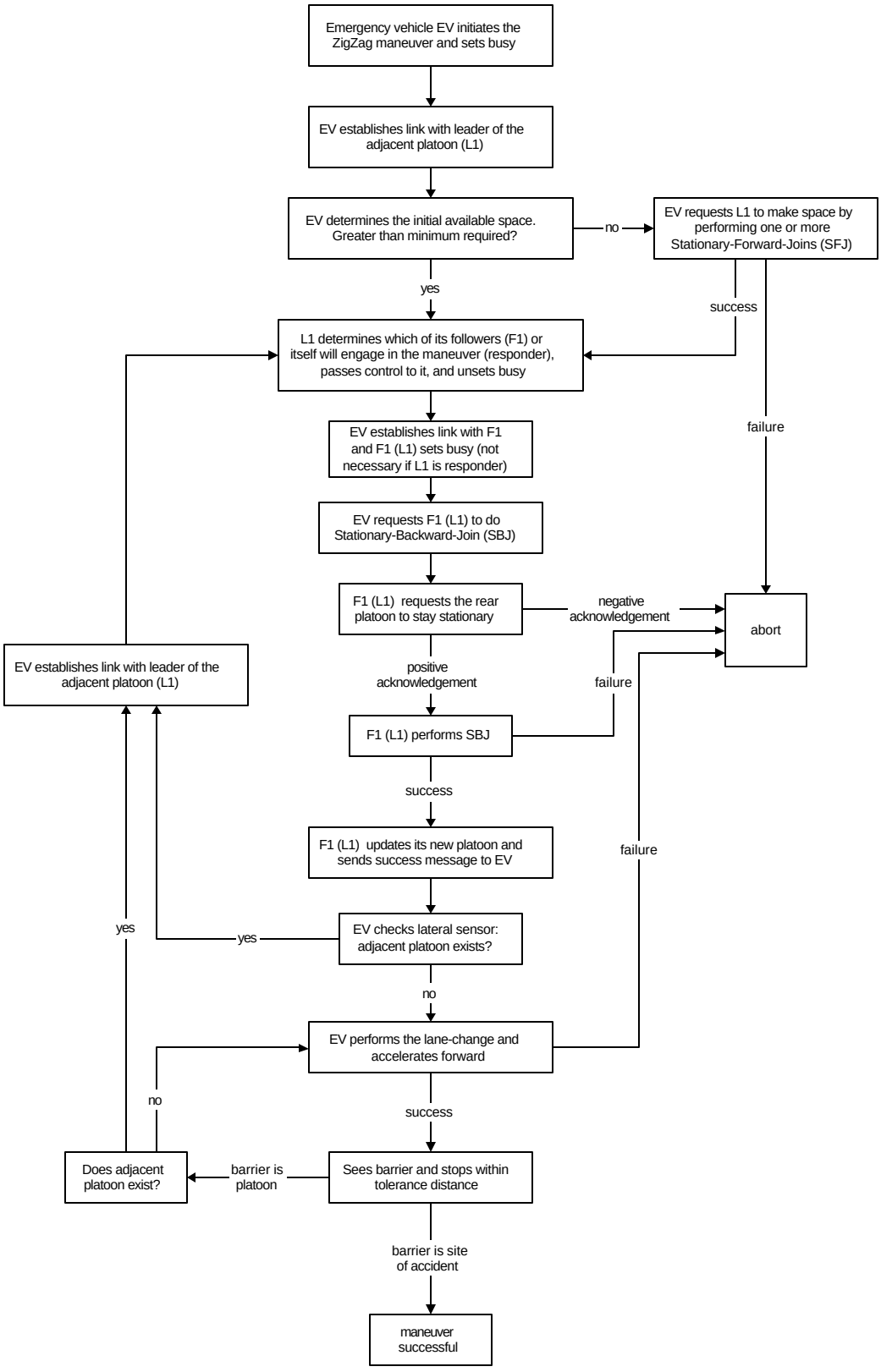

Figure 3.24: Zigzag maneuver flow diagram

The chosen responder along with its followers performs a Stationary-Backward-Join to make space for the EV. With success, the EV can then change lane and accelerate forward until a vehicle is detected ahead, at which time it stops within the tolerance distance. Then the EV checks its lateral sensors, and if no adjacent platoon exists, it will perform the lane-change and accelerate forward as before. If an adjacent platoon does exist, the EV will negotiate the same Zigzag maneuver described. This cyclic procedure continues until the EV arrives at the accident site.

As the interplatoon distances accumulate through the performing of the maneuver, the available space increases (Figure 3.23). Consequently, the number of vehicles from a platoon that can be moved backward increases*. The verified FSMs for this maneuver are shown in Figure 3.25, Figure 3.26 and Figure 3.27.

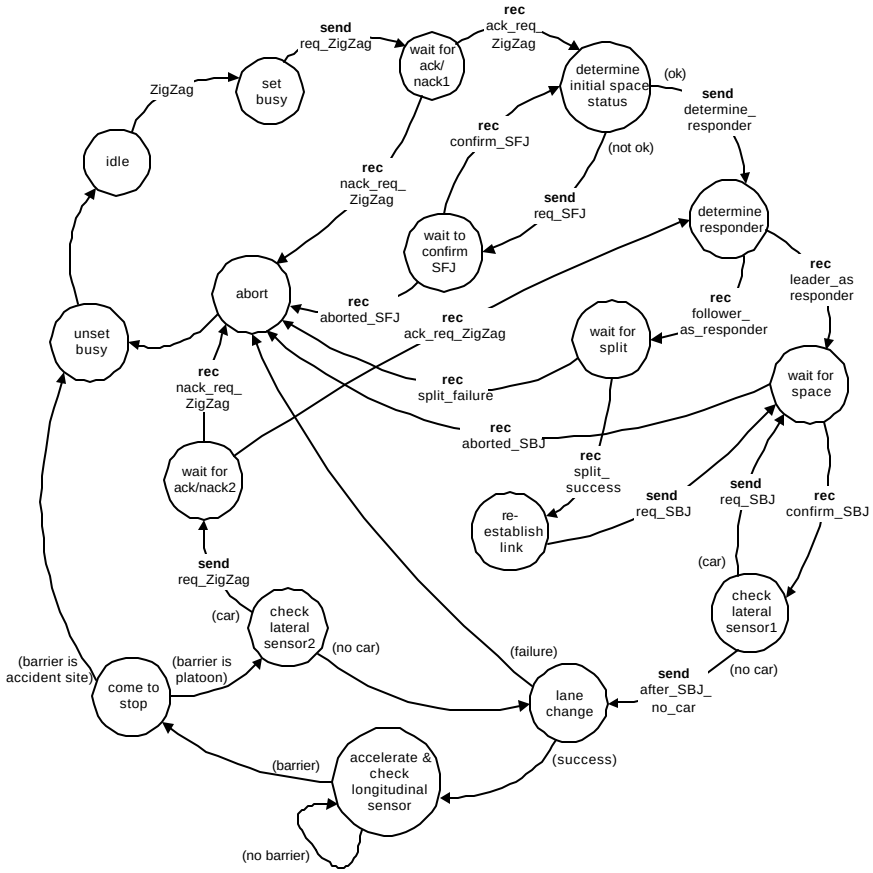

Figure 3.25: Zigzag maneuver initiator's (emergency vehicle) FSM

* If a means of determining the available space at each step exists, and this information can be relayed to the EV. The prime candidate for this task is the Link layer controller.

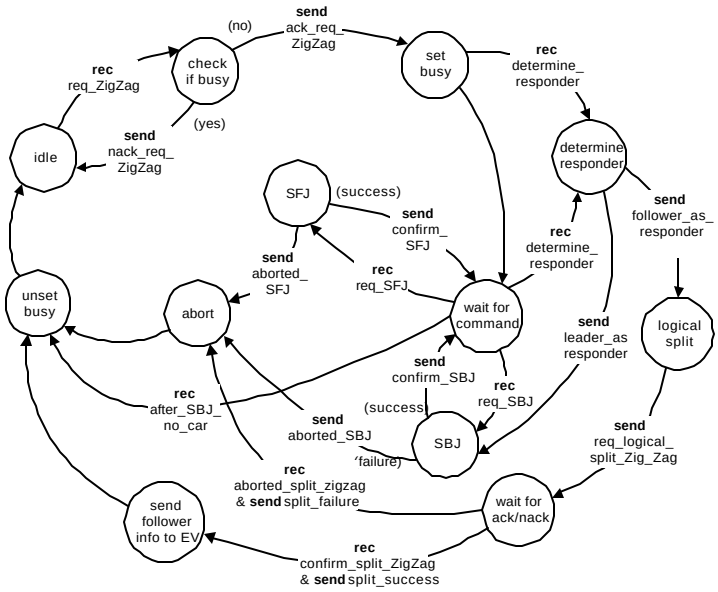

Figure 3.26: Zigzag maneuver responder #1's (adjacent platoon leader) FSM

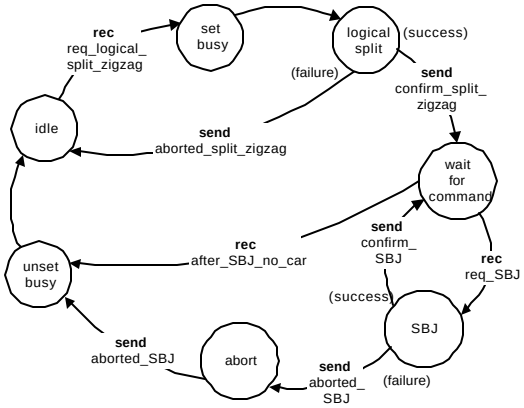

Figure 3.27: Zigzag maneuver responder #2's (adjacent platoon follower) FSM

The current Zigzag maneuver design can be applied to an automated as well as a manually driven EV. In maneuvering the EV in the lane-change, the driver can assist or the vehicle can be fully automated. If driver-assist is chosen, some communication exchanges between the manual EV and the automated traffic must also be supported by the driver as well. For instance, the driver must signal (e.g., push a button) the adjacent platoon to initiate the SBJ at each step.

3.6 Reverse-and-Merge Maneuver

The maneuvers described previously are for moving the EV through the AHS. Here the Reverse-and-Merge maneuver, which is designed for assisting stuck vehicles in a single-lane pile-up to merge into the freely flowing, adjacent lane, is discussed. For the

maneuvering of the EV through an AHS that has one crippled lane, the EV can basically travel on the freely flowing lane, and with the assistance of the Link layer, it can reach the accident site quickly.

However, for vehicles that are piled up on that stopped lane, the Reverse-and-Merge maneuver allows those vehicles to merge into the open lane. The operation of the maneuver is shown in Figure 3.28. The assistance of the Link layer in this maneuver is

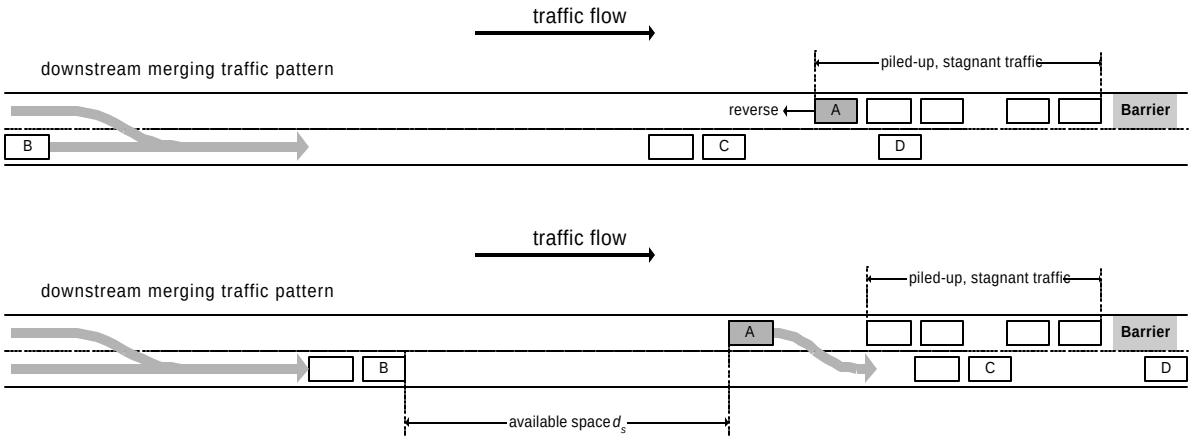

Figure 3.28: Reverse-and-Merge maneuver

crucial. The Link layer must help to significantly decrease the traffic density (i.e., increase interplatoon distance) and decrease traffic speed on the open lane such that the merging by a stopped vehicle is possible. The Link layer control laws for this purpose remain as future research.

When a vehicle engages the Reverse-and-Merge maneuver, it will reverse to a pre-determined distance behind the vehicle in front and merge into adjacent lane when given the *go-ahead* by the Link layer. The merging part of this maneuver is adopted from the Stoplight maneuver (Chen et al., 1997; Godbole et al., 1994). Essentially, the Link layer serves as a stoplight in giving the *green light* to the car so it can begin merging.

The design of this maneuver was generalized for a platoon. Thus, if so chooses, the maneuver can *reverse and merge* an entire platoon of several cars into the open lane. The number of cars that the merging platoon can accommodate will depend on the adjacent lane's upstream traffic and other safety factors (e.g., traffic speed and highway topology). The verified FSMs for this maneuver is shown in Figure 3.29 and Figure 3.30.

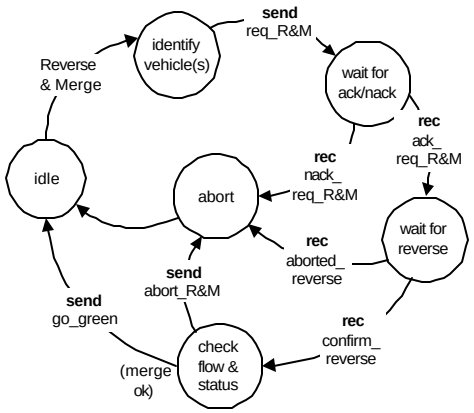

Figure 3.29: Link layer Reverse-and-Merge maneuver initiator's FSM

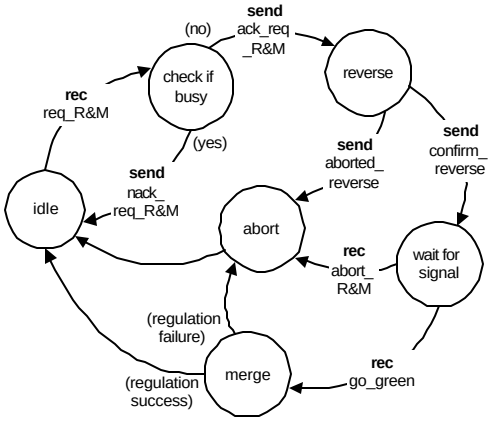

Figure 3.30: Coordination layer Reverse-and-Merge maneuver responder's FSM

Chapter

4 Conclusion

In this report, four completed Coordination layer maneuvers for emergency vehicles? Vortex, Part-and-Go, Zigzag and Reverse-and-Merge? were described. The design of these maneuvers relied on the modeling syntax of the Mealy finite-state-machine (FSM), and the verification was performed with the software tool COSPAN. The entire development procedure consisted of: 1) conceptualizing the maneuver within the scheme of the current PATH architecture and other existing control laws, 2) outlining step-by-step the maneuver in a flow chart format, 3) modeling the maneuver's initiator and responder(s) using FSMs, 4) modeling *all* elements of the maneuver (i.e., Regulation layer, sensors, and decision machines) within the COSPAN language environment, and 5) verifying with the compiled COSPAN program.

The verified maneuvers meet the criteria set forth in the beginning. All four maneuvers require no additional infrastructure and use only the available, automated lanes (two lanes assumed). To minimize the travel time of the EV in a freely flowing AHS, the Vortex maneuver circulates traffic around the EV such that it can reach velocity greater than the normal traffic. Moreover, the Vortex maneuver causes minimal local disturbance to the AHS. On the other hand, the Part-and-Go and Zigzag maneuvers enable the EV to transit through a completely stagnant AHS so that it can rectify the problem causing the breakdown (i.e., a collision). In the scenario of a single-lane pile-up, the travel of the EV is minimized simply if it travels on the open lane, while the Link layer assists in opening space downstream to the EV's travel. No EV maneuver in the Coordination layer was considered for this case. However, to move the stuck vehicles out of the stopped lane, the Reverse-and-Merge maneuver reverses these cars and allows them to merge into the open lane. This maneuver requires the help of the Link layer also. With these four maneuvers, the initial objectives of 1) ensuring rapid EV transit within the AHS and 2) enabling EV transit through a stagnant AHS.

As required by the above four maneuvers, three assisting maneuvers? Platoon-Lane-Change (PLC), Stationary-Backward-Join (SBJ) and Stationary-Forward-Join (SFJ)? were also developed. The PLC maneuver is required by the Vortex maneuver; the SBJ maneuver is used in the Part-and-Go, Zigzag and Reverse-and-Merge maneuvers; and the Part-and-Go maneuver also requires the aid of the SFJ maneuver. As a result of the SBJ maneuver, the current AHS scheme must be changed to accommodate the backward motion.

4.1 Future Research

Because the EV maneuvers were designed only within the Coordination layer, their final applicability will require additional future works in the Regulation and Link layers.

Within the Regulation layer, the following maneuvers will be needed:

1. **EV leader law**: Although expectedly similar to the normal leader law, the EV's leader law must inherently be different from its surrounding platoon leaders in order to gain greater access to the AHS. For instance, its maximum cruise velocity provided by the Link controller will be greater. Furthermore, safety or comfort parameters within the Regulation layer controllers must be investigated and modified to allow better time-efficiency (passenger comfort-level can be sacrificed).
2. **EV lane change**: This maneuver should be the same normal-mode free-agent lane change maneuver when the EV is traveling on a freely flowing AHS. However, for traveling on a stagnant AHS, as in the Part-and-Go and Zigzag maneuvers, the maneuver has to be modified because the traffic is stopped and most important of all, the gap for the lane change is much smaller.
3. **Platoon-Lane-Change**: Description can be found in 3.2.
4. **Backward control**: Lateral and longitudinal control for backward vehicle motion will have to be designed. However, first backward vehicle dynamics must be extensively research because backward travel by a vehicle is unstable at high speeds. Also, relevant Regulation layer parameters need to be modified.

The necessary capabilities, maneuvers and control laws for the Link layer are outlined below:

1. **Determination of EV speed limit for use in the EV leader law**: This limit should be determined based on the traffic pattern and density.
2. **Determination of available space in the AHS link**: In the case of a stopped AHS and for the EV to reach the accident site, the Part-and-Go maneuver is preferred over the Zigzag maneuver. However, its applicability depends on the total vehicle distance (all vehicles plus all intraplatoon distances) and the total free space left (all interplatoon distances plus the free spaces) in both lanes within the link under question. Thus, the Link layer must be capable of determining these two quantities.
3. **Generating a break in traffic**: In the available space is not sufficient to allow the Part-and-Go maneuver, the Link layer can in advance control the upstream traffic and open up "extra" free space to enable the Part-and-Go maneuver. This can be accomplished by creating a "break space."

With the completion of these Regulation and Link layer maneuvers, the designed EV maneuvers can be finalized.

References

Alvarez, L., Horowitz, R., and Li, P. (1996). Link Layer Vehicle Flow Controller for the PATH AHS Architecture. *Proceedings of the 1996 IFAC World Congress, San Francisco,* volume Q, pages 207?212.

Chen, P., Alvarez, L., and Horowitz, R. (1997). Trajectory Design and Implementation of Longitudinal Maneuvers on AHS Automated and Transition Lanes. Technical report UCB-ITS-PRR-97-49, Institute of Transportation Studies, University of California, Berkeley.

Eskafi, F. (1996). Modeling and Simulation of the Automated Highway System. Ph.D. thesis, Department of Electrical Engineering and Computer Sciences, University of California, Berkeley.

Godbole, D., Eskafi, F., Singh, E., and Varaiya, P. (1994). Design of Entry and Exit Maneuvers for IVHS. Technical report, Institute of Transportation Studies, University of California, Berkeley.

Godbole, D., Lygeros, J., Singh, E, Deshpande, A., and Lindsey, A. (1995). Design and Verification of Coordination Layer Protocols for Degraded Modes of Operation of AHS. *Proceedings of IEEE CDC*, pages 427?432.

Har'El, Z., and Kurshan, R. P. (1987). COSPAN User's Guide. Murray Hill, NJ: AT&T Bell Labortories.

Har'El, Z. and Kurshan, R. P. (1990). Software for Analytical Development of Communications Protocols. AT&T Technical Journal, Jan./Feb.: 45-49.

Horowitz, R. (1997). Automated Highway Systems: the Smart Way to Go. *Proceedings of the 8th IFAC Symposium on Transportation Systems (Plennary Presentation)*.

Lygeros, J., Godbole, D., and Broucke, M. E. (1996). Towards a fault tolerant AHS design, part I: Extended architecture. Technical report, Institute of Transportation Studies, University of California, Berkeley.

Rao, B. and Varaiya, P. (1993). Roadside Intelligence for Flow Control in IVHS. Technical report, PATH, University of California, Berkeley.

Ren, W. and Green, D. (1994). Continuous Platooning: A New Evolutionary and Operating Concept for an Automated Highway Systems. Technical report preprint, University of California, Berkeley.

Varaiya, P. (1993). Smart Cars on Smart Roads: Problems of Control. *IEEE Transactions on Automatic Control*, AC-38(2): 195?207.

Varaiya, P. and Shladover, S. E. (1991). Sketch of an IVHS Systems Architecture. Technical Report UCB-ITS-PRR-91-3, Institute of Transportation Studies, University of California, Berkeley.

Part II

Emergency Vehicle Maneuvers and Control Laws for Automated Highway Systems

by

Charmaine Veronica Toy

B.S. (University of California at Berkeley) 1992
M.S. (Stanford University) 1993

A dissertation submitted in partial satisfaction of the
requirements for the degree of
Doctor of Philosophy

in

Engineering - Mechanical Engineering

in the

GRADUATE DIVISION
of the
UNIVERSITY of CALIFORNIA at BERKELEY

Committee in charge:

Professor Roberto Horowitz, Chair
Professor Oliver M. O'Reilly
Professor Carlos Daganzo

Spring 2000

The dissertation of Charmaine Veronica Toy is approved:

Chair Date

Date

Date

University of California at Berkeley

2000

Emergency Vehicle Maneuvers and Control Laws for Automated Highway Systems

Copyright 2000

by

Charmaine Veronica Toy

Abstract

Emergency Vehicle Maneuvers and Control Laws for Automated Highway Systems

by

Charmaine Veronica Toy

Doctor of Philosophy in Engineering - Mechanical Engineering

University of California at Berkeley

Professor Roberto Horowitz, Chair

In this thesis, the problem of high priority transit for emergency vehicles (EV) on automated highway systems (AHS) is investigated. The goal of the EV maneuvers and control laws presented in this thesis is to ensure that EVs travel faster than the nominal AHS traffic in the same highway section in free-flowing traffic conditions. It is assumed that all AHS vehicles are fully automated and that there are no highway shoulders. Both individual vehicle maneuvers and mesoscopic traffic flow maneuvers are needed to maintain this region of low vehicle density around the faster moving EV.

The hierarchical control architecture introduced by California Partners for Automated Transit and Highways (PATH) is used to separate the complex problem of controlling all AHS vehicles into five smaller control layers. The main contribution of this thesis is the development of EV specific control laws and maneuvers for the link and coordination layers of the PATH hierarchical control architecture.

At the link layer, individual vehicles are not identified or controlled; traffic is treated as a continuum. For low traffic density conditions, a traffic flow control law, nicknamed the *Bubble* maneuver in this thesis, is presented which enables the vehicle flow in one lane to be circulated out of the way of the section in which the fast moving EV travels. The *Bubble* maneuver only uses lane changing commands to achieve this circulation. Another traffic flow control law, nicknamed the *Volcano* maneuver in this thesis, is developed for high traffic density conditions. The *Volcano* maneuver requires both traffic flow speed changes and lane changing commands. To achieve the traffic flow speed changes, traffic flow velocity must be varied in a specific way; the idea of a non-stationary velocity profile is introduced. Two link layer stabilizing controllers are developed specifically for accomodating non-stationary velocity profiles.

For the coordination layer, this thesis evaluates the previously designed *Vortex* maneuver, which microscopically moves individual vehicles out of the way of an EV. The *Vortex* maneuver is found to be inadequate because it does not reestablish the original configuration of vehicles after the EV has passed. A new and improved *Vortex2* maneuver, which does reestablish the position of vehicles, is designed and tested.

Professor Roberto Horowitz
Dissertation Committee Chair

To Mom and Dad.

Contents

List of Figures

Acknowledgements

I would like to thank my advisor, Roberto Horowitz, for his guidance and accesibility for my research. I would also like to thank Professors O'Reilly and Daganzo for their sharing of time and ideas for my dissertation. I am grateful to my friends and officemates who have given me help in almost all aspects of my graduate student life: Gabriel Gomes, Jingang Yi, Laura Munoz, Craig Smith, Joel Shields, Perry Li, Rob Bickel, Prabhakar Pagilla, Elisa Bass and Elaine Serina. I owe special thanks to Luis Alvarez-Icaza for our discussions of research ideas over the years.

I will always be grateful to my parents, who have always been my steady guidance and support. I thank David for his love and support during the good and bad times of my graduate career and for being my conscience.

Chapter 1

Introduction

This thesis investigates the design requirements for implementation of high priority emergency vehicle (EV) transit on AHS in order to better understand Automated Highway System (AHS) technology. It specifically focuses upon developing the modifications and additions to AHS control laws that are needed for an EV, such as a police car, ambulance or fire truck, to use the system. Should an AHS be implemented, EVs would benefit from AHS use under two different scenarios: 1) using the AHS to travel to an accident inside the AHS and 2) using the AHS to travel to a location outside of the AHS. In the former case, the AHS's capability to maintain high traffic flows is directly related to its ability to quickly recover from faults. If one assumes a flow of 6000 vehicles per hour on the AHS and 93 incidents per million vehicle miles of travel [1], then it is possible to expect one breakdown per hour on every 2 miles of AHS. In the latter case, EVs, such as police cars or ambulances, may need to travel within the AHS to an incident or medical facility. When one needs to

[1] An efficiency study of the freeway service patrol in Los Angeles estimated this frequency based on incidents requiring any type of assistance. Most incidents were breakdowns on shoulders and are included because this thesis is restricted to the study of shoulderless AHS. See (Skabardonis et al., 1998).

evaluate how potentially useful and realizable an AHS can be, EV specific maneuvers and control laws must be considered.

AHS technology refers to control laws and maneuvers that are needed to conduct a vehicle on a highway without any driver supervision once the vehicle arrives at a highway entrance. Once he/she relays destination information to the AHS, the driver is free from vehicle supervision until the vehicle exits the AHS. Vehicle and roadside control systems are responsible for maintaining safe distances from neighboring vehicles and performing activities, such as lane changes or route choices, so that each individual vehicle reaches its destination safely and in an efficient manner. AHS technology is a subcategory of Intelligent Vehicle Highway Systems (IVHS), which may also include partial driver assisted technologies. Because the supervising AHS control systems ensure consistent cooperation among vehicles, it is possible to decrease intervehicle spacing by organizing groups of vehicles, which share high-speed communication, into platoons. This may lead to an increase in highway capacity while requiring fewer lanes. The design goals of the AHS are to improve individual vehicle safety, vehicle travel efficiency and highway capacity. Any EV control laws or maneuvers designed for this thesis must address these larger goals. As a result, shockwaves caused by the presence of a faster moving EV are very undesirable, and the traffic configuration should always be restored after the EV has passed.

Carefully designed control laws and maneuvers together with AHS communication systems allows automated vehicles to more efficiently respond to an EV requiring high priority transit. On a manual highway, audio and visual cues alert human drivers to the presence of an approaching EV. Many human drivers can not detect the direction of an EV from a siren

and therefore, can not perform evasive maneuvers until the EV is in sight. By utilizing the AHS's communication systems, automated vehicles can obtain additional information, such as EV position, speed and required lane well in advance to respond more efficiently. State law requires drivers to slow their vehicles and move them out of the way of the police car or ambulance to allow the EV to pass. Because the AHS relieves humans of their normal driving responsibilities, it is necessary to develop maneuvers and control laws to promote the passing of a faster moving EV. Because the AHS forces vehicles to cooperate to circulate out of the way, faster EV transit can be achieved than would otherwise be possible in manually driven traffic and with fewer perturbations to the overall traffic flow.

The presence of an EV on the AHS requires nearby non-EVs to interrupt their normal activities in order to move out of the way. Under normal operating conditions, vehicles operate with full capabilities, and AHS design treats all vehicles equally; a non-EV travels no faster than other nearby vehicles with the same destination. Degraded mode operation, which occurs when a vehicle experiences a performance degradation requiring corrective action, may require other nominally operating vehicles to give way to a designated vehicle (usually the disabled one). [2] The presence of an EV on the AHS requires degraded mode operation of the nearby non-EVs, which interrupt normal maneuvers in order to move out of the way. Changes to the controllers of all non-EV AHS vehicles are required to implement specific degraded mode manuevers for high priority EV transit.

The EV maneuvers and control laws in this thesis were developed under the following

[2] It is said, then, that the designated vehicle (and possibly its neighbors if their activities are interrupted) operates in a degraded mode. An EV which needs to travel faster than the rest of the traffic is the designated vehicle in this scenario. See (Lygeros et al., 1995) and (Lygeros et al., 2000) for descriptions of additional degraded modes of operation (e.g. radar failure). Relaxation of certain AHS parameters, such as comfortable maximum deceleration/acceleration levels, may also be possible.

design restrictions:

1. **There are two or more AHS lanes.** In the case of a single lane, the EV is restricted to travel at the same speed as the AHS traffic flow. With multi-lanes the lane in which the EV does not travel is used to circulate vehicles around the EV. In this thesis, all designs and control laws assume that highways have two lanes everywhere. However, the addition of lanes does not change the overall strategies presented.
2. **There is no dedicated shoulder for the EV**. The EV travels through normal automated lanes. [3] One of the purposes of AHS design is to increase traffic capacity while using less roadway space. The rationale arises from the assumption that space used for a shoulder could be utilized for a highway lane instead. This is the case with at least one expressway in California (San Tomas in Santa Clara County), where the shoulder serves as an extra lane depending on traffic demand.
3. **All vehicles on the AHS are fully automated.** There is no mixture of automated and manually driven vehicles on the highway. Mixed traffic has been shown to change the characteristics of traffic flow, specifically leading to faster propagation of shock waves (See (Bose and Ioannou, 1999).) and is an area of current flow research. With mixed traffic, cooperation between vehicles to move out of way of an EV is no longer guaranteed; the efficiency of maneuvers developed under mixed traffic conditions is lower compared to those developed for fully automated highways. This thesis restricts itself to considering only fully automated highways with vehicles assumed capable of satisfying a nominal set of requirements (acceleration, braking, etc) for normal mode

[3] The assumption that AHS does not have shoulders is a design specification of this project. See PATH project MOU311.

function.

1.1 PATH AHS Architecture

As a framework for AHS control systems, this thesis uses the hierarchical control system architecture proposed in (Varaiya and Shladover, 1991), (Varaiya, 1993), (Horowitz, 1997) that partitions the design of the AHS into five layers: network, link, coordination, regulation, and physical. This section describes the hierarchical control architecture in detail. The work contained in this thesis is specifically directed to the link and coordination layers, which are intermediate AHS levels. When considering the technology that would be necessary to implement a fully functional AHS, one needs to look at design specifications needed for each control layer.

The hierarchical organization of the AHS architecture lends itself to the development of non-automated technologies because each control problem is designed separately. For example, regulation layer control laws to steer vehicles and aid them in maintaining safe headway distances can be implemented in individual vehicles, without using the remaining AHS infrastructure for adaptive cruise control. At the highest level of the control architecture, the network layer, research on traffic network optimization is highly related to origin-destination research on manual traffic and can be used to provide information signs to human drivers. The problem of EV transit on AHS reveals what type of coordinated control is needed to promote a faster moving vehicle in traffic flow and how to minimize an EV's impact on the overall traffic flow.

The control laws and coordinated maneuvers presented in this thesis address the fol-

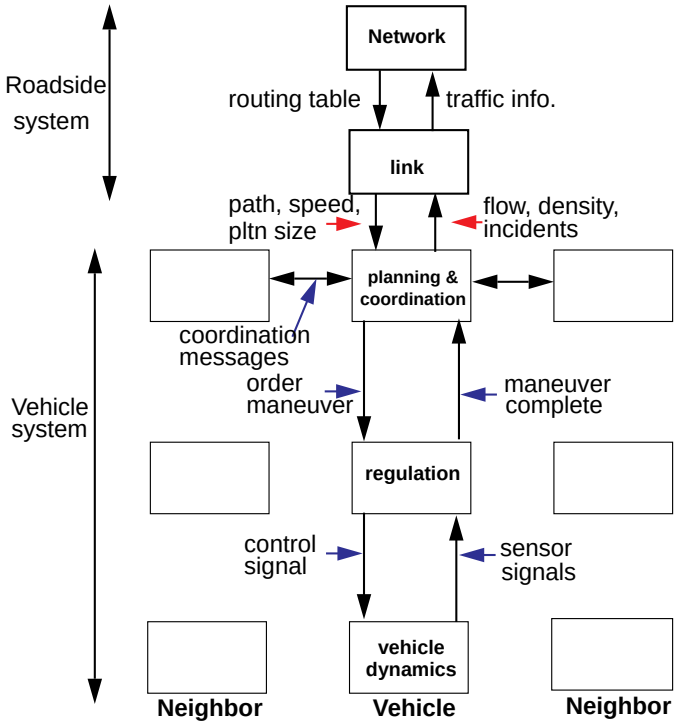

Figure 1.1: PATH hierarchical control architecture

lowing main design objective: *to ensure safe and rapid EV transit within the AHS with minimal impact to the transit of other vehicles.* The EV travels to an incident either inside or outside the AHS at speeds higher than that of normal vehicles. Traffic flow conditions are nominal (free-flowing). For AHS coordination layer maneuvers that have been developed to promote EV transit through stopped traffic see Section 1.4.

In the AHS control architecture proposed in (Varaiya and Shladover, 1991) and (Varaiya, 1993), traffic is organized into platoons of closely spaced vehicles. The use of this strategy has the objective of increasing highway capacity and safety. Platoons have large interplatoon distances (i.e., 30m) and small intraplatoon spacings (i.e., 2m). The first vehicle of a platoon is called the leader, while all other vehicles in the platoon are called followers;

a single vehicle by itself in a platoon is known as a free-agent. To achieve the coordinated acceleration/deceleration needed to maintain the small intraplatoon spacings, each platoon member maintains high speed communications with the leader and preceding vehicle. Direct sensor measurements suffice to provide information about the preceding vehicle's speed/acceleration, but for string stability, the leader's acceleration is provided only through communication.

The design of the AHS architecture shown in Fig. 1.1 consists of five hierarchical layers: network, link, coordination, regulation and physical (see (Varaiya and Shladover, 1991), (Varaiya, 1993)). The first two layers are roadside control systems, and the latter three reside on each vehicle. Each control layer presents a reference model to its adjacent hierarchical layers. We describe each hierarchical layer below.

One network layer controller exists for the entire automated highway network. It is responsible for assigning a specific route to the vehicles based on destination. The network layer controller minimizes the travel time of vehicles by suggesting optimal vehicle routes. Control is exerted by specifying activities at highway junctions to the link layer controller. Little research has been performed for the AHS network layer to date.

An AHS network is divided into links, or sections, that can vary from hundreds of meters to a few kilometers. A single link layer controller controls several links. The link layer controller does not identify individual vehicles, but rather specifies velocities, platoon size, and proportions of activities for a particular vehicle destination or type on each link. Activities may include lane changing, joining a platoon, or splitting from a platoon. Roadside monitors provide density information for the different types of vehicles on each link.

These density monitors are not so much sensors as counters with communication devices that query passing cars for information. Control commands from the link layer are passed to the coordination layer (see (Horowitz, 1997), (Rao and Varaiya, 1993), (Alvarez et al., 1996)). Each vehicle in a link attempts to adjust its activities to match the transmitted commands; whether commands are executed is dependent on the vehicle's current state and environment. For example, a vehicle may not be able to achieve the link layer velocity control law because of a slower moving vehicle in front, or it may exceed the link layer velocity while involved in a maneuver, such as a join. Because capacity constraints on the AHS are guaranteed in the choice of link layer control laws, the real AHS vehicle velocity and proportions of vehicles changing lane agree on average with the commands transmitted from the link layer controller. Previous relevant research for the link layer controller is described in detail in Section 1.3.

The coordination layer determines which maneuvers to perform, manages inter-vehicle communications, and coordinates the actions of the vehicle with neighboring cars. Each coordination layer maneuver is described by a discrete event system. This mathematical system of inputs and outputs can be modeled by sets of finite state machines as in (Eskafi, 1996). The choice of maneuvers and when to execute them depend on safety, the vehicle's route, commands from the link layer, and local traffic conditions as in (Eskafi et al., 1995), (Godbole et al., 1995), (Horowitz, 1997) and (Li et al., 1997a). The vehicle speed transmitted by the link layer to the coordination layer is passed directly to the regulation layer controllers and is not directly utilized by the coordination layer. The proportion of activities broadcasted to each vehicle's coordination layer determines a probability for ma-

neuver initiation (e.g., merge, split, change lane). At present, each vehicle's probability of maneuver execution is independent of its local state. Future work by (Bana, 2000) will provide a state dependent methodology for choosing maneuvers based on the configuration of neighboring platoons.

The regulation layer receives commands from the coordination layer and executes the chosen maneuvers. It is essentially a set of continuous-time, feedback-based controllers. The design of safe regulation layer laws focuses primarily on safety. Several works such as (Carbaugh et al., 1997), (Li et al., 1997a), (Alvarez and Horowitz, 1999) have been devoted to the design of safe trajectories for AHS maneuvers such as joining and splitting a platoon. (Swaroop, 1994) describes string stability requirements for longitudinal vehicle control laws; to achieve vehicle headway error attenuation, a platoon follower must have knowledge of the preceding vehicle's state as well as that of the platoon leader's speed. A platoon leader's desired speed is chosen as

$$v_{desired} = min(v_{link}, v_{safe}) \tag{1.1}$$

where v_{link} is the transmitted link layer speed, and v_{safe} is the speed determined to maintain regulation layer safety. The recent work of (Mahal, 2000) demonstrates that communication delays have significant effect on string stability. This is an example of an instance where the design of specific control law may need to take into account the behavior of lower level functions.

The lowest hierarchical level is the physical layer, which pertains to the vehicle's actuators and sensors. It receives steering, throttle, and brake actuator commands from the regulation layer and returns information such as vehicle speed, acceleration, and engine

state. Hardware selection, signal processing and communication schemes are key design issues for the physical layer.

For safety reasons, vehicle control is exerted with the lower hierarchical level commands taking greater priority over ones from higher levels. Conversely, optimization of overall traffic flow is exerted from the top down. Commands from the roadside link layer controller, such as proportions of vehicles changing lane, are transmitted to each vehicle's on-board coordination layer. The coordination layer controller then interprets the control command without violating the safety conditions imposed at the lower hierarchical levels. For example, a change lane maneuver will not be successful if the vehicles in the destination lane are unable to guarantee safe space.

The purpose of the PATH hierarchical architecture is to partition a complex control problem into several smaller problems which can be separately designed. In order to promote high priority transit for EVs, it is necessary to develop control laws for more than one hierarchical layer. Considering the design requirements for EVs discussed previously, it was determined that the standard set of degraded mode regulation layer control laws would be sufficient for this purpose. However, specific control laws and maneuvers for the link and coordination layers are needed in conjunction with one another to promote high priority EV transit on AHS.

1.2 Traffic Flow Modeling

In order to describe the time evolution of traffic flow, one has to define the basic quantities of traffic flow and density. A stationary observer at location x is able to count the

number of vehicles, N, that pass by in a measurement time interval, τ. The time interval should be sufficiently long for vehicles to cross. Flow rate, Q, is given by

$$Q = \frac{N}{\tau}. \tag{1.2}$$

For a length of highway, dx, the density of vehicles, K, on this portion of road is given by

$$K = \frac{\sum t}{\tau dx} \tag{1.3}$$

where $\sum t$ is the total travel time for vehicles crossing dx. The length of highway chosen for measurement, dx, should be sufficiently large for K to be meaningful. Vehicle density can also be expressed as the difference in vehicle counts between spaced observers.

$$K = \frac{\Delta N}{dx}. \tag{1.4}$$

One treatment of K is to define a specific length over which to measure ΔN centered at x; however, this leads to a discontinuous function. An alternative, which is assumed in this thesis, is to define a "smooth" function N for vehicle density as shown in Fig. 1.2. (see (Daganzo, 1997)). (Lighthill and Whitham, 1955) and (Richards, 1956) were the first to model traffic flow as a continuum utilizing the notions of vehicle density and flow (known as LWR theory). Conservation of vehicles imposes the following constraint on the traffic flow model:

$$\frac{\partial K(t,x)}{\partial t} + \frac{\partial Q(t,x)}{\partial x} = 0. \tag{1.5}$$

The problem is identical to that of one dimensional fluid flow or string theory. In addition to the conservation law of Eq. (1.5), LWR theory postulates that the flow $Q(t,x)$ is a function

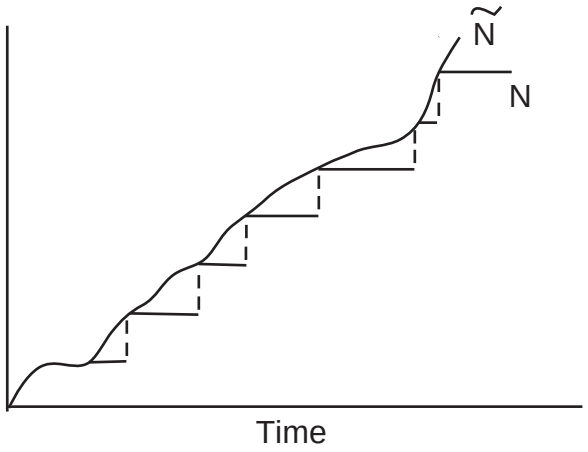

Figure 1.2: Cumulative vehicle count versus time. The function is "smoothed" for a continuous approximation.

of the vehicle density $K(t, x)$. Experimental results provided by (Lighthill and Whitham, 1955) support this hypothesis. Another useful definition is that of mean traffic speed:

$$V = \frac{Q}{K}. \tag{1.6}$$

Here, V is an average vehicle speed weighted by the time each vehicle spends on the length of interest.

In order to use the traffic flow continuum model to investigate shocks and stability, researchers attempted to develop higher order models. One class of manual traffic flow models, known as microscopic models, extends asumptions about individual vehicle behavior to predict the macroscopic behavior of traffic flow under varying traffic density. (Payne, 1971) presented a well-known car following model, in which each vehicle's behavior is determined by that of the preceding vehicle. By considering reaction times and inverting vehicle density to obtain spacing information, (Payne, 1971) determined a dynamic equation for

the traffic flow speed:

$$\frac{dV}{dt} = -\frac{1}{T}\left(V - V_e(K) - \frac{V_e'(K)}{2K}K_x\right), \tag{1.7}$$

here $V_e(K)$ is the steady-state speed-density relationship, which can be chosen to describe a particular microscopic behavior. Eq. (1.7) together with the conservation equation produces a second order model which attempts to predict the behavior of manual traffic flow. (Payne, 1971) also discretized this model for simulation purposes. The discrete traffic flow model of (Payne, 1971) was refined by (Cremer and Papageorgiou, 1981) to include relaxation, convection and density gradient terms. (Cremer and Papageorgiou, 1981) utilized nonlinear programming to solve for the optimal traffic model parameters using experimental data from a section of autobahn between Frankfurt and Basel. Validation of the optimal parameters using different data showed improvement relative to the authors' nominal model parameters. (Papageorgiou et al., 1990) took one step further and performed both discrete model parameter optimization and real-time traffic control based on the generated model. Linear quadratic optimal control was utilized to regulate on-ramp flow for the Boulevard Peripherique in Paris. None of the models discussed in this paragraph attempt to describe the effects of lane changing, which is done in this thesis. To describe manual traffic flow, a relation such as Eq. (1.7) is always needed to relate traffic flow to vehicle density. On an AHS, the influence of vehicle density upon traffic flow is specified by the control law developed in this thesis, so that complete behavior of automated traffic is described without finding model parameters.

The continuum model used in (Li et al., 1997b), (Alvarez et al., 1999) and in this thesis extends the framework of (Lighthill and Whitham, 1955) to include terms that describe

various vehicle activities such as lane changing. This idea has also been investigated by (Holland and Woods, 1995) and (Holland and Woods, 1997), who propose a two lane traffic lane model. (Holland and Woods, 1995) present a two lane traffic flow model:

$$\begin{aligned}(k_1)_t + c_1(k_1)_x &= a(k_2 - k_1),\\ (k_2)_t + c_2(k_2)_x &= a(k_1 - k_2).\end{aligned} \tag{1.8}$$

k_1 and k_2 are the vehicle densities in lanes 1 and 2 respectively. The two wavespeeds, c_1, c_2, are allowed to be different. Both the wavespeeds and the rate of lane change, a, are assumed constant. The fact that the rate of lane changing is represented by a single term, a, signifies that the exchange of vehicles between the two lanes is equal in the two directions (change lane left and change lane right). (Holland and Woods, 1995) find an explicit solution by first rewriting Eq. (1.8) in a frame moving with the average of two wavespeeds and with non-dimensionalized time. The resulting two equations can be then combined into a single Telegraph equation utilizing either the sum or difference of concentrations, which is solved explicitly. The model presented in Chapter 2 differs from that of Eq. (1.8) in two ways: 1) the wavespeeds, c_1 and c_2, are allowed to vary in time and 2) the rate of lane changing is allowed to be inequal in the two directions. (Holland and Woods, 1997) improves on the model of Eq. (1.8) by allowing the rate of lane changing to be inequal:

$$\begin{aligned}(k_1)_t + c_1(k_1)_x &= a(k_2 - \lambda k_1),\\ (k_2)_t + c_2(k_2)_x &= a(\lambda k_1 - k_2).\end{aligned} \tag{1.9}$$

The notation here is identical to that of Eq. (1.8). The additional term, λ, allows the rate of vehicles leaving lane 1, $a\lambda$, to differ from the rate of vehicles leaving lane 2, a. Using the

same techniques as in (Holland and Woods, 1995), (Holland and Woods, 1997) also obtain a general solution and illustrate the results using a sinusoidal traffic flow input to a lane moving slower than its neighbor. Asymptotically, a single pulse of traffic flow which enters the highway is Gaussian shaped. The modeling framework is also extended by (Holland and Woods, 1997) to three lane traffic flow to obtain a mean speed and distribution width for the asymptotic behavior. Lastly the authors consider wavespeeds that vary linearly with concentration to obtain a more complex two-lane model. The model presented in Chapter 2 allows wavespeeds to vary in a more general manner than in (Holland and Woods, 1997).

1.3 Link Layer

The link layer controller is comprised of two subsystems: feedforward and stabilizing controllers (see Fig. 1.3). The feedforward controller uses traffic demand information (inlet, outlet and junction condition) to design desired highway flow trajectories. The desired properties of the highway flow, which is specified by vehicle density, traffic speed and activity proportions, does not necessarily match the actual highway conditions. The stabilizing controller determines **speed and activity commands** to transmit to AHS vehicles such that the actual highway flow properties converges to those of the desired highway flow.

For the feedforward link layer controller, (Gomes et al., 2000) has approached the design of desired highway flow trajectories as a linear optimization problem. The overall highway flow is maximized subject to fairness constraints, and minimization of lane changing and travel time. For EV transit, overall optimization of the AHS flow has second priority compared to the circulation of vehicles around a faster moving police car or ambulance.

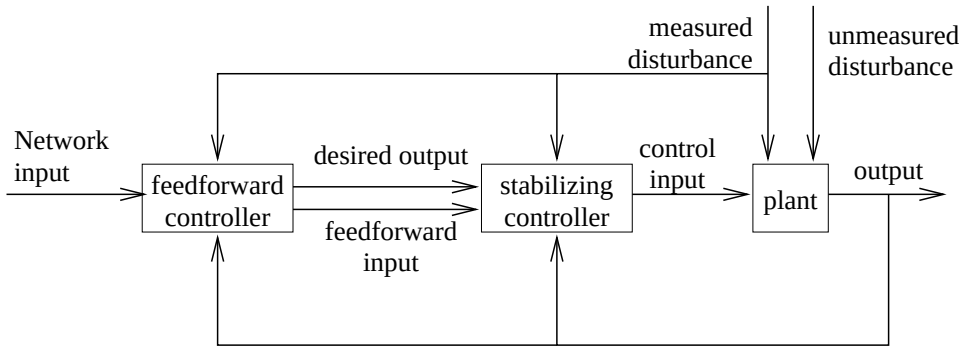

Figure 1.3: Link layer controller is comprised of feedforward and feedback portions.

Any traffic flow optimal feedforward control would be turned off in a vicinity of the EV, but it will be shown in the next chapter how the design of desired traffic flow profiles can be used for high priority EV transit.

Previous research for the link layer stabilizing controller can be found in (Li et al., 1997b) and (Alvarez et al., 1999). Two stabilizing traffic flow controllers capable of handling time varying desired lane change commands and stationary desired velocity profiles were developed. (Li et al., 1997b) utilized a coordinate transformation to convert vehicle density into a variable which better reflects the influence of velocity fields upon lane change activity. The coordinate transformation is independent of the highway vehicle density and can be calculated a-priori. The desired lane change proportions are, however, restricted to be non-time varying. In (Alvarez et al., 1999), a simpler controller is used to demonstrate the circulation of traffic around a fixed section of highway. Lane change commands were used to achieve a local stationary region of low vehicle density; the desired lane change proportions for the presented example are non-time varying. This controller differs from that of (Li et al., 1997b) in that 1) the controller does not utilize an a-priori calculated coordinate

transformation and 2) the lane change proportions can be time varying.

In the next chapter, two different maneuvers; *Bubble* and *Volcano*, are presented. The *Bubble* maneuver utilizes a new EV specific feedforward control law and the controller of (Alvarez et al., 1999) to circulate traffic around the faster moving EV. The *Volcano* maneuver utilizes new EV specific feedforward and stabilizing control laws to achieve the same goal but in higher density traffic. The feedforward design uses a steady moving velocity profile to achieve compression and decompression of highway traffic in a neighborhood of the EV. The stabilizing controllers of (Alvarez et al., 1999) and (Li et al., 1997b) are modified to produce two controllers which can accomodate steady moving velocity profiles.

1.4 EV Specific Coordination Control Laws

In (Leung, 1994), several coordination layer maneuvers are presented for high priority EV operation on AHS. The *Vortex* maneuver, which is used to move a faster moving police car or ambulance through free flowing traffic, is described in detail in Chapter 3 and in (Leung, 1994). Additional maneuvers: the *Zig-Zag* and *Part-and-Go* maneuvers; were developed for moving an EV through stopped AHS traffic to the site of an incident. The *Part-and-Go* maneuver is named for the EV's path through stopped traffic. In the two lane case, platoons in lane 1 are commanded to back up away from the incident and to form a single superlarge platoon. Platoons in lane 2 are directed to move forward towards the incident and to also form a single superlarge platoon. The EV travels in lane 2 and then switches to lane 1 to reach the incident. The size of the superlarge platoons would exceed the maximum allowable under normal conditions. The *Zig-Zag* maneuver is named

for the movement of the EV as it weaves between the two lanes. Each AHS vehicle is serially requested to back up away from the accident, starting with the vehicle in the neighboring lane and immediately downstream of the EV. The EV changes lane into the vacated space, and the cycle repeats itself. While the *Zig-Zag* maneuver requires less initial space to initiate the maneuver, the *Part-and-Go* maneuver facilitates higher EV speeds through platoons of stopped vehicles. Several supporting maneuvers: *Platoon Lane Change, Stationary Forward Join* and *Stationary Backward Join*; are required for the EV specific maneuvers. All maneuver protocols were verified using COSPAN (see (Har'El and Kurshan, 1987)), a software package specifically designed for testing of finite state machines by random activitation of transitions. Using COSPAN, the protocols were shown to be deadlock free. No simulation is included in (Leung, 1994).

In Section 3.1.1 experimental simulation and improvement of the *Vortex* maneuver is described. The original *Vortex* maneuver is modified to produce a new improved *Vortex2* maneuver. Unlike the *Vortex*, the new maneuver returns individual vehicles to their original lanes and relative configuration. The *Vortex2* maneuver protocol is verified, tested and compared to the original *Vortex* maneuver of (Leung, 1994).

1.5 Contributions

The specific technical contributions of this thesis are summarized below:

- **Development of the Bubble Maneuver:** A feedforward link layer controller design is presented for high priority EV transit through low density traffic, which only uses lane change commands.

- **Development of the Volcano Feedforward Link Layer Maneuver:** To accomodate high vehicle density highways, traffic flow speed changes and lane change commands are needed. The traffic flow speed must vary in a specific manner to reestablish flow after the EV has passed. Non-stationary velocity profiles are defined and utilized in the design of a feedforward link layer controller for the high vehicle density case.

- **Development of Stabilizing Controllers for Non-Stationary Velocity Profiles:** Two link layer stabilizing controllers are shown to work with the Volcano maneuver, with comparative performance.

- **Evaluation of the Vortex Maneuver:** The *Vortex* maneuver designed by (Leung, 1994) for the coordination layer is tested using a microscopic vehicle simulator. Drawbacks of the maneuver are discussed.

- **Development of the Vortex2 Maneuver:** A new *Vortex2* maneuver for the coordination layer is developed to address the weaknesses found in the Vortex maneuver. The maneuver is also tested using the miscroscopic vehicle simulator.

Chapter 2 describes the link layer maneuvers: the *Bubble* and *Volcano*, together with the two link layer stabilizing controllers developed for non-stationary velocity profiles. Results for coordination layer maneuvers: *Vortex* and *Vortex2* are covered in Chapter 3. Chapter 4 contains concluding remarks.

Chapter 2

Link Layer Control Laws

The link layer does not seek to control or identify individual AHS vehicles; instead, it seeks to control the overall traffic flow properties of the AHS. To facilitate high priority EV transit, we present mesoscopic traffic maneuvers that move other vehicles out of the EV's section while the EV travels at speeds higher than the nominal traffic. It will be shown that different strategies are needed for low and high vehicle density situations.

2.1 Physical Implementation

Fig. 2.1 depicts the physical implementation of the link layer. The link layer controller is comprised of feedforward and stabilizing controllers. The feedforward link layer controller measures inlet conditions and uses this information to generate a desired traffic profile. The feedforward link layer controller also monitors and compensates for link layer faults, which result in degraded monitor operating conditions for the link (e.g. traffic accident, lane shutdown, presence of an EV). An EV entering the highway informs the feedforward

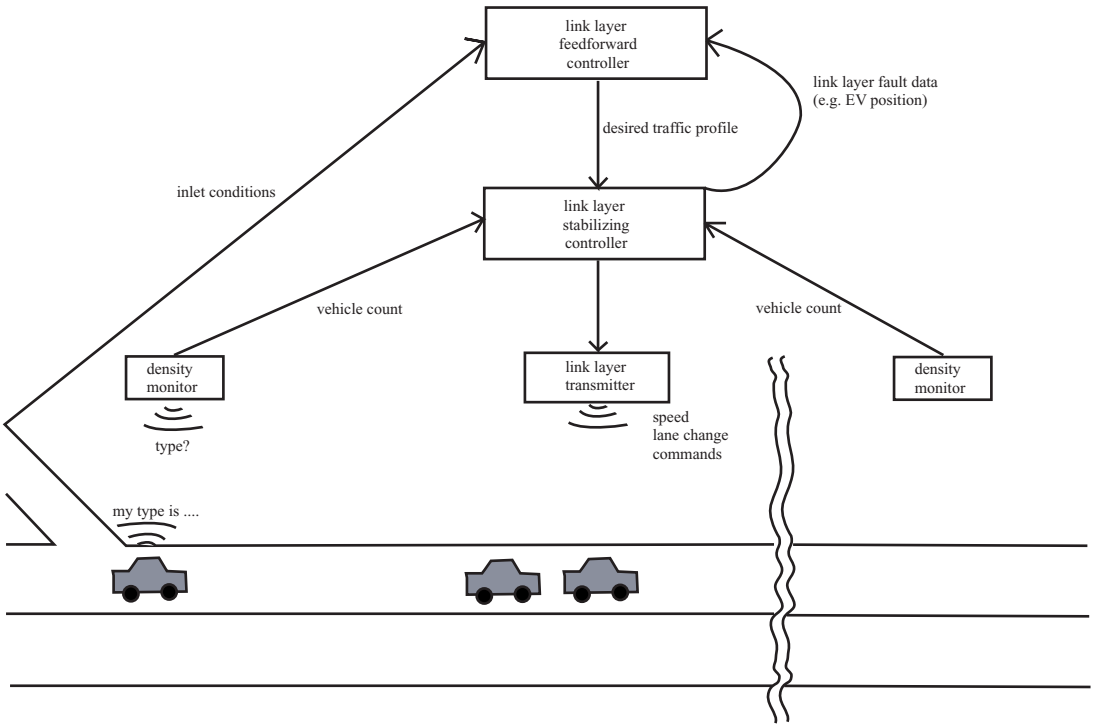

Figure 2.1: Physical hardware components needed for link layer implementation

link layer to change the desired traffic profile to move traffic out of the EV's way. To determine speed and lane change commands to broadcast to AHS vehicles, the stabilizing controller combines the desired traffic profile with vehicle count numbers from dozens of highway density monitors. Each highway density monitor queries passing vehicles about their type/destination and lane number, and counts the number of vehicles entering the section, which can range in length from 0.5 km to a mile in length. As the EV travels within the AHS, its location is passed to the feedforward link layer controller to move vehicles out of the EV's way. In the maneuvers presented in this chapter, the EV is designed to travel from 5 to 10 m/s faster than the nominal traffic speed, which is about 20 m/s.

2.2 Modelling and Notation

Following the ideas of LWR theory, the link layer flow is modeled as a continuum, which is described by a set of partial differential equations based on a conservation of vehicles principle. Vehicle density, K, is expressed in *cars per m* and parameterized by time (t), lane, and lateral highway position (x). Time and spatial dependencies are implicit in the notation except where noted.

- $\mathbf{K}(t,x) = [K_1\ K_2\ \ldots\ K_m]^T$, vector of vehicle densities in lanes 1 through m,
- $\mathbf{V}(t,x) = diag(V_1, V_2, \ldots, V_m)$, diagonal matrix of vehicle velocities in lanes 1 through m,

- $\mathbf{N}(t,x) = \begin{bmatrix} -n_{1,2} & n_{2,1} & & \cdots 0 \\ n_{1,2} & -n_{2,1}-n_{2,3} & n_{3,2} & \cdots 0 \\ 0 & n_{2,3} & -n_{3,2}-n_{3,4} & \cdots 0 \\ & \vdots & & \\ 0 & \cdots & n_{m-1,m} & -n_{m,m-1} \end{bmatrix}$.

  Here $n_{i,j}(t,x)$ is the proportion of vehicles changing lane from lane i to lane j per unit time. These proportions apply only to vehicles at position x and time t.

Physical highway constraints impose certain conditions on the variables involved: $V_i \geq 0$ (vehicles can only travel forward in free-flowing traffic) and $n_{i,j} \geq 0$ for two adjoining generic lanes i and j (the number of vehicles leaving a lane is dependent on the originating rather than destination lane). In this modeling framework, the notation for a multilane highway is introduced, but various vehicle types and destinations are not distinguished (Alvarez et al., 1999). This model is retained for straightforward explanation. Later only two types of vehicles are considered: EVs and non-EVs. The conservation of vehicles principle is expressed as

$$\mathbf{K}_t = -[\mathbf{VK}]_x + \mathbf{NK}. \tag{2.1}$$

Throughout this thesis, subscripts of t and x denote partial derivatives with respect to those variables. Eq. (2.1) is the model used for the actual physical behavior of the AHS.

The goal of the link layer controller is to achieve a desired traffic flow behavior. This desired behavior must also obey a conservation law for vehicles because the desired traffic flow behavior must be physically realizable. The subscript d refers to desired traffic flow behavior. The quantities $\mathbf{K}_d$, $\mathbf{V}_d$, and $\mathbf{N}_d$ are produced by the link layer feedforward control

and passed as inputs to the link layer stabilizing controller:

$$[\mathbf{K}_d]_t = -[\mathbf{V}_d\mathbf{K}_d]_x + \mathbf{N}_d\mathbf{K}_d. \tag{2.2}$$

The design of a link layer traffic flow controller consists of

1. specification of desired traffic flow behavior for the feedforward link layer controller,
2. an appropiate stabilizing feedback control law which asymptotically minimizes an error norm for the difference between the actual and desired traffic flow behavior.

Controller performance is measured by use of the vehicle density error. Define the vehicle density error to be $\widetilde{\mathbf{K}} = \mathbf{K}_d - \mathbf{K}$. Control action is exerted by specification of velocity and change lane commands to vehicles along the highway:

$$\begin{aligned} \mathbf{V} &= \mathbf{V}_d + \mathbf{V}_f, \\ \mathbf{N} &= \mathbf{N}_d + \mathbf{N}_f. \end{aligned} \tag{2.3}$$

$\mathbf{V}_f$ and $\mathbf{N}_f$ are feedback terms for speed and lane changing respectively. They are determined by the link layer stabilizing controller and will be discussed in more detail later on. The error dynamics of the traffic density flow are

$$\widetilde{\mathbf{K}}_t = -\left[\mathbf{V}_d\widetilde{\mathbf{K}} - \mathbf{V}_f\ \mathbf{K}\right]_x + \mathbf{N}_d\widetilde{\mathbf{K}} - \mathbf{N}_f\mathbf{K}. \tag{2.4}$$

2.3 Low Capacity Highways - The Bubble Maneuver

Vehicles in front of the EV must move of the way in order for the faster moving police car or ambulance to pass. At any given moment, the highway section which has the EV

inside should be devoid of vehicles. Due to vehicle conservation, all the vehicles in the EV's lane must be moved to an adjacent lane. Whether or not the transfer of vehicles to the adjacent lane can be achieved is governed by capacity constraints. This section discusses the feedforward control law that can be used for high priority EV transit only on uncrowded highways and illustrates the maneuver's dependence upon vehicle density.

To ensure that EVs have high priority AHS transit, two design specifications for the link layer are required. First, EV type vehicles should have higher specified velocities than other AHS vehicles. Second, a region of low vehicle density around the EV is desirable from a safety standpoint. Because of its resemblance to a bubble in a fluid, this region of low vehicle density is referred to as a bubble in the thesis. Without the bubble, the EV is unable to travel faster than the rest of the traffic because of interference with downstream vehicles.

2.3.1 Control Law

In the modeling framework used, one can distinguish between vehicles with different destinations and lanes. (Alvarez et al., 1996) introduces a link layer stabilizing controller that is used to produce a stationary vehicle density hole:

$$\mathbf{V}_f = \gamma(t,x)\, diag\left\{\left[\mathbf{V}_{des}(x)\,\widetilde{\mathbf{K}}\right]_x\right\}. \tag{2.5}$$

$\gamma(t,x)$ is a positive control gain parameter which is user selected. Its magnitude affects the velocity controller's responsiveness to density error. For stability, no control is exerted at the boundaries of the controller's domain, $x \in [0, L]$, so that $\gamma(t,0) = \gamma(t,L) = 0$. Recall

that the vehicle density error is defined as $\widetilde{\mathbf{K}} = \mathbf{K}_{des} - \mathbf{K}$. The elements of $\mathbf{N}_f$ have the same sign convention as $\mathbf{N}$ and are defined to be zero except for the following case. Let $i, j, i \neq j$ be subscripts denoting lanes 1 and 2. The following applies to the elements of $\mathbf{N}_f$:

$$n_{f,i,j} = max\left(0, \zeta\ (t,x)\left[\widetilde{K}_i V_{d,i}(x) - \widetilde{K}_j V_{d,j}(x)\right]\right). \tag{2.6}$$

$\zeta\ (t,x)$ is an adjustable positive gain parameter, which can be selected to control the rapidness of the lane change feedback response. As with the velocity feedback, no lane change control may be imposed at the controller boundaries $x \in [0, L]$ so that $\zeta(t,0) = \zeta(t,L) = 0$. The controller allows for convergence of actual traffic flow conditions to desired quantities specified by the link layer feedforward controller. The design of velocity control $\mathbf{V}$ requires specification of desired velocity profile $\mathbf{V}_d(x)$. Likewise, the lane change control $\mathbf{N}$ assumes the existence of a defined desired lane change activity profile $\mathbf{N}_d$.

In (Alvarez et al., 1996) the expressions for the feedback terms $\mathbf{V}_f$ and $\mathbf{N}_f$ in Eq. 2.5 are shown to guarantee convergence of the link layer controller. (Alvarez et al., 1996) assume that the desired traffic velocity profile $\mathbf{V}_d(x)$ is time independent. It is important to note that while the desired velocity field can not vary in time, the desired lane change profile, on the other hand, may be specified as a function of time. The design of the *Bubble* maneuver exploits this property. The link layer stabilizing controller of (Li et al., 1997b) assumes that the desired lane change profile and velocity profile are both time independent. Consequently, their controller of (Li et al., 1997b) can not be used for the *Bubble* maneuver.

Creation of the *Bubble* maneuver is achieved by specifying a time varying $\mathbf{N}_d\ (t,x)$. EVs need to be assigned a specific type and destination. Assume that the EV travels in lane 2, and let the EV be located at highway coordinate x_e. A rate of lane change can be specified

such that vehicles other than the EV in lane 2 are removed and placed in lane 1 to make way for the EV. Moreover, the excess of cars in lane 1 are returned to lane 2 after the faster moving EV has passed. To achieve this *bubble* profile, the desired rates of lane change obey

$$\begin{aligned} n_{d,2,1}(t, x_e) &> 0 \quad \text{all non-EVs}, \\ n_{d,2,1}(t, x_e) &= 0 \quad \text{EV}, \\ n_{d,1,2}(t, x_e) &= 0 \quad \text{all non-EVs}, \\ n_{d,1,2}(t, x_e) &> 0 \quad \text{EV}, \end{aligned}$$

where x_e is the location of the EV at time t. These restrictions on the rates of lane change force the EV to occupy lane 2.

2.3.2 Simulation Results and Discussion

Simulation results are obtained using SmartCap (Broucke et al., 1996), a mesoscopic traffic flow simulation package, of a hypothetical EV circulating on a two lane highway. SmartCap is a C program which evaluates traffic management plans for user-defined highway geometries. A traffic management plan consists of:

- traffic velocities for different sections along the highway,
- spacing required for activities such as cruising or lane change,
- permitted exit flows,
- desired entry flows.

SmartCap integrates the specified traffic management plan starting at the highway exits and proceding upstream. Entrance flows are automatically adjusted so that the user-defined

highway spacing policy is not violated. SmartCap discretizes the highway into sections. Within a section, one or more lanes are contained in parallel.

The numerical integration method for SmartCap is derived heuristically and is given by

$$K_b^{a+1} = \left[1 - V_b^a \frac{k}{h}\right] P_b^a K_b^a + V_{b-1}^a \frac{k}{h} P_{b-1}^a K_{b-1}^a. \tag{2.7}$$

The subscripts k and h refer to the time and spatial discretizations, respectively. Superscript a and subscript b refer to the time and space indices, respectively. P refers to the proportion of vehicles remaining in the section after lane changing for the time interval has taken place. The first term represents the proportion of vehicles remaining in the section after one time period, and the second term contributes vehicles entering from the previous section. Note that this equation implies that lateral integration (lane changing) takes place entirely before calculation of the longitudinal flows (due to velocity).

The numerical integration methods of SmartCAP may be improved by considering algorithms based on the conservation equation, Eq. (2.1). For this purpose a Strang splitting method for hyperbolic equations (Strang, 1998; LeVeque, 1997) is suggested. The conservation equation is rewritten as

$$\mathbf{K}_t + \mathbf{V}\mathbf{K}_x = (\mathbf{N} - \mathbf{V}_x)\,\mathbf{K}. \tag{2.8}$$

The Strang splitting method separates the problem by considering the source term separately. The scheme for a single step of the overall problem is

1. Solve $\mathbf{K}_t = (\mathbf{N} - \mathbf{V}_x)\,\mathbf{K}$ for $\Delta t/2$.

2. Solve $\mathbf{K}_t + \mathbf{V}\mathbf{K}_x = 0$ for Δt.

3. Solve $\mathbf{K}_t = (\mathbf{N} - \mathbf{V}_x)\,\mathbf{K}$ for $\Delta t/2$.

The exchange of vehicles due to lane changing is split up in steps 1 and 2, before and after the longitudinal integration respectively. By provision of second order accurate numerical schemes for each of the steps, the composite scheme is second order accurate (Strang, 1998). Combining the three steps using notation similar to that of Eq. (2.7), gives

$$K_b^{a+1} = P_b^a(3)\left[1 - V_b^a\frac{k}{h}\right]P_b^a(1)K_b^a + P_b^a(3)V_{b-1}^a\frac{k}{h}P_{b-1}^a(1)K_{b-1}^a, \tag{2.9}$$

where $P(1)$ and $P(3)$ are the proportions of vehicles remaining after steps 1 and 3, respectively. The two numerical integration schemes, Eqs. (2.7) and (2.9), are similar, but Eq. (2.7) assumes implicitly that the dynamics of lane changing are much faster than the longitudinal movement due to velocity flow. An area of future work for SmartCap would be the implementation of Eq. (2.9) for additional consistency with the partial differential conservation equation.

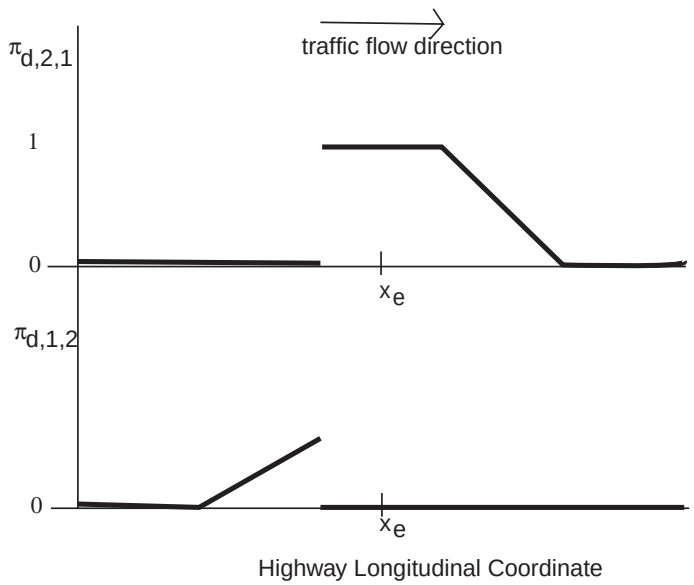

Figure 2.2: Desired change lane proportions versus highway longitudinal coordinate for the *Bubble* maneuver. The profile moves along with the EV keeping the vehicle centered at x_e.

The proportion of vehicles remaining in a section after lane changing, P, and the proportion of vehicles changing lane, π, in a single SmartCap time step are related by

$$\pi = 1 - P. \tag{2.10}$$

The lane change rate, N (lane changes per second), in the continuum description of the traffic flow (Eq. 2.1) is related to the discrete proportion of vehicles changing lane by

$$\pi = Nk \tag{2.11}$$

where k is the SmartCap time step. The desired lane change proportions profile used for the *Bubble* maneuver is shown in Fig. 2.2. The profile moves at the EV's speed so that the the EV is always centered inside the profile.

In the SmartCAP simulations presented in this thesis, all vehicles are assumed independent (i.e. no platoons). All highway sections are $500m$ long, and there are two highway lanes everywhere. We assume a conservative safety policy which imposes constraints on vehicle spacing depending on activity and vehicle speed. For example, a vehicle cruising at $20m/s$ requires approximately $23m$ of headway space. Activities such as changing lane require additional space in both the originating and destination lane. In these simulations, the low density bubble extends over 7 sections of the highway by design of the desired lane change proportions (see figure 2.2).

In the first simulation, all vehicles are cruising at $20m/s$ at a steady flow before the EV enters the highway. We assume capacity conditions so that it is possible at this speed to move all non EVs into a single lane in the EV's section without violating safety conditions. Fig. 2.3 depicts the results. The results are expressed in number of vehicles per section.

In the first plot, the vehicle densities in both lanes are the same. At $t = 800s$, a *static* low density bubble is created around section 10. The creation of the low density bubble is achieved in one sampling period, approximately 15 seconds. After the entry of the EV onto the AHS, all vehicles maintain the cruising speed of $20m/s$. In section 10, the density of non-EVs in lane 2 drops to zero while the density in lane 1 doubles, reflecting movement of all non-EVs into lane 1. The bubble begins to move at $t = 1000s$ with a velocity of $25m/s$, which is the speed of the EV. The EV remains centered in the bubble as they travel together. At $t = 1280s$, the bubble has left the highway, and at $t = 1400s$, traffic conditions are fully recovered. During the EV maneuver, the desired velocity of all non-EVs remains $20m/s$. The low density bubble travels along the highway at a velocity of $25m/s$, allowing the EV inside to travel at faster speeds than the rest of the traffic.

The simulation results indicate that an EV can travel faster than other AHS vehicles under the illustrated circumstances. The size of the low density bubble can be enlarged to allow non-EVs more time to change lane. The opportunity to change lane is dependent upon the availability of space in the destination lane, but can also be provided by acceleration/deceleration of neighboring vehicles which requires time. Increasing vehicle density on the AHS would require the low density bubble to extend over more links. The tradeoff associated with a larger bubble is a longer recovery time for nominal traffic conditions.

The second set of results is obtained for more crowded traffic conditions (Fig. 2.4). Prior to the entry of the EV, all vehicles cruise at a speed of $20m/s$. Under the imposed vehicle spacing policy for safety, the speed of $20m/s$ imposes a maximum of 20 vehicles which can occupy each lane of each $500m$ highway section. For this example, we choose

an initial inlet flow of $1800\frac{vehicles}{hr}$ for each of the two lanes. The resulting vehicle density at $20m/s$ is greater than 10 vehicles per lane and section. Moving all vehicles laterally into a single lane, while maintaining the speed of $20m/s$, exceeds the safety capacity of 20 vehicles per lane in a section. At $t = 800s$, a *static* low density bubble for the EV is created. Immediately, inlet traffic flow must be restricted (see Fig. 2.5) to permit the non-EVs to change lane from lane 2 into lane 1. The velocity of non EVs needs to also be decreased to $10m/s$ so that less spacing is needed for each vehicle (slower moving vehicles require less headway). At $t = 1000s$, the EV enters the highway and travels together with the low vehicle density bubble at a speed of $30m/s$. Traffic conditions are recovered more quickly than in the first simulation. Inlet flow is again unrestricted at $t = 1200s$. The *Bubble* maneuver is capable of accomodating higher inlet flows, but the presence of an EV impacts both the AHS inlets and traffic speeds. Expanding the bubble spatially does not improve the flow or speed requirements. Ultimately, all vehicles in the two lanes must be moved into a single lane in the same section as the EV. As a rule, traffic shocks should be avoided to maintain safety; therefore, the *Bubble* maneuver may not be suitable for high vehicle density scenarios. In the next section, a high capacity maneuver is developed which eliminates a reduction in inlet flows and which localizes the reduction in traffic speed.

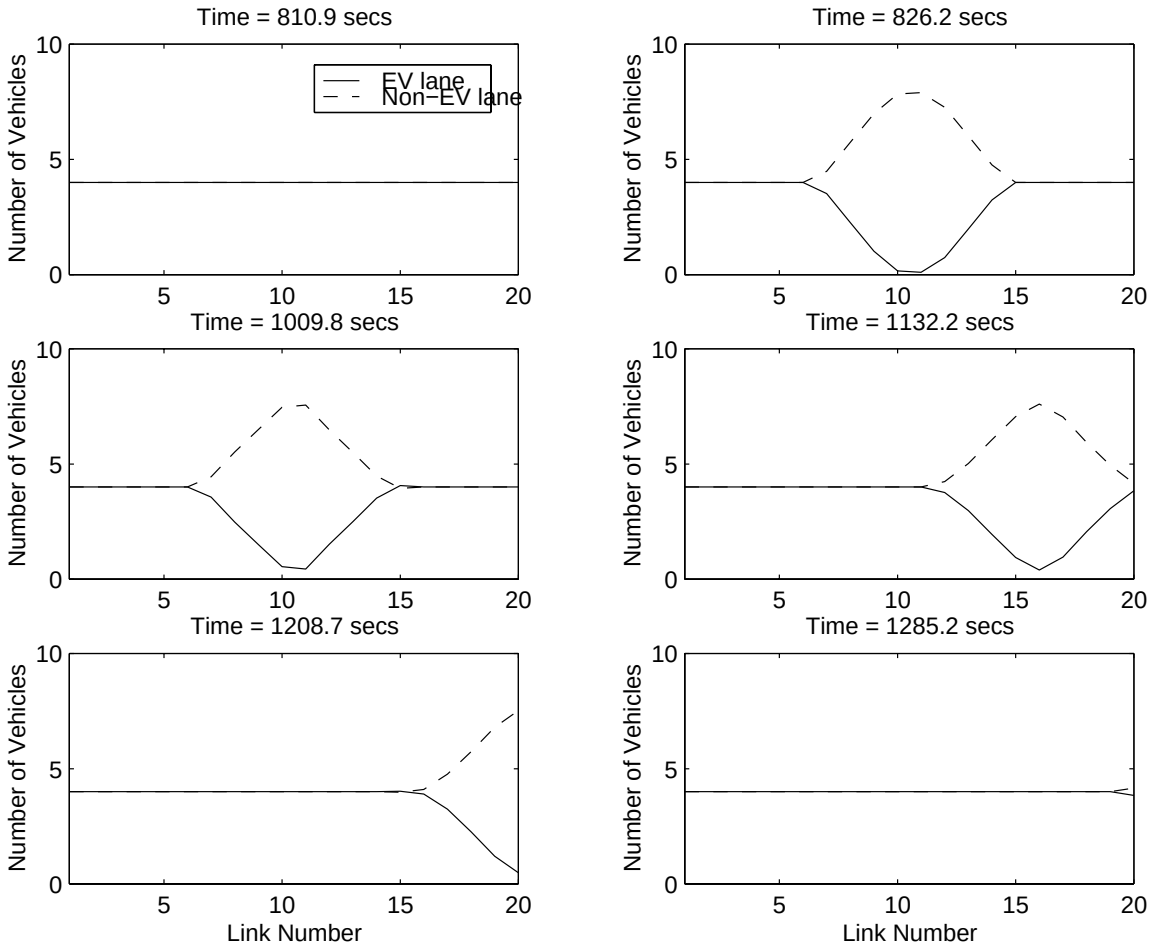

Figure 2.3: Simulation 1 - Vehicle densities for both lanes. The highway is initially unperturbed, and traffic flow is low. When the EV enters the AHS, the link layer controller vacates vehicles from the EV lane. This region of zero vehicles accompanies the EV as it moves along the AHS (to the right).

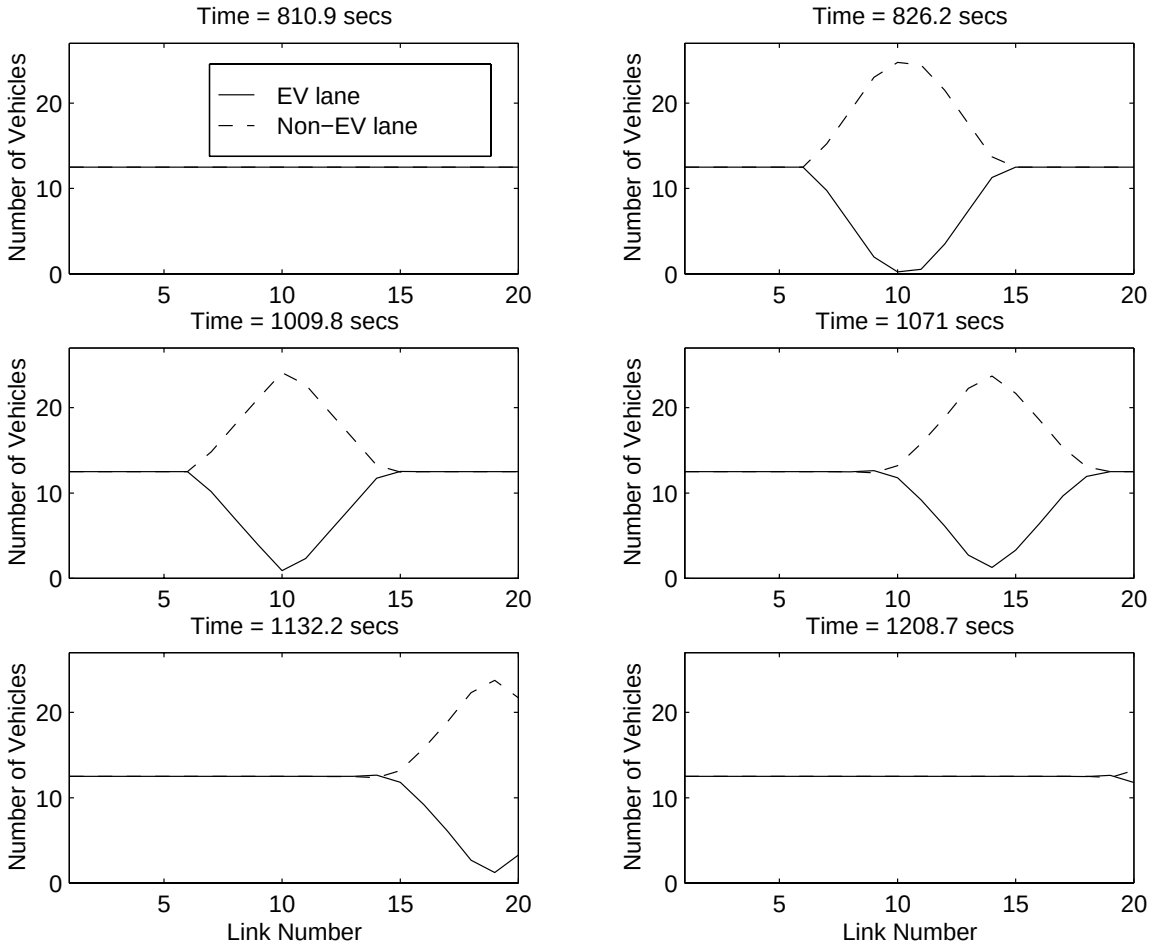

Figure 2.4: Simulation 2 - Vehicle densities for both lanes. Prior to the appearance of the EV, traffic flow is high and uniform in both lanes. When the EV enters the AHS, the link layer controller commands all vehicles in section 10 to change lane out of the EV's lane as seen at $t = 826.2s$. The "bubble" of vehicle density accompanies the EV as the link layer controller always commands vehicles out of the EV's way prior to its arrival.

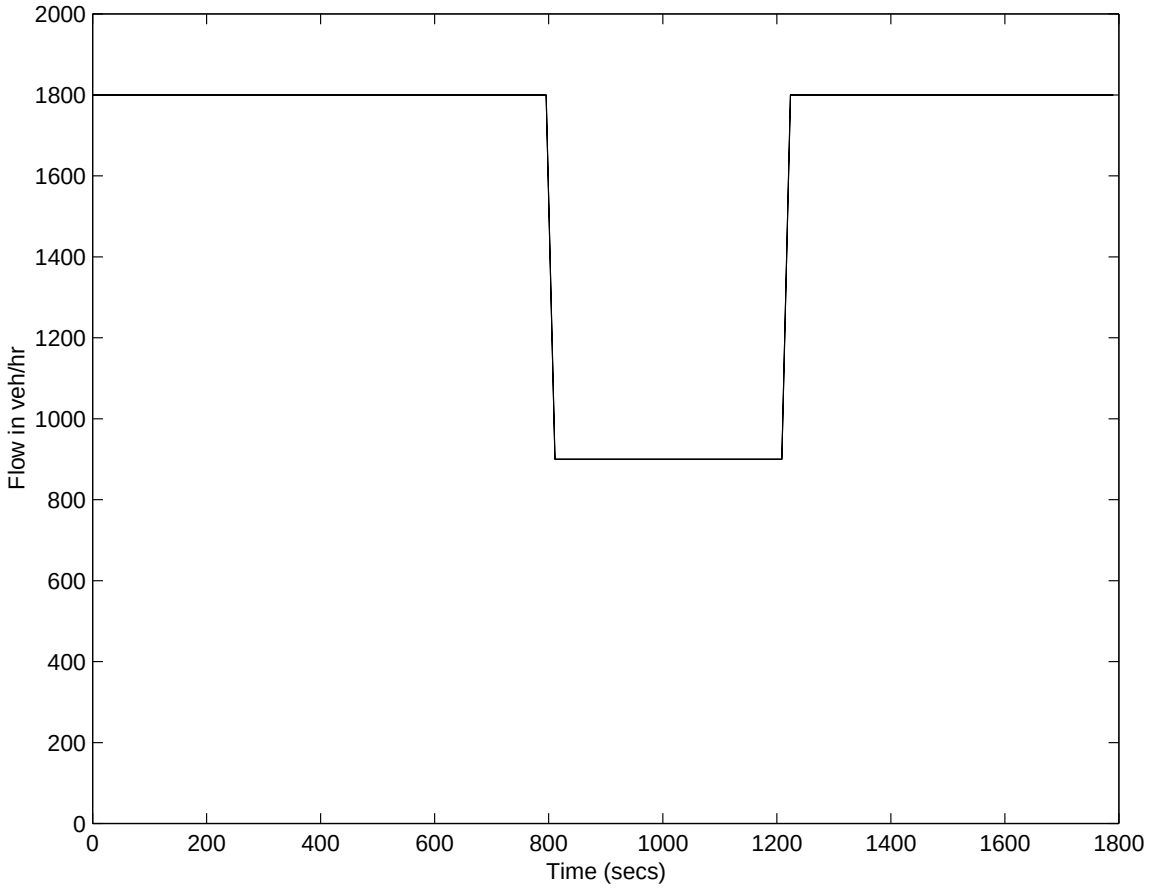

Figure 2.5: Simulation 2 - AHS inlet flow in each lane. This figure illustrates the drop in inlet traffic flow that is needed to push all vehicles of the EV's lane in a particular section. Prior to the EV's entrance, the flow is high but drops to half the nominal value for the entire time that the EV remains on the AHS.

2.4 High Capacity Highways - The Volcano Maneuver

The goal of the work in this section is to design a maneuver similar to the *Bubble* maneuver, which does not restrict inlet flows under high capacity conditions (as defined in the previous section). Non-stationary velocity profiles are found to solve this problem. In addition, a non-stationary velocity profile restricts traffic speed changes to a local neighborhood of the EV.

In this section, the usefulness of non-stationary velocity profiles for high priority emergency vehicle transit on automated highways is explored. Non-stationary velocity profiles are intended for use in designing different link layer feedforward controllers. The notion of a non-stationary velocity profile is defined and its effects on traffic flow are explored. A specific non-stationary velocity profile which can be used to circulate traffic around a faster moving emergency vehicle is introduced. The shape of this profile resembles a volcano, for which the maneuver is named. Because previously developed link layer stabilizing controllers are not capable of dealing with non-stationary velocity profiles, a new type of link layer stabilizing controller had to be developed. This chapter compares two new, distinct link layer stabilizing controllers, which derive from the work of (Li et al., 1997b) and (Alvarez et al., 1999) respectively.

2.4.1 Determination of Desired Traffic Profile

Non-Stationary Velocity Profiles

A non-stationary velocity profile is defined to be a velocity function which moves with a determined speed. Fig. 2.6 shows an example of a non-stationary velocity profile.

The graph depicts the traffic speed versus highway coordinate at a particular snapshot in time. The shape shown in the figure travels along at the highway at specified speed, $w(t)$, which is greater than the traffic flow speed anywhere on the AHS. It does not change as it moves on the highway. This thesis is restricted to non-stationary velocity profiles which are parameterized by a single coordinate s:

$$s = x - \int_0^t w(\varepsilon) d\varepsilon. \tag{2.12}$$

Non-stationary velocity profiles can be utilized to produce circulating regions of low vehicle density. Consider Fig. 2.6 as an example of a possible profile for a single lane. The non-stationary velocity profile has a speed of $w(t)$, and. vehicles in each of the highway sections travel on average more slowly than the profile. Note that the region $[a, b]$ moves with the velocity profile, which retains its shape, at speed $w(t)$. To determine the associated changes in density due to this velocity profile under steady state conditions, the time derivative of the integral $\int_a^b K_d dx$ is evaluated in the region $[a, b]$:

$$\frac{d}{dt} \int_a^b K_d dx = \dot{b} K_d(t, b) - \dot{a} K_d(t, a) + \int_a^b [K_d]_t \, dx. \tag{2.13}$$

Here, steady state conditions refer to a velocity profile which is able to travel for an indefinite time period without the accumulation of vehicle density within the profile. The accumulation of vehicles inside of the profile would result in changes to the profiles's speed and shape (see Appendix A); hence, a steady-state velocity profile retains its traffic flow properties. For a steady-state solution, set the derivative of the left hand side of Eq. (2.13) to zero and utilize the conservation equation for a single lane [1]

$$K_t = -[VK]_x, \tag{2.14}$$

[1] This relation is derived from Eq. (2.1), neglecting any lane changes.

to obtain Eq. refeqeq:drop. This equation relates the densities at locations a and b to each other, after and before encountering the velocity profile, respectively:

$$K_d(t,a) = \frac{\dot{b} - V_d(t,b)}{\dot{a} - V_d(t,a)} K_d(t,b). \tag{2.15}$$

If the velocity profile does not change shape and travels faster than all vehicles at speed $w(t)$, then let $w(t) = \dot{a} = \dot{b} > V_d(t,x)\ \forall x,t$. It can be noted from the velocity profile shape in Fig. 2.6 that $V_d(t,b) > V_d(t,a)$ and, thus, that $K_d(t,a) < K_d(t,b)$ from Eq. (2.15). The non-stationary velocity profile creates a region of low vehicle density which coincides with the dip in velocity in Fig. 2.6. The non-stationary velocity profile in Fig. 2.6 expands and contracts the vehicle density as it moves along the highway.

The traveling region of low vehicle density can also been seen from the perspective of the approximate time-space (TS) diagram in Fig. 2.7 for the velocity profile shown in Fig. 2.6. On the plot of highway distance versus time, the trajectories of many highway vehicles are depicted. Each line represents the path of a single vehicle. At $t = 0s$, vehicles are spaced every $100m$ and travel at $20m/s$, which is the initial slope. The velocity profile travels at $30m/s$. When vehicles encounter the profile, they slow to $10m/s$, which is reflected in the decrease in slope. After exiting the profile, vehicles return to their initial slope/speed of $20m/s$. To observe the effects of the velocity profile, note what happens in the highway section between $7000m$ and $7500m$. At $t = 40s$, there are 6 vehicles in this section of highway (inclusive). During the traffic slowdown at $t = 100s$ to $10m/s$ there are 3 vehicles in the same section. The vehicle density returns to 6 vehicles after the velocity wavelet passes. It can be seen that the non-stationary velocity profile (shown in Fig. 2.6) produces a region of low-vehicle density which travels with the profile.

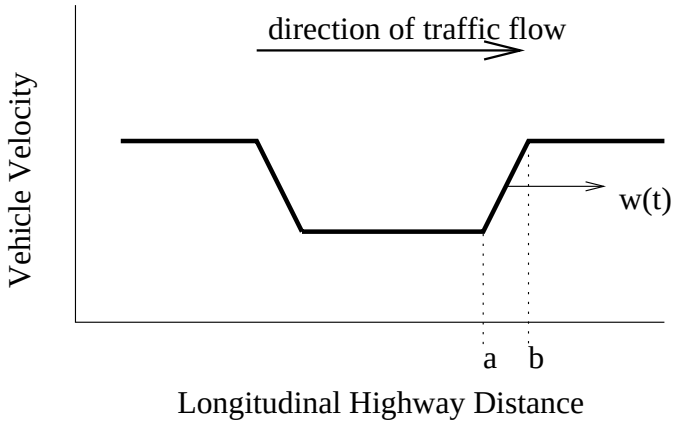

Figure 2.6: One lane non-stationary velocity profile

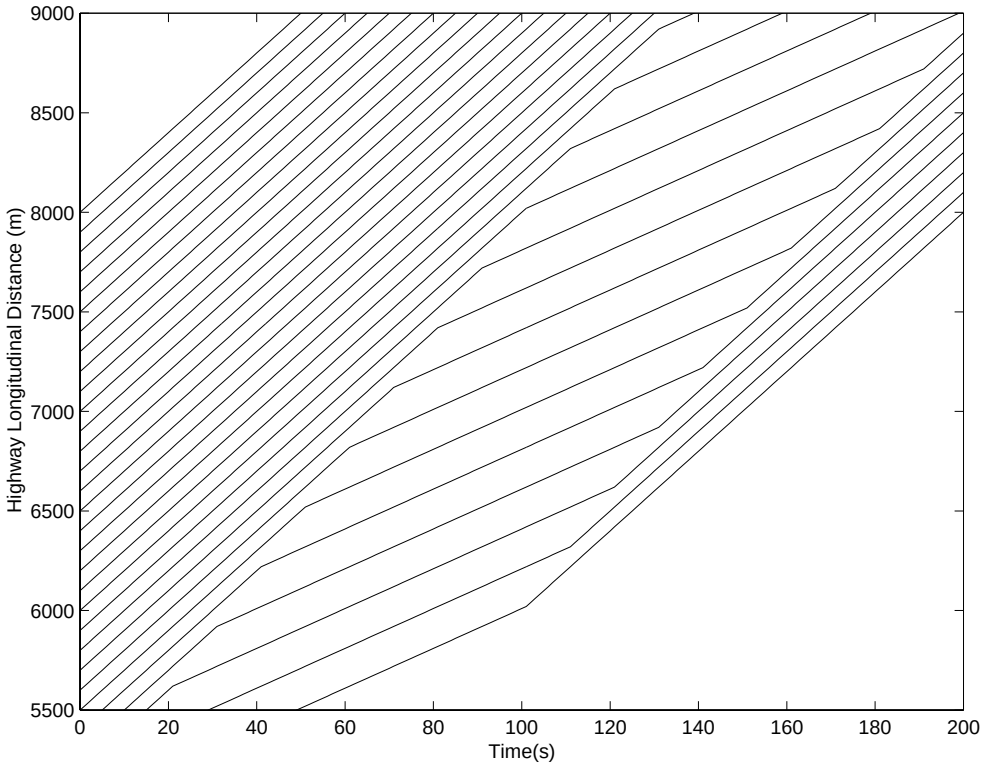

Figure 2.7: Time-space diagram for Fig. 2.6

Regions of low vehicle density can be desirable from a safety standpoint; they allow vehicles inside the regions more opportunity to perform maneuvers such as lane changing under decreased traffic density conditions. Slower moving vehicles require less headway space for safety so that a wider variety of maneuvers are allowable; a vehicle which would otherwise be unable to change lane may be able to do so when there are fewer vehicles nearby. A moving region of low vehicle density, which results from the non-stationary velocity profile, can be used to perform vehicle maneuvers which are otherwise not possible due to capacity and safety constraints.

Depending on shape and traveling speed, velocity profiles can also lead to point accumulations of vehicles and can have a detrimental effect on traffic. Fig. 2.8 illustrates a single lane example of a bad non-stationary velocity profile. The speed of the non-stationary velocity profile, $w(t)$, is equal to the traffic flow speed at certain locations including $x = a$. In this case $w(t) = \dot{a} = \dot{b} = V_d(t, a) > V_d(t, b)$. Eq. (2.15) implies an infinite increase in the vehicle density, $K_d(t, a)$, at highway location $x = a$. Slower moving vehicles in front of $x = a$ are caught up by the rapidly moving velocity profile traveling at $w(t)$. Once a vehicle's position coincides with point a, its velocity becomes the same as that of the velocity profile, $w(t)$; the vehicle is forced to travel with the velocity profile, which accumulates the slower moving vehicles in front of it.

Fig. 2.9 depicts the approximate TS diagram for the velocity profile shown in Fig. 2.8. At $t = 0s$, vehicles are spaced every $100m$ and travel at $20m/s$. The profile travels at $30m/s$. As vehicles encounter the traveling velocity profile from behind, they speed up to $30m/s$, which is shown as an increase in the slope of each trajectory. At the lower boundary of the

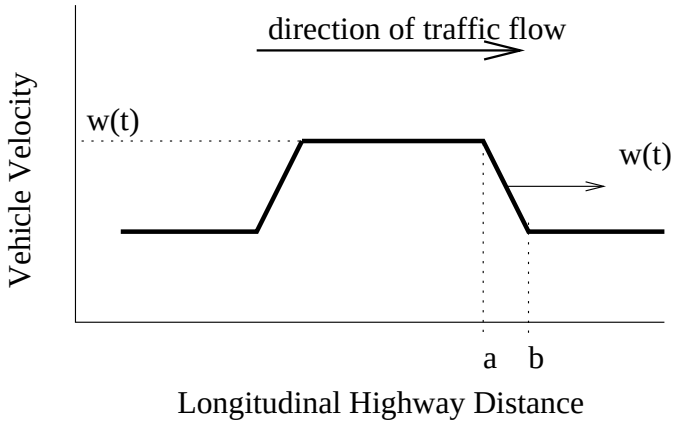

Figure 2.8: One lane non-stationary velocity profile

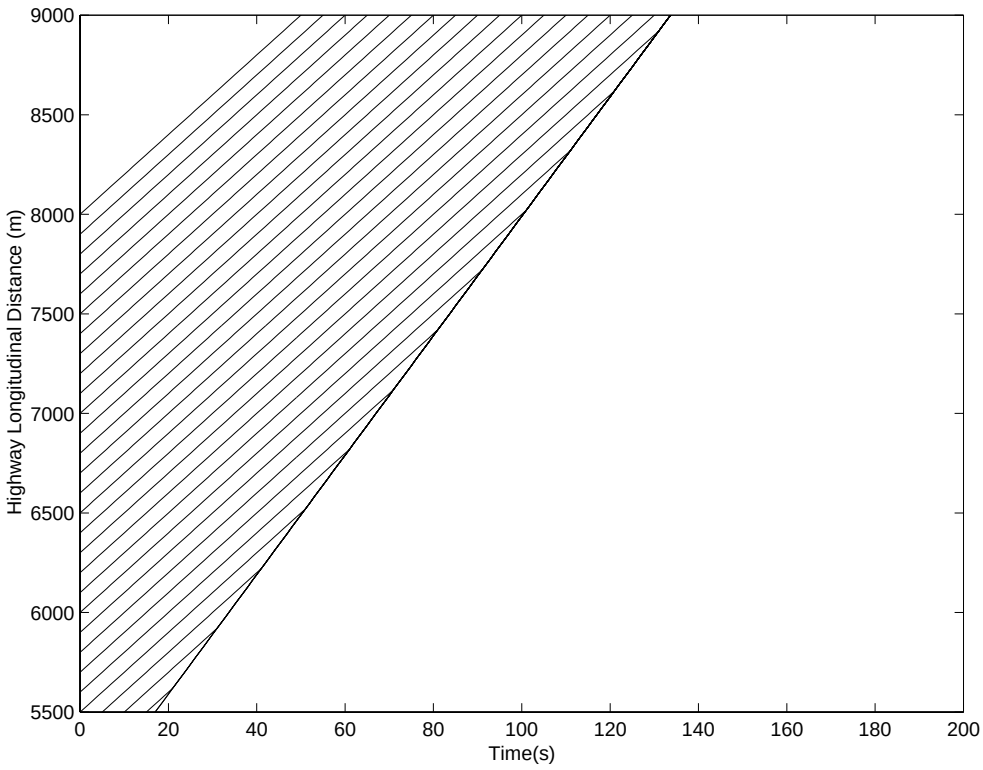

Figure 2.9: Time-space diagram for Fig. 2.8

graph, all the vehicles join together in a single path; this corresponds to an accumulation of vehicle density along this trajectory ($x = a$). This can be thought of as vehicles joining the velocity profile as it moves along the highway and those cars being unable to escape the profile. Because the non-stationary velocity profile overtakes all cars and retains them, the number of vehicles inside the profile increases indefinitely.

If there is more than one highway lane, this accumulation of vehicles can be cancelled by use of lane changes. Lane changes are utilized in front of the point of accumulation $x = a$, to empty the lane of vehicles so that they are not caught up in the shock wave. The vehicles that change lane can return to the original lane after the wave has passed. For safety considerations and spacing requirements, lane changing should not occur between lanes with a large difference in speed.

Fig. 2.10 shows a set of velocity profiles for two lanes which utilize lane changing. The two profiles travel together at speed $w(t)$, which is equal to the maximum speed in lane 1, V_{high}. The overall number of vehicles on the AHS is high, such that vehicles in both lanes cannot be moved into a single lane while maintaining the nominal speed due to safe spacing constraints (see section 2.3.2). As vehicles in both lanes encounter the velocity profile, the vehicles decelerate to V_{low}. The deceleration has the same effect as illustrated in the case shown in Fig. 2.6, i.e. vehicle density decreases in the trough of V_{low} by the proportion given in Eq. (2.15). This region of low speed and low vehicle density can be utilized for lane changing. Because $V_{high} = w(t)$ at $x = x_e$, any vehicles which remain in lane 1 will be caught up in the shock wave if not moved out of the way, as illustrated in Fig. 2.8. The proportion of vehicles that needs to move out of lane 1 and into lane 2 must be determined.

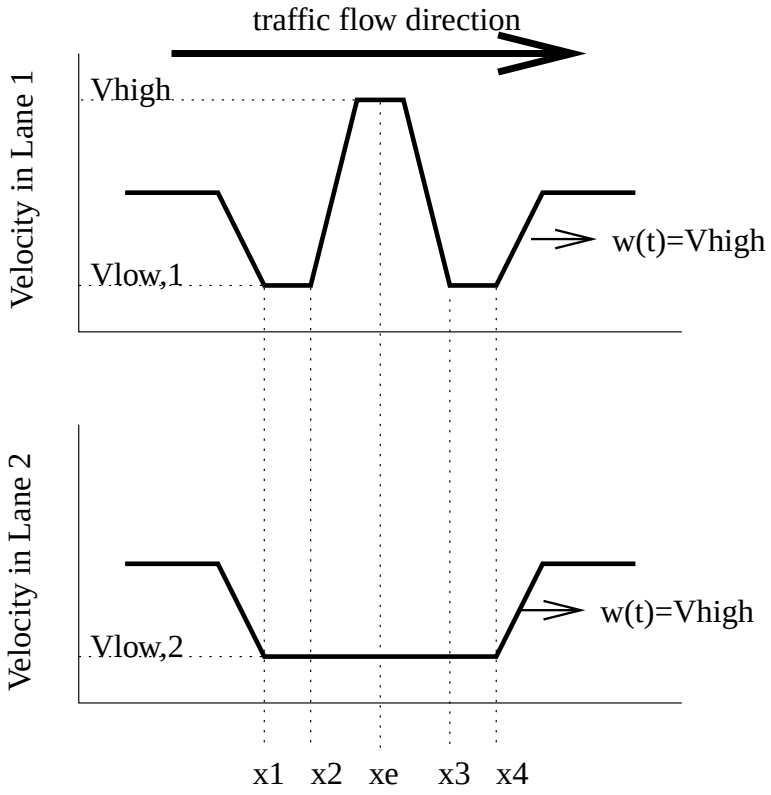

Figure 2.10: Non-stationary velocity profiles for two lanes - used to circulate vehicles out the way of the faster moving EV.

For safety reasons, vehicles are allowed to change lane only in regions where both lanes have the same highway speed. Assume that

$$n_{d,1,2}(t,x) \neq 0 \quad x \in [x_3, x_4], \tag{2.16}$$

$$n_{d,2,1}(t,x) = 0.$$

For the EV to pass, the feedforward link layer controller should attempt to move all vehicles out of the way; i.e. $K_{d,1}(t, x_3) = 0$. To derive an expresion for the lane change proportions,

use Eq. (2.13) together with Eq. (2.2) to obtain

$$\begin{aligned}\frac{d}{dt}\int_{x_3}^{x_4} K_{d,1}dx &= w(t)\left[K_{d,1}(t,x_4) - K_{d,1}(t,x_3)\right] \\ &\quad - \int_{x_3}^{x_4}\left(\left[V_{d,1}K_{d,1}\right]_x + n_{d,1,2}K_{d,1}\right)dx \\ &= \left(w(t) - V_{low,1}\right)K_{d,1}(t,x_4) - \int_{x_3}^{x_4} n_{d,1,2}K_{d,1}dx.\end{aligned} \tag{2.17}$$

To guarantee the removal of vehicles from in front of the EV, the density in lane 1 at x_3 must be set to zero. To determine a steady state solution that does not allow the accumulation of vehicles in $x \in [x_3, x_4]$, set the left hand side of Eq. (2.17) to zero. If it is assumed that the proportion of vehicles changing lane per unit time is constant in this interval, Eq. (2.18) is obtained.

$$n_{d,1,2}(t,x) = \frac{\left[V_{high} - V_{low}\right]K_{d,1}(t,x_4)}{\int_{x_3}^{x_4} K_{d,1}dx}, \quad x \in [x_3, x_4], \tag{2.18}$$

here, $\int_{x_3}^{x_4} K_{d,1}dx$ is the number of vehicles between x_3 and x_4. In the case of no vehicles (as in the denominator of Eq. (2.18)), we can safely set $n_{d,1,2}(t,x) = 0$ for $x \in [x_3, x_4]$.

For $x < x_e$ in Fig. 2.10, lane 1 is void of vehicle density because of the lane changing downstream in the sections $x \in [x_3, x_4]$. To restore the original traffic flow configuration after the EV has passed, we derive a similar expression for lane 2 for $x \in [x_1, x_2]$ to describe the return of vehicles to lane 1. We assume the following holds true for the proportions of lane changing:

$$\begin{aligned} &n_{d,2,1}(t,x) \neq 0, \quad x \in [x_1, x_2], \\ &n_{d,1,2}(t,x) = 0. \end{aligned} \tag{2.19}$$

In a similar manner to deriving the lane change proportions for $x \in [x_3, x_4]$, we combine the expression for the density changes associated with the velocity profile, Eq. (2.13), with the conservation equation, Eq. (2.2), to obtain

$$\begin{aligned} \frac{d}{dt}\int_{x_1}^{x_2} K_{d,2}dx &= w(t)\left[K_{d,2}(t,x_2) - K_{d,2}(t,x_1)\right] \\ &\quad - \int_{x_1}^{x_2} \left(\left[V_{d,2}K_{d,2}\right]_x + n_{d,2,1}K_{d,2}\right) dx \\ &= \left(w(t) - V_{low,2}\right)\left[K_{d,2}(t,x_2) - K_{d,2}(t,x_1)\right] - \int_{x_1}^{x_2} n_{d,2,1}K_{d,2}dx. \end{aligned} \tag{2.20}$$

This expression differs from Eq. (2.17) because the number of vehicles to keep in lane 2 after the velocity profile has passed, $K_{d,2}(t,x_1)$, can be chosen; the goal of the maneuver should be to restore the highway conditions before the EV came along. For a steady state solution, set the left hand side of Eq. (2.21) and assume that the proportion of vehicles changing lane $n_{d,2,1}$ is constant in the interval $x \in [x_1, x_2]$ to obtain

$$n_{d,2,1} = \frac{(V_{high} - V_{low})\left[K_{d,2}(t,x_2) - K_{d,2}(t,x_1)\right]}{\int_{x_1}^{x_2} K_{d,2}dx}, \quad x \in [x_1, x_2]. \tag{2.21}$$

The denominator of Eq. (2.21), $\int_{x_1}^{x_2} K_{d,2}dx$, is the number of vehicles in lane 2 in the interval $x \in [x_1, x_2]$. If there are no vehicles in this region, $n_{d,2,1}$ is set to zero because there are no vehicles to control.

Using the velocity profile shown in Fig. 2.10, a vehicle or priority group of vehicles is able to travel along the highway at speed $w(t)$, faster than the rest of the traffic. The velocity profile indicates that if there is high traffic density on the AHS, the vehicles downstream of the EV should decelerate in order to change lane out of the way, which is counter-intuitive. The speed and spatial shape of the velocity profile should be chosen such that the maximum acceleration/deceleration capabilities of vehicles is not violated. For a discussion of the

limitations that physical vehicle capabilites place upon non-stationary velocity profiles, see Appendix A. On a non-automated highway system, this coordinated deceleration and lane changing is difficult to achieve.

Because the desired non-stationary velocity profile involves a time varying velocity function $\mathbf{V}_d$, neither of the link layer stabilizing controllers previously developed by (Li et al., 1997b) and (Alvarez et al., 1999) will work. A new type of stabilizing controller is needed. In the next section, the coordinate transformation properties of the non-stationary velocity profile are explored to produce two link layer stabilizing controllers.

2.4.2 Stabilizing Control

Coordinate Transformation

A non-stationary velocity profile is a velocity function parameterized by a single coordinate s. Assume that the velocity profile travels at velocity $w(t)$ and propose the following coordinate transformation for $(x,t) \rightarrow (s,\tau)$:

$$\begin{aligned} s &= x - \int_0^t w(\varepsilon)d\varepsilon, \\ \tau &= t. \end{aligned} \tag{2.22}$$

The time and partial derivatives transform in the following manner:

$$\begin{bmatrix} \frac{\partial}{\partial x} \\ \frac{\partial}{\partial t} \end{bmatrix} = \begin{bmatrix} 1 & 0 \\ -w(t) & 1 \end{bmatrix} \begin{bmatrix} \frac{\partial}{\partial s} \\ \frac{\partial}{\partial \tau} \end{bmatrix}. \tag{2.23}$$

Under this coordinate transformation, the conservation equation, Eq. (2.1), may be rewritten as:

$$[\mathbb{K}]_\tau = -[\mathbb{V}_{rel}\mathbb{K}]_s + \mathbb{N}\mathbb{K}. \tag{2.24}$$

The subscript s refers to partial derivatives with respect to that variable. $\mathbb{K}(t,s)$ and $\mathbb{N}(t,s)$ are the vehicle density and lane change terms, respectively, after the change of coordinates. The blackboard boldface type refers to matrix quantities in the new coordinate system (t,s). Eq. (2.24) describes vehicle densities in the moving coordinate frame in terms of the relative velocity $\mathbf{V}_{rel} \equiv \mathbf{V} - w(t)\mathbf{I}$. The coordinate transformation removes the desired velocity's time dependence and casts the flow equation into a form similar to the original conservation expression (Eq. (2.1)). The difference here is that the absolute velocity $\mathbf{V}$ is replaced by the speed of traffic flow relative to the non-stationary velocity profile, $\mathbb{V}_{rel}$. The conservation equation for the desired traffic flow behavior, Eq. (2.2), transforms similarly:

$$[\mathbb{K}_d]_\tau = -[\mathbb{V}_{d,rel}\mathbb{K}_d]_s + \mathbb{N}_d\mathbb{K}_d. \tag{2.25}$$

The error dynamics, expressed in the new coordinate system are

$$\left[\widetilde{\mathbb{K}}\right]_\tau = -\left[\mathbb{V}_{d,rel}\widetilde{\mathbb{K}}\right]_s + [\mathbb{V}_f\mathbb{K}]_s + \mathbb{N}_d\widetilde{\mathbb{K}} - \mathbb{N}_f\mathbb{K}, \tag{2.26}$$

where $\mathbb{V}_f$ are $\mathbb{N}_f$ are the velocity and lane change feedback control terms (respectively) produced by the link layer stabilizing controller in the new coordinate frame.

Because the desired velocity profile travels at speed $w(t)$, the desired relative velocity, $\mathbb{V}_{d,rel}(s) \equiv \mathbb{V}_d(t,s) - w(\tau)\mathbb{I}$, is time invariant under the coordinate transformation. It is also assumed that the profile velocity, $w(t)$, travels faster than the average traffic flow speed:

$$w(t) > V_{i,d}(t,s), \qquad \forall t,s,i,$$

and for all lanes $i = 1$ to m. As a result of this assumption, the speed of the traffic flow relative to the non-stationary velocity profile, $\mathbb{V}_{d,rel}(s)$, is negative definite everywhere.

Stabilizing Controller without Matrix Transformation

The objective of the stabilizing link layer controller is to provide velocity and lane change feedback control laws such that the actual highway density distribution, $\mathbf{K}$, converges to the desired behavior, $\mathbf{K}_d$, which is determined by the link layer feedforward controller. The stabilizing link layer controller presented in this section uses a weighted error signal and is based upon the ideas of (Alvarez et al., 1999). No precomputation of a matrix transformation is needed.

Theorem 1 *For smooth traffic flow, assume that the desired vehicle density* $\mathbb{K}_d(t,s)$ *is prescribed to be bounded throughout the highway; i.e.* $|K_{d,i}(t,s)| < M$ *for all lanes* i *and* $\forall(t,s)$ *and that* $\mathbb{V}_{d,rel}(s)$ *is dependent only on* s*. Under these conditions, the stabilizing controller in Eq. (2.27) achieves* L_2 *stability:*

$$\begin{aligned} \mathbb{V}_f(t,s) &= -\alpha(t,s)\, diag\left[\mathbb{V}_{d,rel}\widetilde{\mathbb{K}}\right]_s, \\ n_{i,j,f}(t,s) &= max\left(\zeta_{i,j}(t,s)\left[\widetilde{K}_i V_{d,rel,i} - \widetilde{K}_j V_{d,rel,j}\right], 0\right), \end{aligned} \tag{2.27}$$

with gains: $\alpha(t,s) > 0$ *and* $\zeta_{i,j}(t,s) > 0$*.* $n_{f,i,j}$ *is the proportion of vehicles changing lane out of lane* i *into lane* j*. Here* $x \in [0, L]$ *denotes the link layer controller's domain.*

Proof: In this case, the boundedness of the integral of the density error squared is shown. Using the following Lyapunov candidate,

$$W = -\int_0^L \widetilde{\mathbf{K}}^T \mathbf{V}_{d,rel}\widetilde{\mathbf{K}}dx = -\int_{-\int_0^t w(\tau)d\tau}^{L-\int_0^t w(\tau)d\tau} \widetilde{\mathbb{K}}^T \mathbb{V}_{d,rel}\widetilde{\mathbb{K}}ds, \tag{2.28}$$

the stability properties of the control law will be discussed.

Recall the important assumption that the velocity profile travels with speed $w(t)$. By using the conservation equations in the new coordinate frame, Eqs. (2.24) and (2.25),

together with the control law, Eq. (2.27), the time derivative of W can be written as:

$$\begin{aligned}\dot{W} = w(t)\left[\widetilde{\mathbb{K}}^T\mathbb{V}_{d,rel}\left(\mathbb{V}_{d,rel}+w(t)\mathbb{I}\right)\widetilde{\mathbb{K}}\right]\Big|_{s=-\int_0^t w(\tau)d\tau}^{s=L-\int_0^t w(\tau)d\tau} \\ +2\left[\widetilde{\mathbb{K}}^T\mathbb{V}_{d,rel}\,diag\left(\left[\mathbb{V}_{d,rel}\widetilde{\mathbb{K}}\right]_s\right)\alpha\left(t,s\right)\mathbb{K}\right]\Big|_{s=-\int_0^t w(\tau)d\tau}^{s=L-\int_0^t w(\tau)d\tau} \\ -2\int_{-\int_0^t w(\tau)d\tau}^{L-\int_0^t w(\tau)d\tau}\left[\widetilde{\mathbb{K}}^T\mathbb{V}_{d,rel}\right]_s diag\left(\left[\widetilde{\mathbb{K}}^T\mathbb{V}_{d,rel}\right]_s\right)\alpha\left(t,s\right)\mathbb{K}ds \\ -2\int_{-\int_0^t w(\tau)d\tau}^{L-\int_0^t w(\tau)d\tau}\widetilde{\mathbb{K}}^T\mathbb{V}_{d,rel}\mathbb{N}_d\widetilde{\mathbb{K}}ds+2\int_{-\int_0^t w(\tau)d\tau}^{L-\int_0^t w(\tau)d\tau}\widetilde{\mathbb{K}}^T\mathbb{V}_{d,rel}\mathbb{N}_f\mathbb{K}ds. \quad (2.29)\end{aligned}$$

Under assumptions for the boundary conditions, $\widetilde{\mathbf{K}}(t,x=0)=\widetilde{\mathbf{K}}(t,x=L)=0$ and $\alpha(t,x=0)=\alpha(t,x=L)=0$, the first two terms are zero. The third term is negative definite because $\mathbb{V}_{d,rel}$ is negative definite $\forall s$. The choice of lane change feedback, Eq. (2.27), allows one to set the last term in Eq. (2.29) to be negative definite. Thus, the first three terms and last term of Eq. (2.29) contribute to the controller's stability in a straightforward manner. Consider now the expression inside the integrand of the fourth term of Eq. (2.29) for generic adjoining lanes i and j:

$$-2\widetilde{\mathbb{K}}^T\mathbb{V}_{d,rel}\mathbb{N}_d\widetilde{\mathbb{K}}=2n_{d,i,j}\widetilde{K}_i\left[\widetilde{K}_iV_{d,rel,i}-\widetilde{K}_jV_{d,rel,j}\right]+2n_{d,j,i}\widetilde{K}_j\left[\widetilde{K}_jV_{d,rel,j}-\widetilde{K}_iV_{d,rel,i}\right]. \quad (2.30)$$

For the desired profile, desired lane changes are specified to take place only in one direction; i.e. $n_{d,i,j}>0\Longrightarrow n_{d,j,i}=0$. The reason for this restriction is that the desired lane change proportions can always reduced to a **net** flow of vehicles in one direction. Because of symmetry, consider only one of the terms on the right hand side of Eq. (2.30):

$$2n_{d,i,j}\widetilde{K}_i\left[\widetilde{K}_iV_{d,rel,i}-\widetilde{K}_j\left(t,s\right)V_{d,rel,j}\right]. \quad (2.31)$$

To analyze the sign of the expression in Eq. (2.31), there are six separate cases to consider in the event that $n_{d,i,j}>0$.

1. $\widetilde{K}_i \equiv 0,\ \widetilde{K}_j \equiv 0,$

2. $sign(\widetilde{K}_i) \neq sign(\widetilde{K}_j),$

3. $\widetilde{K}_i, \widetilde{K}_j < 0$ and $\widetilde{K}_i V_{d,rel,i} < \widetilde{K}_j V_{d,rel,j},$

4. $\widetilde{K}_i, \widetilde{K}_j < 0$ and $\widetilde{K}_i V_{d,rel,i} > \widetilde{K}_j V_{d,rel,j},$

5. $\widetilde{K}_i, \widetilde{K}_j > 0$ and $\widetilde{K}_i V_{d,rel,i} < \widetilde{K}_j V_{d,rel,j},$

6. $\widetilde{K}_i, \widetilde{K}_j > 0$ and and $\widetilde{K}_i V_{d,rel,i} > \widetilde{K}_j V_{d,rel,j}.$

Case 1 is trivial. Cases 2, 4 and 5 result in a negative definite expression for Eq. (2.31). Additional analysis is required for cases 3 and 6.

Case 3:

The expression in Eq. (2.31) is combined with its companion term arising from the lane change feedback (last term in Eq. (2.29)):

$$2\left(\widetilde{K}_i V_{d,rel,i} - \widetilde{K}_j V_{d,rel,j}\right)\left(n_{d,i,j}\widetilde{K}_i + n_{f,j,i}K_j\right). \tag{2.32}$$

By choosing $\zeta_{j,i}(t,s)$ in Eq. (2.27) to satisfy

$$\zeta_{j,i}(t,s)\left[\widetilde{K}_j V_{d,rel,j} - \widetilde{K}_i V_{d,rel,i}\right] K_j \geq n_{d,i,j}|\widetilde{K}_i|, \tag{2.33}$$

the expression in Eq. (2.32) becomes negative semidefinite.

Case 6:

Consider the remaining case where $\widetilde{K}_i, \widetilde{K}_j > 0$ and $\widetilde{K}_i V_{d,rel,i} > \widetilde{K}_j V_{d,rel,j}$ in the region Ω. In this region, there are fewer cars than desired in both lanes. Without loss of generality, consider the two lanes i, j independently of the other lanes; the more general multilane case

is proven similarly. Let $W_{i,j} = W_i + W_j$ be the components of W associated with lanes i and j. Then consider the time derivative of this term:

$$\begin{aligned}\dot{W}_{i,j}\Big|_{\Omega} &\leq \int_{\Omega} 2n_{d,i,j}\widetilde{K}_i\left[\widetilde{K}_i V_{d,rel,i} - \widetilde{K}_j V_{d,rel,j}\right] ds \\ &\leq -2W_{i,j}\Big|_{\Omega} \inf_{\Omega}\{n_{d,i,j}\} + M^2 \sup_{\Omega}\{|V_{d,rel,j}|\} \sup_{\Omega}\{n_{d,i,j}\} \int_{\Omega} ds,\end{aligned}$$

where the constant M is an upper bound of the desired density in the region Ω,

$$0 \leq K_{d,i}, K_{d,j} < M. \tag{2.34}$$

Because the desired density is prescribed to be bounded, boundedness of the error terms follows (Alvarez and Horowitz, 1997).

Stabilizing Controller with Matrix Transformation

In this section a stabilizing controller based on the work of (Li et al., 1997b) which utilizes a matrix transformation for the vehicle error density. The purpose of the matrix transformation is to absorb the contribution of the desired lane change proportions. In the moving coordinate frame described by s, the matrix transformation is time invariant but is allowed to vary with s. First, we define the matrix transformation and its time derivative.

Lemma 1 *Let $\mathbb{A}(s)$ be a matrix transformation for the vehicle density $\widetilde{\mathbb{K}}(t,s)$ such that $\frac{d}{ds}\mathbb{A}(s) = -\mathbb{A}(s)\,\mathbb{N}_d(s)\,\mathbb{V}_{d,rel}^{-1}(s)$ and that $\mathbb{A}(0)$ is invertible. Define $\mathbb{G}(t,s) \equiv \mathbb{A}(s)\,\widetilde{\mathbb{K}}(t,s)$. Then it follows that*

$$\mathbb{G}_t(t,s) = -\left[\mathbb{A}(s)\,\mathbb{V}_{d,rel}(s)\,\mathbb{A}^{-1}(s)\,\mathbb{G}(t,s)\right]_s + \mathbb{A}(s)\left[\mathbb{V}_f(t,s)\,\mathbb{K}(t,s)\right]_s - \mathbb{A}(s)\,\mathbb{N}_f(t,s)\,\mathbb{K}(t,s). \tag{2.35}$$

Proof: Both $\mathbb{N}_d$ and $\mathbb{V}_{d,rel}$ are non-singular matrices by assumption. It follows that $\mathbb{A}(s)$ is invertible under the given dynamics $\forall s$. To obtain the time derivative of the matrix transformed density, differentiate $\mathbb{G}$.

Lemma 2 *Suppose* $\mathbb{V}_{d,rel}(s) = \delta \cdot \mathbb{I}$ *and* $\mathbb{A}_s(s) = -\mathbb{A}(s)\,\mathbb{N}_d(s)\,\mathbb{V}_{d,rel}^{-1}(s)$. *Then it follows that*

$$\mathbb{G}_t(t,s) = -\left[\mathbb{V}_{d,rel}(s)\,\mathbb{G}(t,s)\right]_s + \mathbb{A}\left[\mathbb{V}_f(t,s)\,\mathbb{K}(t,s)\right]_s - \mathbb{A}(s)\,\mathbb{N}_f(t,s)\,\mathbb{K}(t,s). \tag{2.36}$$

Proof: Substitute $\mathbb{A}\mathbb{V}_{d,rel}\mathbb{A}^{-1} = \mathbb{A}\delta \cdot \mathbb{I}\mathbb{A}^{-1} = \mathbb{V}_{d,rel}$ into the expression for $\mathbb{G}_t$ derived in Lemma 1.

The restriction on the relative velocity matrix $\mathbb{V}_{d,rel}(s) = \delta \cdot \mathbb{I}$ is derived from the fact that lane changes should only take place in locations where the lane traffic flows have the same speed. Here, $\mathbb{A}(s)$ is a time independent coordinate transformation and is also required to be non-singular $\forall s$, and $\mathbb{V}_{d,rel}(s)$ is non-singular everywhere because the desired profile should specify forward free-flowing traffic. Note that $\mathbb{N}_d(s)$ is also non-singular by assumption. Because of the time independence of $\mathbb{A}(s)$, the matrix can be precomputed a priori. $\mathbb{N}_d(s)$ must also be time independent as well, in order for $\mathbb{A}(s)$ to remain time independent with the dynamics derived in Lemma 2. Compared to the stabilizing controller shown in section 2.4.2, this is a more stringent requirement on $\mathbb{N}_d$, but as shown in the following theorem, stability results are demonstrated more easily.

Theorem 2 *Let* $\mathbb{V}_{d,rel}(s) = \delta \cdot \mathbb{I}$ *and* $\mathbb{A}_s(s) = -\mathbb{A}(s)\,\mathbb{N}_d(s)\,\mathbb{V}_{d,rel}^{-1}(s)$. *Define the velocity*

feedback law to be

$$\mathbb{V}_f\left(t,s\right)=-\psi\left(t,s\right)diag\left[\mathbb{A}^T\left(s\right)\mathbb{V}_{d,rel}\left(s\right)\mathbb{A}\left(s\right)\widetilde{\mathbb{K}}\left(t,s\right)\right]_s \tag{2.37}$$

and the lane change feedback law to be

$$n_{f,i,j}=max\left[0,\mu\left(t,s\right)\left(F_i\left(t,s\right)K_i\left(t,s\right)-F_j\left(t,s\right)K_j\left(t,s\right)\right)\right] \tag{2.38}$$

where $\mathbb{F}\left(t,s\right)=\mathbb{A}^T\left(s\right)\mathbb{V}_{d,rel}\left(s\right)\mathbb{A}\left(s\right)\widetilde{\mathbb{K}}\left(t,s\right)$. *The boundary conditions are* $\widetilde{\mathbf{K}}(0,t)=0$. *Then* L_2 *stability follows.*

Proof: Use the Lyapunov function

$$W(t)=-\frac{1}{2}\int_0^L\mathbf{G}^T\left(t,x\right)\mathbf{V}_{d,rel}\left(t,x\right)\mathbf{G}\left(t,x\right)dx=\frac{1}{2}\int_{\alpha(t)}^{\beta(t)}\mathbb{G}^T\left(t,s\right)\left[-\mathbb{V}_{d,rel}\left(s\right)\right]\mathbb{G}\left(t,s\right)ds \tag{2.39}$$

where $\alpha(t)=-\int_0^t w(\tau)d\tau$ and $\beta(t)=L-\int_0^t w(\tau)d\tau$. Recall that $\mathbb{V}_{d,rel}$ is negative definite:

$$\begin{aligned}\dot{W}(t)&=\frac{1}{2}\beta'(t)\mathbb{G}^T\left[-\mathbb{V}_{d,rel}\right]\mathbb{G}\Big|_{s=\beta(t)}-\frac{1}{2}\alpha'(t)\mathbb{G}^T\left[-\mathbb{V}_{d,rel}\right]\mathbb{G}\Big|_{s=\alpha(t)}\\&\quad+\frac{1}{2}\int_{\alpha(t)}^{\beta(t)}\left[\mathbb{G}^T\left[-\mathbb{V}_{d,rel}\right]\mathbb{G}\right]_t ds\\&=-w(t)\mathbb{G}^T\left[-\mathbb{V}_{d,rel}\right]\mathbb{G}\Big|_{s=\alpha(t)}^{s=\beta(t)}+\int_{\alpha(t)}^{\beta(t)}\mathbb{G}^T\mathbb{V}_{d,rel}\left[\mathbb{V}_{d,rel}\mathbb{G}\right]_s ds\\&\quad-\int_{\alpha(t)}^{\beta(t)}\mathbb{G}^T\mathbb{V}_{d,rel}\mathbb{A}\left[\mathbb{V}_f\mathbb{K}\right]_s ds+\int_{\alpha(t)}^{\beta(t)}\mathbb{G}^T\mathbb{V}_{d,rel}\mathbb{A}\mathbb{N}_f\mathbb{K}ds.\end{aligned} \tag{2.40}$$

Using integration by parts and noting that $\mathbb{G}^T \mathbb{V}_{d,rel} \left[\mathbb{V}_{d,rel}\mathbb{G}\right]_s = \left[\mathbb{G}^T \mathbb{V}_{d,rel}\right]_s \mathbb{V}_{d,rel}\mathbb{G}$, we obtain

$$\begin{aligned}
\dot{W}(t) = & -w(t)\mathbb{G}^T \left[-\mathbb{V}_{d,rel}\right] \mathbb{G}\Big|_{s=\alpha(t)}^{s=\beta(t)} + \frac{1}{2}\int_{\alpha(t)}^{\beta(t)} \left[\mathbb{G}^T \mathbb{V}_{d,rel}^2 \mathbb{G}\right]_s ds \\
& - \int_{\alpha(t)}^{\beta(t)} \left[\mathbb{G}^T \mathbb{V}_{d,rel} \mathbb{A} \mathbb{V}_f \mathbb{K}\right]_s ds + \int_{\alpha(t)}^{\beta(t)} \left[\mathbb{G}^T \mathbb{V}_{d,rel} \mathbb{A}\right]_s \mathbb{V}_f \mathbb{K} ds \\
& + \int_{\alpha(t)}^{\beta(t)} \mathbb{G}^T \mathbb{V}_{d,rel} \mathbb{A} \mathbb{N}_f \mathbb{K} ds \\
= & \frac{1}{2}\mathbb{G}^T \mathbb{V}_{d,rel} \left[\mathbb{V}_{d,rel} + 2w(t)\cdot \mathbb{I}\right] \mathbb{G}\Big|_{\alpha(t)}^{\beta(t)} - \left[\mathbb{G}^T \mathbb{V}_{d,rel} \mathbb{A} \mathbb{V}_f \mathbb{K}\right]_{\alpha(t)}^{\beta(t)} \\
& + \int_{\alpha(t)}^{\beta(t)} \left[\mathbb{G}^T \mathbb{V}_{d,rel} \mathbb{A}\right]_s \mathbb{V}_f \mathbb{K} ds + \int_{\alpha(t)}^{\beta(t)} \mathbb{G}^T \mathbb{V}_{d,rel} \mathbb{A} \mathbb{N}_f \mathbb{K} ds.
\end{aligned} \tag{2.41}$$

Impose the restriction that no stabilizing control is used at the boundaries, $\mathbf{V}_f(t, x=0) = \mathbf{V}_f(t, x=L) = 0$. Thus,

$$\begin{aligned}
\dot{W}(t) = & \frac{1}{2}\mathbb{G}^T \mathbb{V}_{d,rel} \left[\mathbb{V}_{d,rel} + 2w(t)\cdot \mathbb{I}\right] \mathbb{G}\Big|_{\alpha(t)}^{\beta(t)} + \int_{\alpha(t)}^{\beta(t)} \left[\mathbb{G}^T \mathbb{V}_{d,rel} \mathbb{A}\right]_s \mathbb{V}_f \mathbb{K} ds \\
& + \int_{\alpha(t)}^{\beta(t)} \mathbb{G}^T \mathbb{V}_{d,rel} \mathbb{A} \mathbb{N}_f \mathbb{K} ds.
\end{aligned} \tag{2.42}$$

Recall the definition $\mathbb{F}(t,s) \equiv \mathbb{A}^T(s)\, \mathbb{V}_{d,rel}(s)\, \mathbb{A}(s)\, \widetilde{\mathbb{K}}(t,s)$,

$$\int_{\alpha(t)}^{\beta(t)} \left[\mathbb{G}^T \mathbb{V}_{d,rel} \mathbb{A}\right]_s \mathbb{V}_f \mathbb{K} ds = \int_{\alpha(t)}^{\beta(t)} -\psi(t,s) \sum_i K_i F_i^2 ds \leq 0, \tag{2.43}$$

$$\begin{aligned}
\int_{\alpha(t)}^{\beta(t)} \mathbb{G}^T \mathbb{V}_{d,rel} \mathbb{A} \mathbb{N}_f \mathbb{K} ds &= \int_{\alpha(t)}^{\beta(t)} \mathbb{F}^T \mathbb{N}_f \mathbb{K} ds \\
&= \int_{\alpha(t)}^{\beta(t)} \sum_{\substack{i\neq j=1 \\ |i-j|\leq 1}}^{m} -\mu(t,s)\left(F_j K_j - F_i K_i\right)^2 \leq 0 \quad \forall \mu(t,s) \geq 0.
\end{aligned} \tag{2.44}$$

Combining the results of Eqs. (2.43) and (2.44) with the general expression for $\dot{W}(t)$, one obtains

$$\dot{W}(t) \leq \frac{1}{2}\mathbb{G}^T \mathbb{V}_{d,rel} \left[\mathbb{V}_d + w(t)\cdot \mathbb{I}\right] \mathbb{G}\Big|_{\alpha(t)}^{\beta(t)}. \tag{2.45}$$

Under the following assumption for the boundary conditions, $\widetilde{\mathbf{K}}(0,t) = 0$, one obtains the following inequality:

$$\dot{W}(t) \leq \frac{1}{2}\mathbb{G}^T \mathbb{V}_{d,rel} \left[\mathbb{V}_d + w(t) \cdot \mathbb{I}\right] \mathbb{G}\Big|_{\beta(t)} \leq 0. \tag{2.46}$$

Eq. (2.46) holds because the following matrix quantity in Eq. (2.47) is also diagonal, positive definite under the assumption that the $\mathbb{V}_d\,(t,s)$ is positive definite and diagonal.

$$\mathbb{V}_d + w(t) \cdot \mathbb{I} > 0. \tag{2.47}$$

$\mathbb{V}_{d,rel}\,(s) < 0$ is negative definite and diagonal, and $\mathbb{A}$ is a non-singular matrix transformation $\forall s$. Thus, L_2 stability follows for the density error.

2.4.3 Simulation Results

The following scenario for emergency vehicles (EVs) illustrates the operation of the two controllers. From a safety standpoint, an area of low vehicle density is desired around the moving EV so that other vehicles can circulate around it. This region of low vehicle density is achieved by moving a low velocity profile in the non-EV lane, as discussed in Section 2.4.1. In the EV lane, vehicles are requested to move out of the way; these vehicles must also decrease velocity to provide safe lane changing space. The non-stationary velocity profile to be used is shown in Fig. 2.10 and was discussed in section 2.4.1. The EV travels at the location of the peak velocity in lane 1 and at speed $w(t) = V_{high}$. To avoid vehicle pile-up in front of the EV and to restore the nominal flow of the highway after the EV passes, lane changing is required.

Simulation results are also obtained using SmartCap (Broucke et al., 1996). In these simulations, all vehicles are assumed independent (i.e. no platoons). All highway sections

are 100 m long, and there are two highway lanes. A conservative safety policy imposes constraints on vehicle spacing dependent on activity and vehicle speed. A vehicle cruising at 20 m/s requires approximately 23 m of space, including the length of the vehicle itself. Changing lane requires space in the originating and destination lane.

In Figs. 2.11 and 2.12, SmartCap results are shown for the two lane non-stationary profile without control feedback. At $t = 0$, the highway is empty, and we allow a net inflow of 4800 vehicles per hour distributed equally over the lanes. These vehicles travel at the nominal speed of 20 m/s. By $t = 1000s$, the highway is filled evenly with 3.3 vehicles per section. At this time the velocity profile is formed and begins to travel at 30 m/s. The vehicles inside the profile decelerate the 10 m/s in order to change lane out of the way of the EV.

It is important to note that vehicles at the nominal velocity of 20 m/s can not change lane out of the way of the EV while maintaining that speed due to capacity constraints. The time delay between its deceleration and that of the car in front causes vehicles to "spread out". In this low density region, vehicles are then able to change lane out of the EV's lane. While the adjacent lane's vehicles continue to travel at 10 m/s, the EV travels along with the velocity profile at 30 m/s. After the EV has passed, vehicles in the adjacent lane are able to change lane back into the EV lane while maintaining the slow speed of 10 m/s. Vehicles in both lanes then accelerate to the nominal traffic speed upon leaving the non-stationary velocity profile. It is important to note that highway capacity conditions do not permit all vehicles to change lane into a single lane at the speed of 30 m/s. At slower speeds, headway space demands can be relaxed. The non-stationary velocity profile allows

fast circulation of local traffic around an emergency vehicle without restriction of highway inflow.

In Fig. 2.12 the velocity profile retains the shape shown in Fig. 2.10 in the absence of feedback. Due to the fact that vehicles must be moved out of the way to create space for the EV, a pile-up of vehicle density results upstream of the profile. In the absence of feedback control, this pile-up persists during the simulation and travels down the highway at the nominal speed. When space for the EV is initially formed in lane 1, vehicles must change lane into lane 2. Because the vehicles do not return to their original lane 1, there is a greater pile-up of vehicle density in lane 2 than in lane 1 upstream of the profile.

Figs. 2.13 and 2.14 depict the results of a simulation with the same highway conditions but utilizing the coordinate transformation controller of Section 2.4.2 for feedback. Prior to simulation, the matrix transformation, $\mathbb{A}(s)$ is precomputed in Matlab. The overall effect of the feedback control is a smoother vehicle density distribution. After the initial formation of space for the EV, the peak number of vehicles in a section is greater in the absence of feedback control, resulting in greater perturbation.

The pile-up of vehicle density upstream of the profile is dissipated as time progressed due to feedback control. The velocity profile shown in Fig. 2.14 is similar in general shape to Fig. 2.12 except for a very slight "bowing" of the speed curve where the pile-up is located. It was observed that very slight modifications of the speed curve resulted in significant vehicle density dissipation. This suggests that using control feedback for dissipation of local density peaks may have little negative impact on large scale highway capacity. The vehicle density is also equalized in the two lanes upstream of the profile due to lane change feedback. The

amount of lane changing activity behind the profile is significant. Restoration of nominal highway conditions behind the EV is desirable from a capacity standpoint. Simulations utilizing the controller in Section 2.4.2 produce similar results.

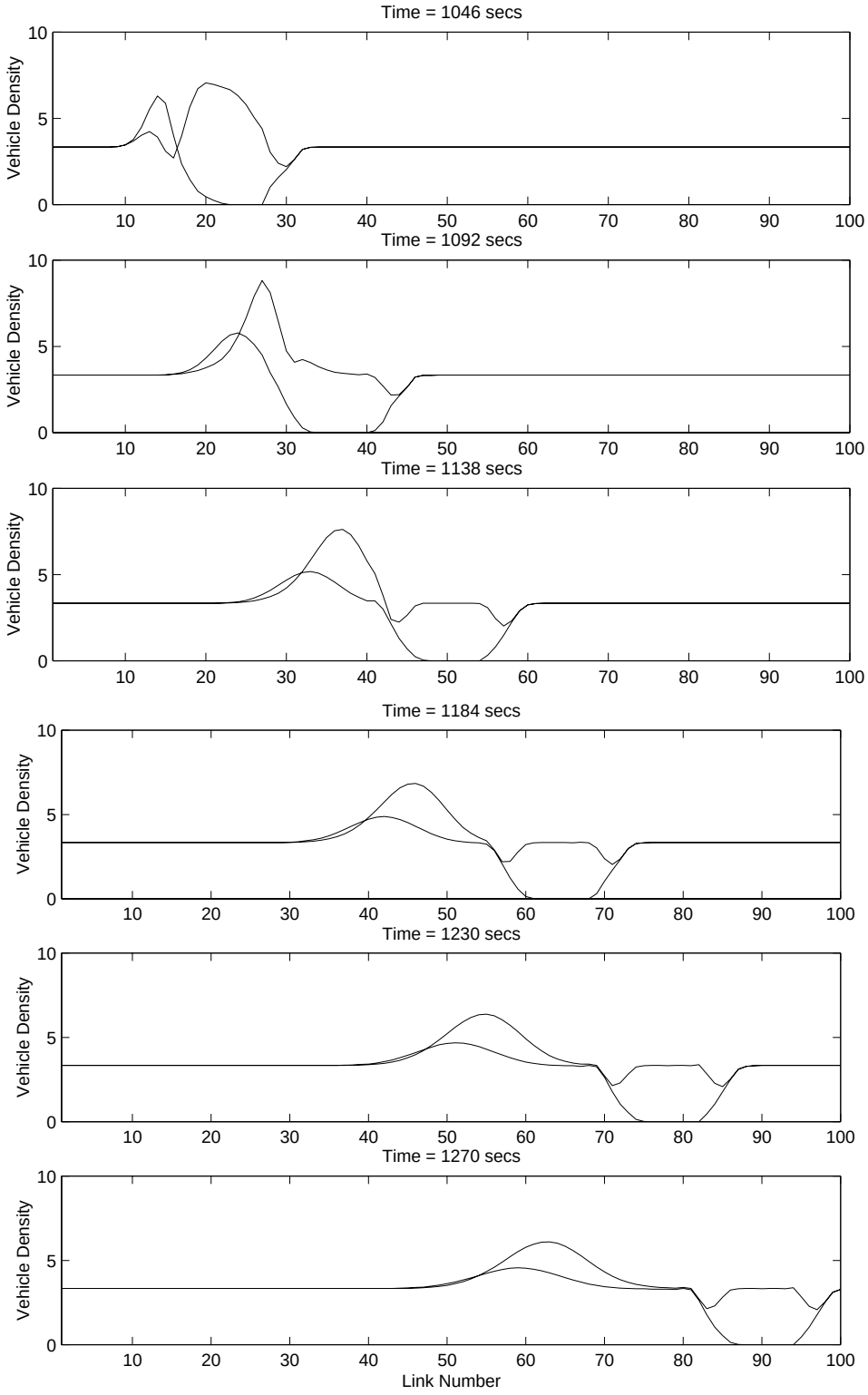

Figure 2.11: Vehicle density versus longitudinal section - No feedback control is used. To form the vehicle density hole, more vehicles are moved out of the EV's lane, resulting in a larger pileup of vehicles behind the EV. This larger pileup persists in the EV lane even after the maneuver.

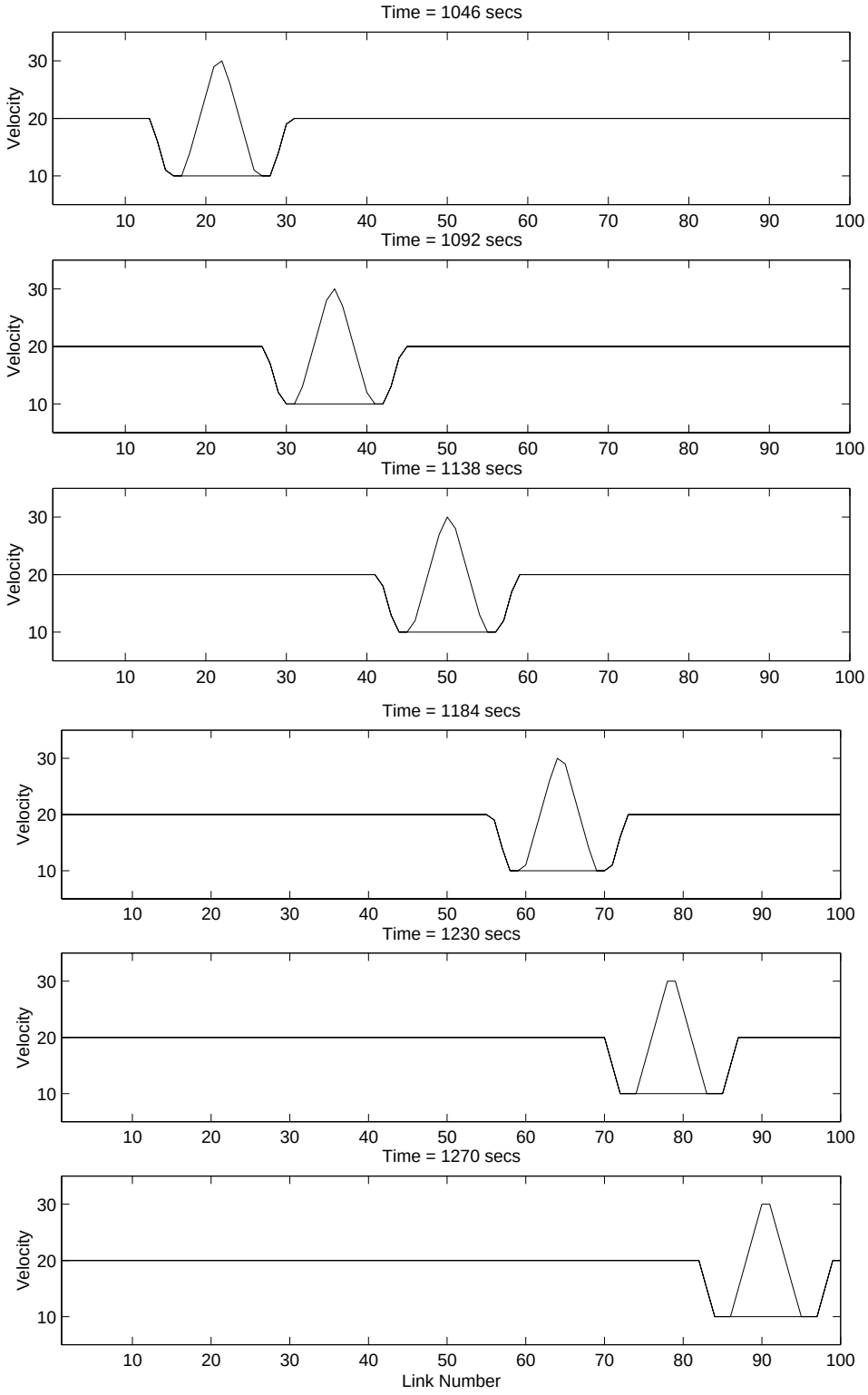

Figure 2.12: Traffic velocity versus longitudinal section - No feedback control is used. The profile is the same as the designed velocity profile shown in Fig. 2.10.

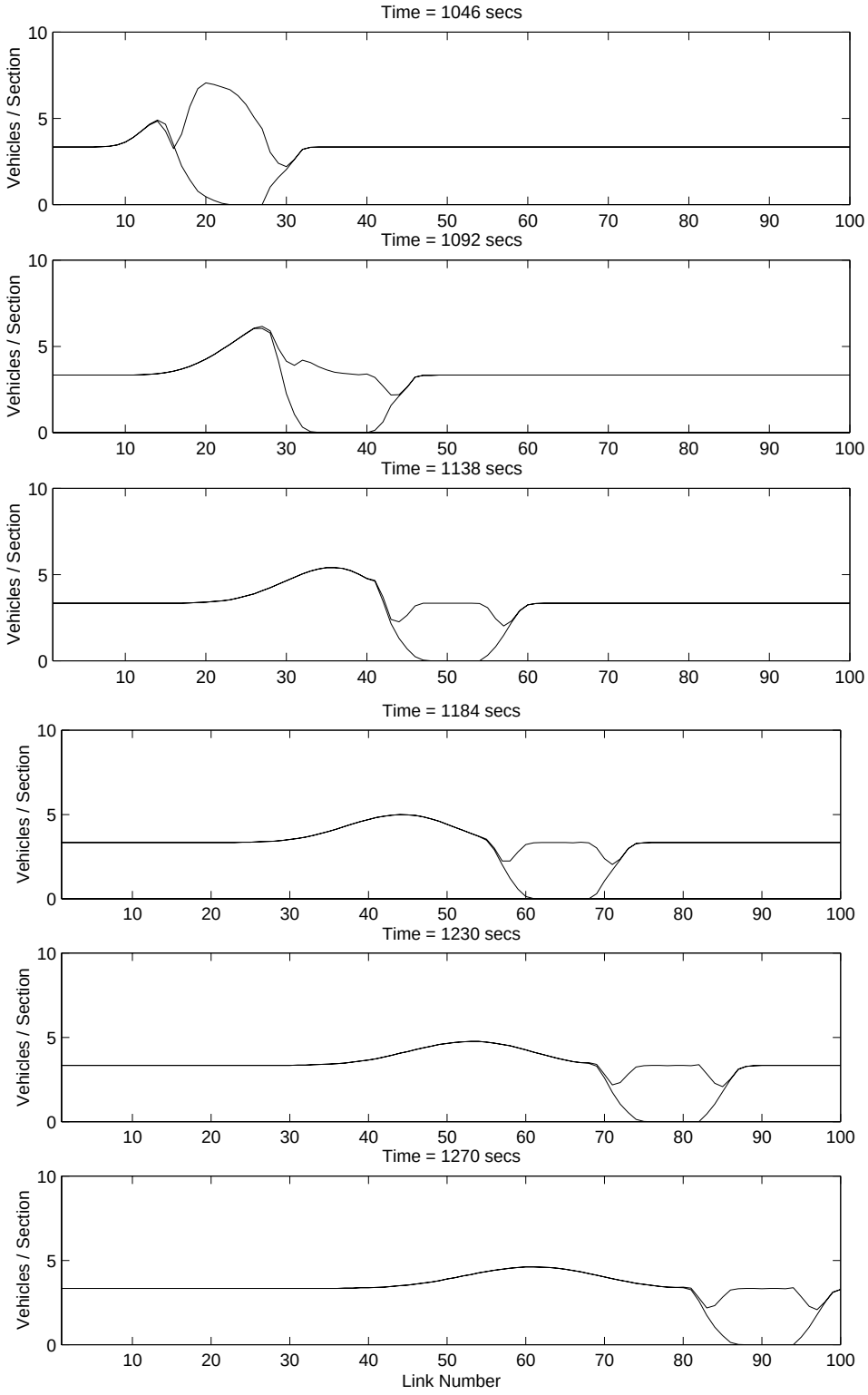

Figure 2.13: Vehicle density versus longitudinal section - Feedback control is used. The feedback control for lane changing equalizes the error in both lanes after the EV has passes. The "lump" of vehicles is equally distributed between the two lanes.

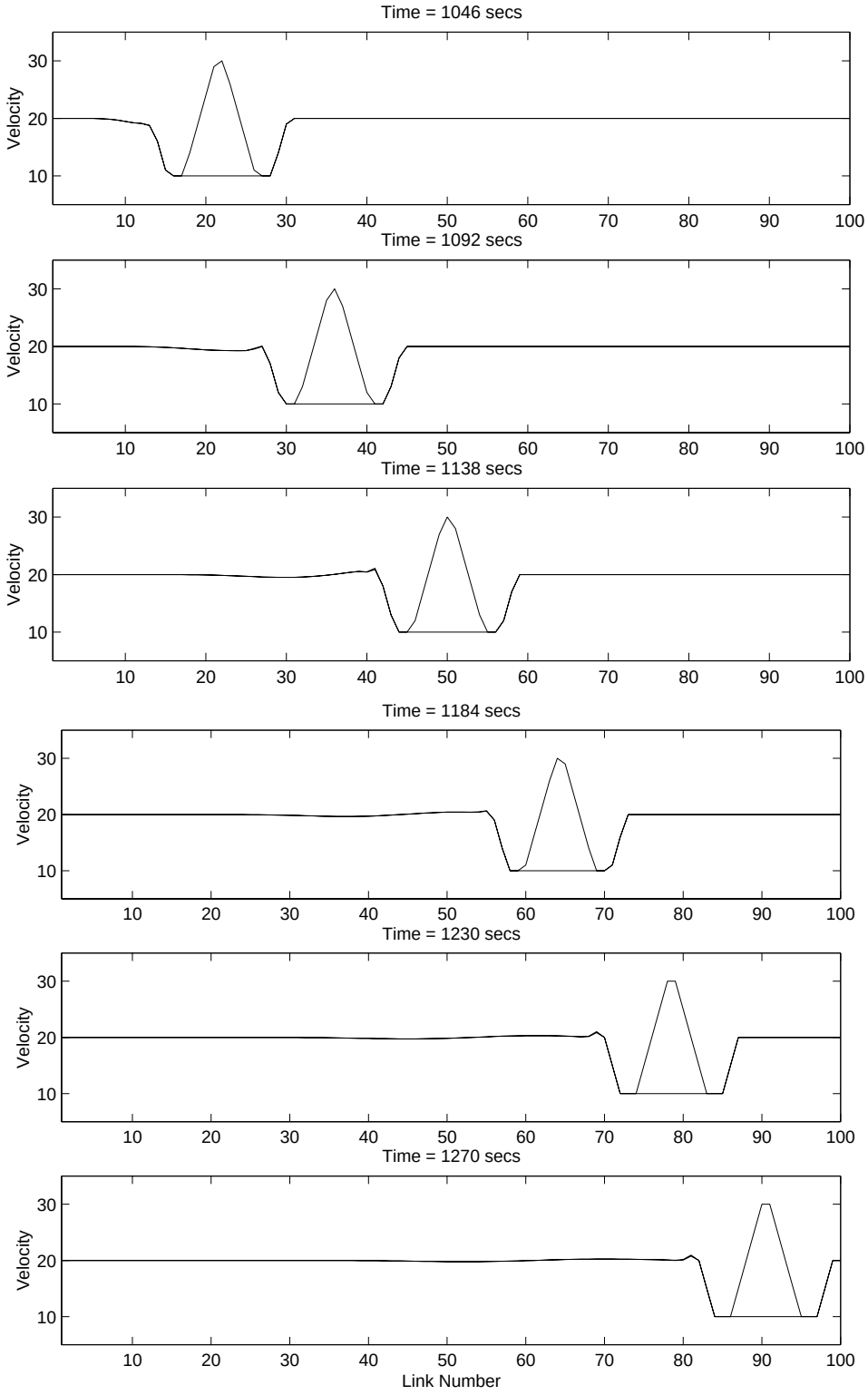

Figure 2.14: Traffic velocity versus longitudinal section - Feedback control is used. The velocity feedback attempts to spread out the "lump" of vehicles left after the initial hole is created. This results in a "bowing out" of the traffic speed behind the velocity profile.

Chapter 3

Coordination Layer Control Laws

In the previous chapters, different link layer strategies for moving vehicles out the way of an emergency vehicle were discussed. Whether or not an individual AHS vehicle executes a link layer command depends on the vehicle's state. For example, a car may be prevented from achieving the link layer's speed command by a slower moving vehicle downstream merging onto the highway. Local deviations from the link layer behavior occur because the link layer models the highway as a continuum with a distributed vehicle density without regard for individual vehicles' safety conditions. Because the link layer may fail to vacate all vehicles immediately downstream of the EV, a corrective coordination layer maneuver is needed to move the remaining vehicles out of the way. In (Leung, 1994) the *Vortex* maneuver was developed for the coordination layer to perform actions analagous to those of the *Bubble* and *Volcano* maneuvers. Microsimulation results for the *Vortex* maneuver are analyzed in this chapter. The simulations showed the necessity to modify some aspects of this maneuver leading to the design of the *Vortex2*, as an improved *Vortex* maneuver that

is described in this chapter.

3.1 Original Vortex Maneuver

3.1.1 Maneuver Description

Several coordination layer maneuvers specific for emergency vehicles on AHS, including the *Vortex*, were designed by (Leung, 1994). These were described briefly in Chapter 1. This chapter specifically focuses on simulation and evaluation of the *Vortex* maneuver, which serves the same purpose as both the *Bubble* and *Volcano* link layer strategies: to circulate vehicles around a faster moving EV by use of lane changes.

The operation of the *Vortex* manuever is depicted in Fig. 3.1. The EV utilizes the same coordination layer leader law as all automated vehicles on the highway. When no downstream vehicles are detected, the EV travels at the maximum speed allowable by the link layer, which exceeds that of all the non-EVs. When a downstream platoon (A) is detected, the EV maintains a safe distance from the other platoon and sends a platoon lane change (PLC) maneuver request. If platoon A isn't busy, it attempts a PLC and may request assistance from neighboring lane platoon B. Platoon B decelerates to make space for A in the neighboring lane. Once platoon A has changed lane, A sends a PLC complete message to the EV. The EV no longer has a downstream platoon in its radar and accelerates. Once the EV has advanced downstream past, A requests platoon B to perform a PLC to take advantage of the space created behind the EV. B returns a message to A indicating its sucess/failure for the PLC maneuver. Regardless of B's success or failure, A in turn replies to and unlinks itself from the EV. A and B are now independent of the

EV, and the EV is free to repeat the cycle with another detected downstream platoon. A's PLC maneuver is utilized to generate headway for the EV, and B's PLC maneuver is used to reestablish distributed vehicle density over the two highway lanes. Details for the finite-state machines (FSM) for the initiator (EV) and two responders (platoons A and B) can be found in (Leung, 1994).

In the *Vortex* maneuver, the EV "talks" to only one platoon (A) at a time. One reason for this restriction is the PATH's hierarchical control system specification of point-to-point communication; i.e. a vehicle only communicates with one other vehicle at a time for coordination layer maneuvers. This assumption is necessary for verification of the maneuver protocols and for correct coordination layer design (Varaiya, 1993). The second reason for the restriction is the design criteria that the EV should minimal impact on the rest of the traffic. If the EV requested more than one downstream platoon to move out of the way at the same time, larger shockwaves would be imposed on the non-EV lane.

3.1.2 Simulation Results

The *Vortex* maneuver was evaluated using SmartAHS, a traffic microsimulator (Gollu and Varaiya, 1998). SmartAHS is written in the SHIFT language (Deshpande et al., 1998), which is specifically designed for straightforward coding of hybrid automata. SmartAHS simulates the continuous dynamics of individual vehicles and provides a framework for defining highway topologies. California PATH projects MOU-310 and MOU-383 have produced SmartAHS code to simulate PATH's regulation, coordination and link layer controllers. Only the normal regulation and coordination layer controllers were used for these simula-

tions; the link layer was disabled. [1]

In this simulation nine vehicles and one EV are placed on a two lane AHS. The EV is the vehicle farthest upstream and must move through the group of vehicles. The simulation probably best represents the real-life scenario where an EV has to move through a cluster of vehicles on a medium density highway before encountering the next cluster some distance downstream.

Results are shown in Fig. 3.2 as a TS diagram. The implementation and testing of the *Vortex* maneuver utilized only free agents. (Leung, 1994) developed the *Platoon Lane Change (PLC)* maneuver for use with the *Vortex*, but the *PLC* cannot be implemented due to lack of safety criteria. The simplified regulation layer controllers developed as part of PATH MOU-383 are used; comfort limits on acceleration/deceleration of all vehicles are removed. The traffic flows downstream towards the right of the figure. The ten vehicles enter the two lane AHS after approximately 10 seconds with approximately 44 meters between vehicles. The link layer speed of the non-EVs is set at 22 m/s, and that of the EV is set at 32 m/s. Each curve denotes the trajectory of a single vehicle. Blue and green denote vehicles in lanes 1 and 2, respectively. The EV is the vehicle farthest upstream, and travels in lane 2. Its trajectory is indicated in red. Upon receiving a vortex initiation request from the EV, the vehicle immediately downstream (*Vortex* responder 1, which is denoted in green) decelerates to obtain safe headway space in the destination lane and forces the vehicles upstream in the target lane to also decelerate. Once there is enough space it changes lane, which is depicted by the change of color in the vehicle's trajectory from green to blue. The

[1] The ability to simulate enough vehicles to populate a length of AHS large enough to test several sections for the link layer is currently beyond the scope of SmartAHS. Current research associated with California PATH project MOU-383 attempts to provide large scale highway simulation by integrating SmartCap-like mesosimulation with SmartAHS.

vehicle behind the *Vortex* responder 1 is requested to change lane, in turn.

Finite state machine diagrams and a description for the SmartAHS change lane protocol are contained in the Appendix. The change lane protocol described in the Appendix and implemented in SmartAHS is more complicated than the analagous PLC maneuver described in (Leung, 1994). A vehicle performing a change lane maneuver may have to decelerate and at the same time request the upstream vehicle in the destination lane to also decelerate. The PLC maneuver assumes that the upstream vehicle in the destination lane does not participate in the maneuver, which is an oversimplification.

During the simulations for the *Vortex* maneuver, the following observations were made:

- The time required to overtake the vehicle furthest downstream was 85 seconds. This cycle time seems slow considering that high priority EV transit is desired.

- As designed, the *Vortex* maneuver, forces platoons in the position of B in Fig. 3.1 to change lane into the EV's lane behind the EV. However, these platoons may not wish to be in the EV's lane because of their ultimate objective (e.g. a particular lane for a specific destination/color). If platoons A and B are of different length, the *Vortex* maneuver does not reestablish the vehicle density distribution after the vortex has passed.

- While platoon A negotiates with platoon B, the EV must remain on standby, waiting for a signal from platoon A. This signal sent from platoon A to the EV is transmitted regardless of the outcome of any maneuvers by platoon A or B. Both A and B are located in a lane different from that of the EV after A has moved out of the way. The EV's actions are independent of A and B at this point. Forcing the EV to remain on

standby seems unnecessary.

- After the EV has moved through the entire cluster of vehicles, the cluster has "spread out". This represents an expansion in the space the vehicles occupy, which implies that nearby vehicles not directly in contact with the EV could be affected adversely.

In view of these design issues, modifications were incorporated in a new maneuver.

3.2 Improved Vortex2 Maneuver

3.2.1 Maneuver Description

Several improvements were incorporated in the design of the *Vortex2* maneuver. To improve the cycle time of the *Vortex* maneuver, the EV's wait for confirmation from platoon A was eliminated. platoon B's PLC maneuver, while it does take advantage of the space created behind the EV, is eliminated because platoon B's ultimate objective may not to be present in that lane. In addition, if platoon B's length is not equal to that of A, there is no vehicle conservation. Instead, platoon A returns to its original lane once the EV has accelerated past. The operation of the *Vortex2* maneuver is shown in Fig. 3.3.

The finite state machine (FSM) diagrams for the involved vehicles are shown in Figs. 3.4 and 3.5. The *Vortex* initiator protocol is used by the EV, and the *Vortex* responder protocol is used by the platoon detected downstream of the EV. Like the original *Vortex* maneuver, the *Vortex2* maneuver requires the use of the *Platoon Lane Change* protocol (Leung, 1994). The protocols were verified to be deadlock-free using the software verification tool Uppaal (Larsen et al., 1997), which performs random activation of the finite state

machine transitions. The operation of the *Vortex2* protocol is the same as the *Vortex* up to the point where platoon A moves out of the EV's way. Once this is done, the EV unhooks its communication with platoon A and begins to accelerate past. In this way, the EV is free to initiate communication with any downstream platoons that it encounters. Platoon A monitors the EV's progress on the highway and waits until EV passes to return to the original lane. Once platoon A has returned to its original lane, it accelerates to reduce its headway space and also requests platoon B to reduce its headway. These two headway reductions are necessary to compress the space that was needed for platoon A's lane change. The *Vortex2* responder 2 protocol is used by platoon B to answer the request for headway reduction.

3.2.2 Simulation Results

In Fig. 3.6, the results of the SmartAHS simulation for the *Vortex2* maneuver are shown in a TS diagram. All vehicles are freeagents. The EV travels in lane 2, and its trajectory is shown in red. The non-EVs in lane 1 and 2 are denoted by blue and green, respectively. Vehicles are initially spaced approximately every 44m as freeagents. The non-EVs and EV have link layer commanded speeds of $22m/s$ and $32m/s$ respectively. Upon entering the highway, each freeagent's leader law adjusts its acceleration and desired velocity (Alvarez and Horowitz, 1999). The EV enters the highway after the other vehicles have achieved a steady state, and it immediately initiates a *Vortex2* request with the vehicle immediately downstream (*Vortex2* responder). The *Vortex2* responder negotiates with vehicles in the adjacent lane to perform a changelane maneuver (see Appendix), which causes deceleration in its lane and the destination lane. The *Vortex2* responder's changelane is depicted by

a transition from green to blue in the vehicle's trajectory. The EV establishes contact with the next vehicle immediately, which is shown by the rapid deceleration of the next downstream vehicle. Once the EV has passed the *Vortex2* responder (intersection of red trajectory with blue segment) and travelled a sufficient distance away for safe headway, the *Vortex2* responder changes lane again (blue back to green).

In comparing the *Vortex* and *Vortex2* maneuvers, some improvements are noted.

- The time required for the EV to overtake the group of vehicles is approximately 80 seconds, a slight time reduction compared to the original *Vortex* maneuver.

- All vehicles downstream of the EV are returned to their original locations relative to the other vehicles. The vehicle cluster's original configuration is preserved.

- After the EV has passed, the vehicle cluster has "spread" out $+38m$ in spite of the addition of acceleration maneuvers by the two *Vortex2* responders to close the generated headway gaps. This spread is approximately the same as that of the original *Vortex* maneuver; this result is surprising considering that vehicles are commanded to decrease their headway after the EV has passed to counteract the effects of the *Changelane* maneuver (See Appendix). One possible reason for spread is that regulation layer safety conditions do not allow reestablishment of the initial configuration. The *Vortex2* simulation is run for longer time than the *Vortex* simulation to verify the results.

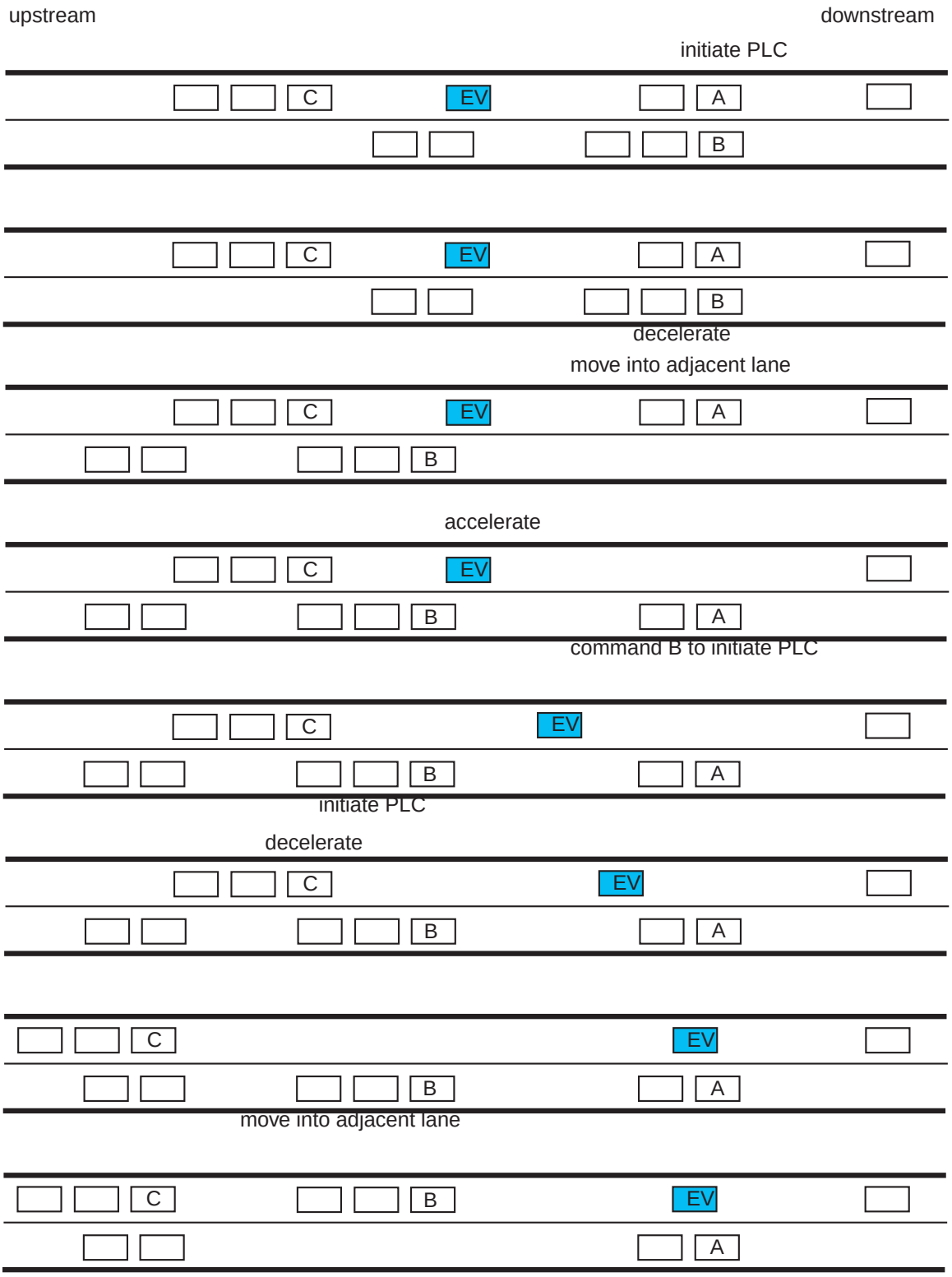

Figure 3.1: Vortex maneuver schematic - Vehicles downstream of the EV are moved out of the way but do not return to their original lane. Vehicle lanes are "switched" by the passing of the EV.

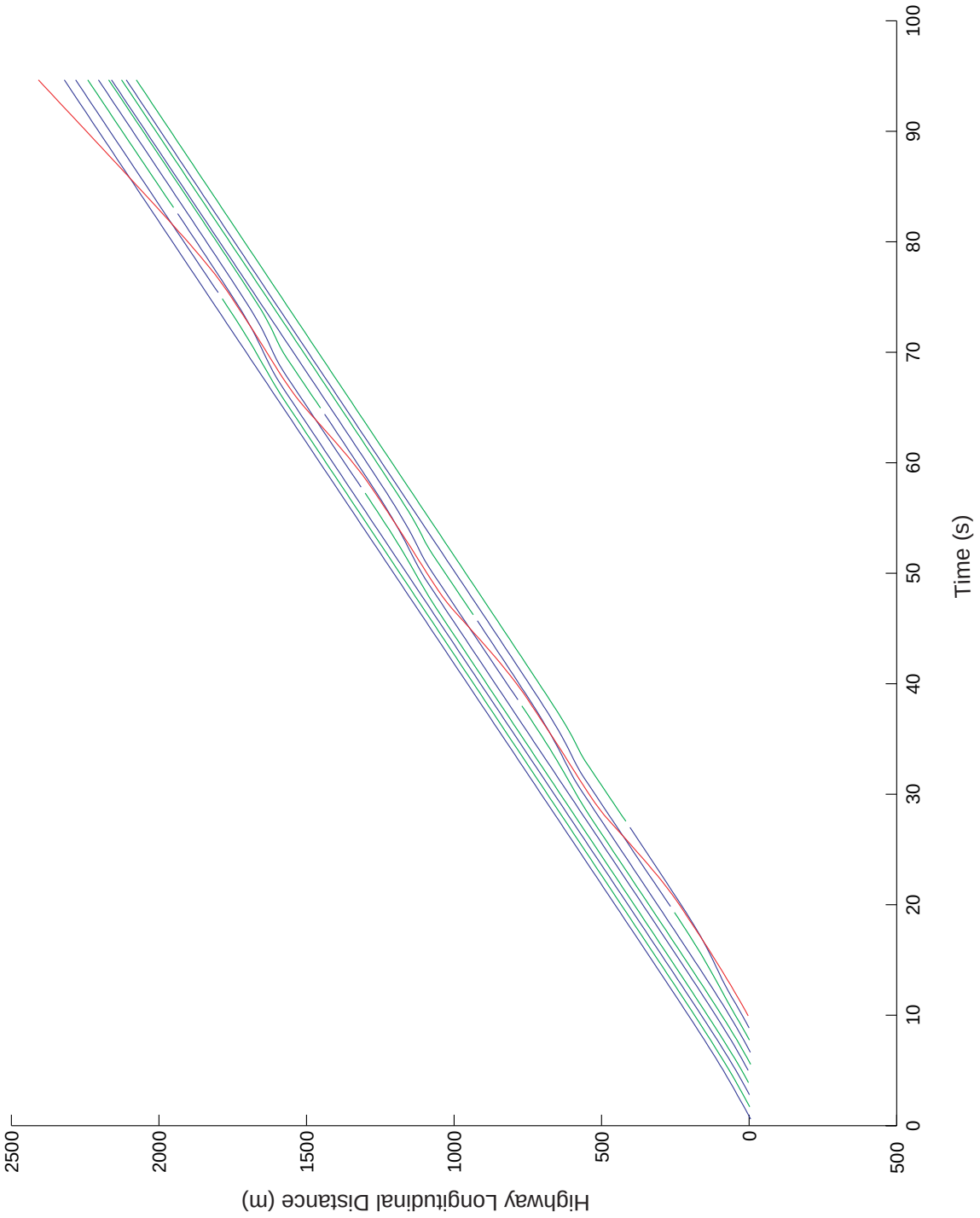

Figure 3.2: Time-space diagram for the SmartAHS simulation of the Vortex maneuver

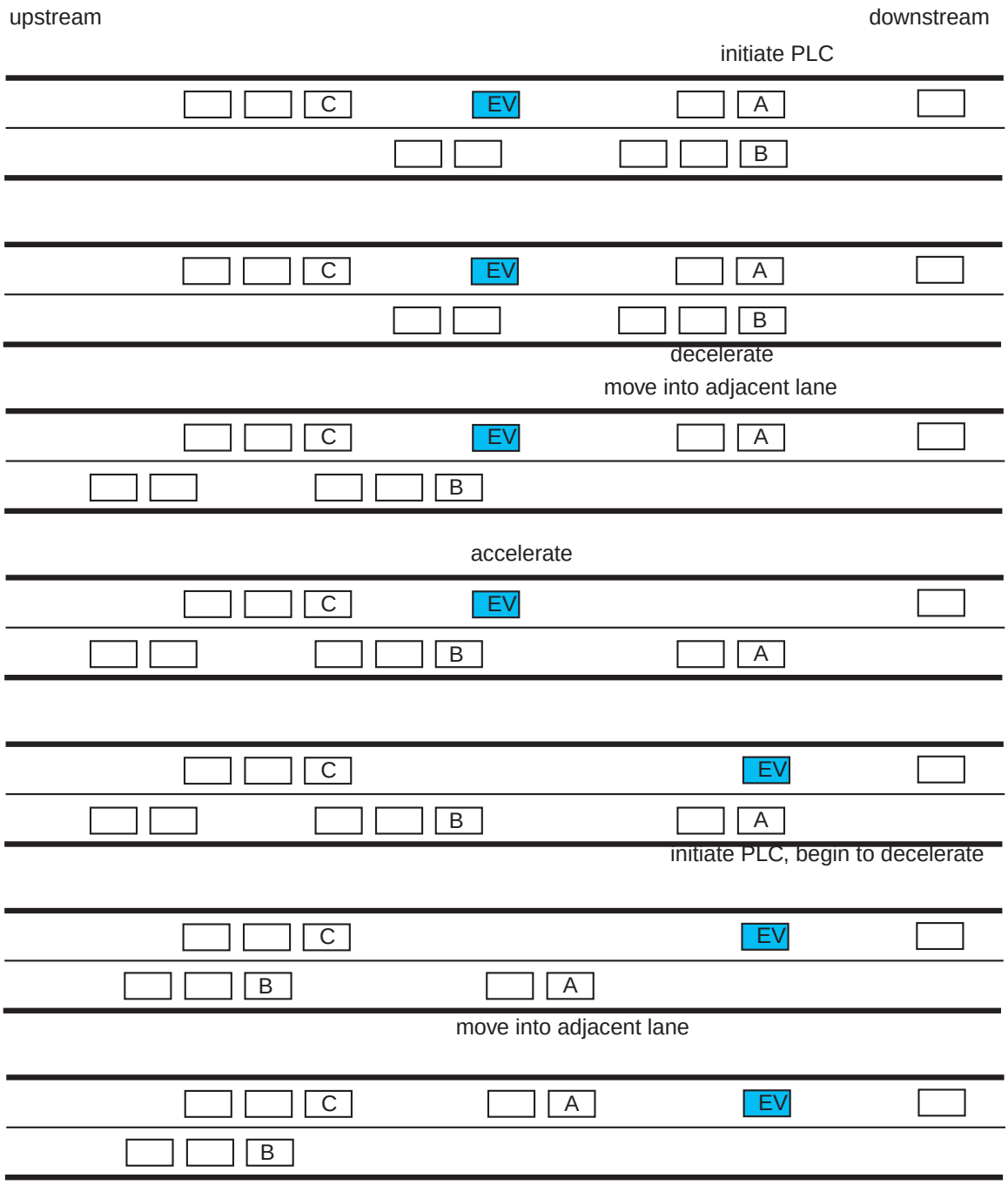

Figure 3.3: Vortex2 maneuver schematic - Vehicles downstream of the EV are returned to their original lane.

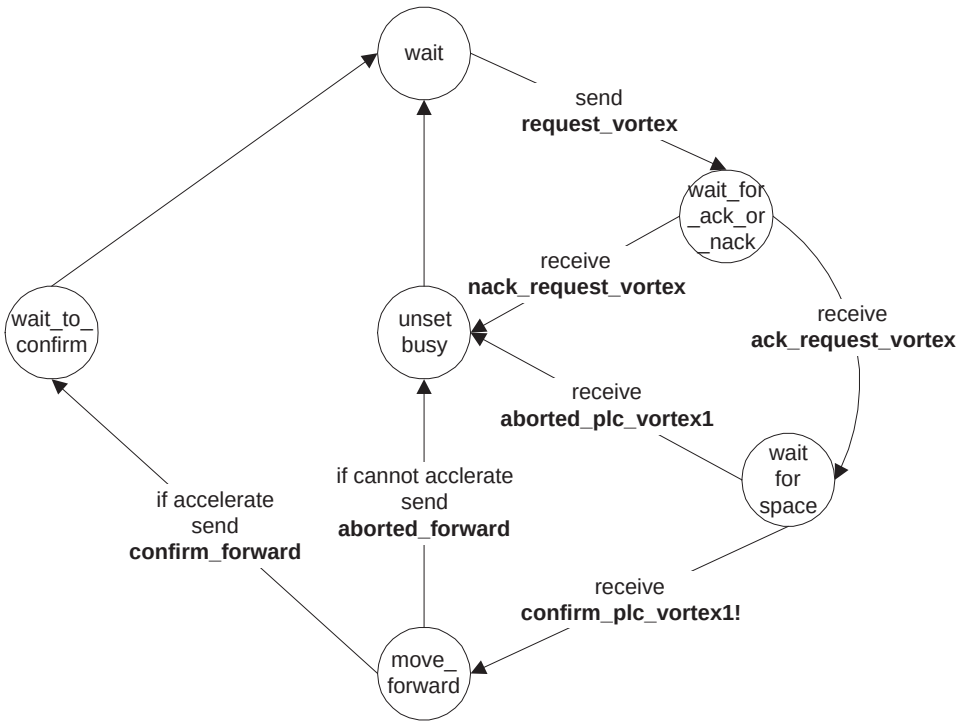

Figure 3.4: Vortex2 initiator protocol used by the EV.

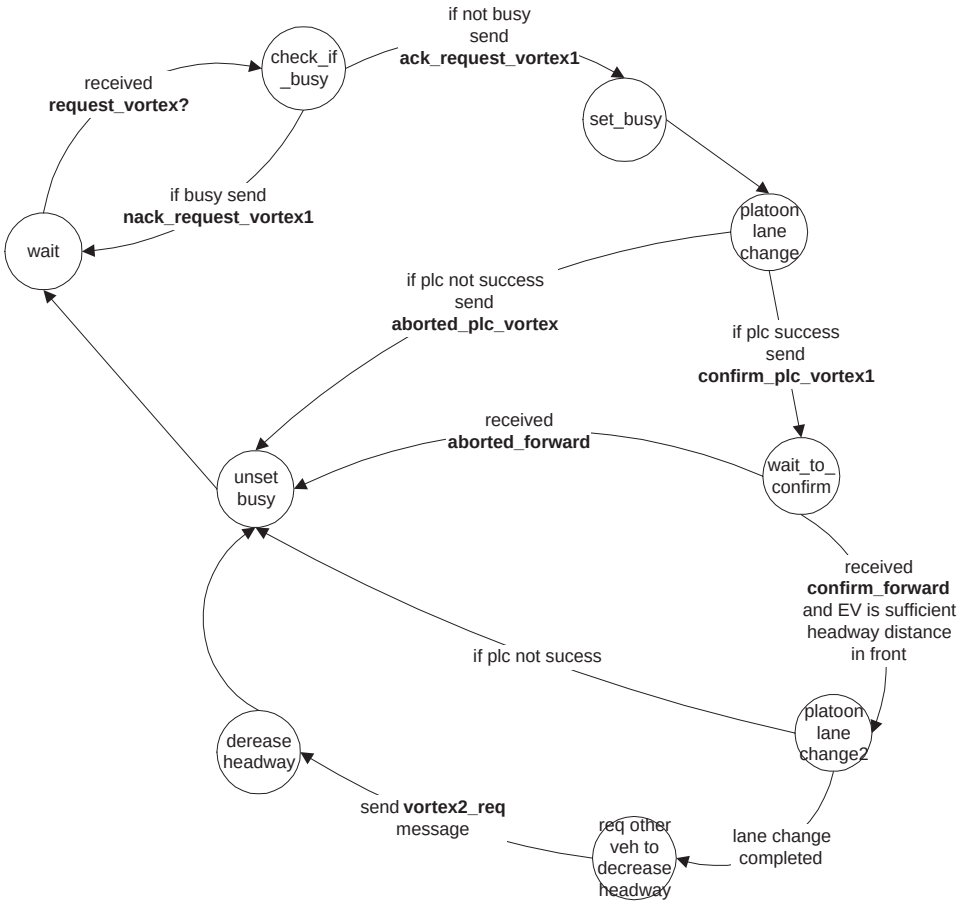

Figure 3.5: Vortex2 responder protocol used by vehicles immediately downstream of the EV.

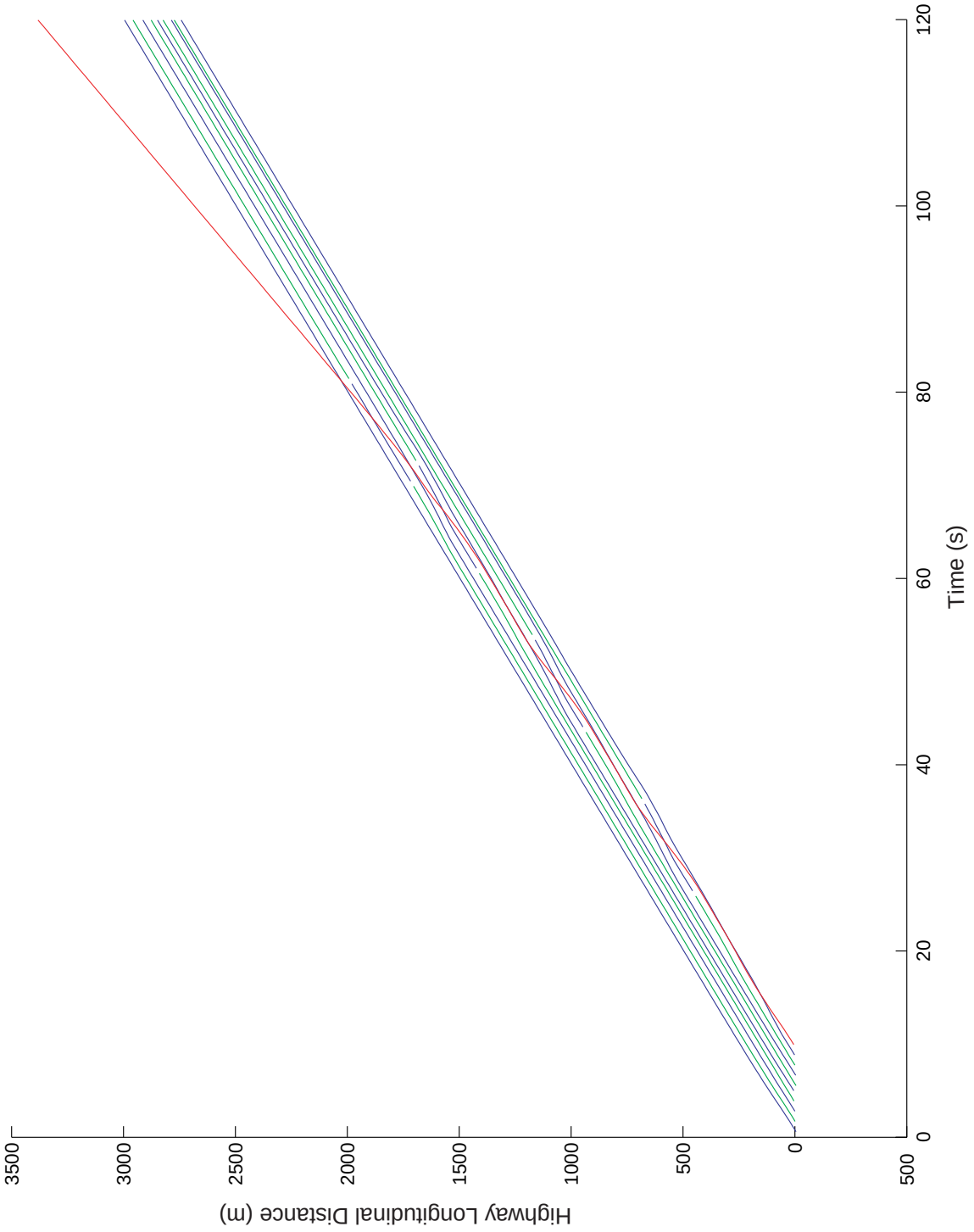

Figure 3.6: TS diagram for the SmartAHS simulation of the Vortex2 maneuver.

Chapter 4

Conclusions

In this thesis, several maneuvers were developed for high priority emergency vehicle (EV) transit on AHS. The *Bubble* and *Volcano* maneuvers were developed for the link layer while the *Vortex2* was developed for the coordination layer. No changes were needed for the other hierarchical control layers (regulation or network), but non-EVs in the vicinity of the EV need to operate in a **degraded** operation mode to assign higher priority to the EV's commands.

The *Bubble* maneuver (developed for the link layer feedforward controller) was found to facilitate the movement of vehicles out of the way of a faster moving EV upstream. However, if a highway exceeds a critical capacity (more vehicles present in a portion of the highway immediately downstream of the EV than could fit into a single lane at the same speed), both the inlet flows and speed of traffic already on the AHS need to be decreased. The impact of the *Bubble* maneuver on a high capacity highway globally restricts the highway traffic flow and would not be desirable if there are too many vehicles. Non-stationary

velocity profiles were investigated as a means of changing AHS traffic flow speed to perform maneuvers that would otherwise not be possible due to capacity constraints. To minimize the impact of the EV on high capacity highways, a non-stationary velocity profile for the link layer feedforward controller was developed to decompress the traffic flow. This *Volcano* maneuver allows vehicles to change lane under high capacity conditions because of the extra space gained by the use of a class of non-stationary velocity profiles such as used for this maneuver. Because previously developed link layer stabilizing controllers can not accomodate non-stationary velocity profiles, two new stabilizing controllers were derived. The performances of the new stabilizing controllers are comparable.

Strategies for the EV's operation at the link layer were found to be highly capacity dependent. Non-stationary velocity profiles can alleviate problems arising from capacity, and it is apparent that the desired traffic flow speed can not be varied arbitrarily. Any future link layer work, not necessarily on EV transit, should focus on analyzing capacity related issues and developing fault and incident detection methods for the link layer feedforward controller. The latter is already a controversial topic in manual traffic research.

The *Vortex* maneuver, which was developed by (Leung, 1994), was evaluated using the SmartAHS vehicle microsimulator and found to require design improvements. The most important problem discovered was that the *Vortex* maneuver did not restore the original configuration of vehicles in the highway lanes. All vehicles downstream of the EV are switched into the opposite lane as a result of the EV passing by. When different sizes of platoons are involved, vehicle conservation is not preserved, and shockwaves may be produced. The design of the *Vortex2* maneuver attempted to correct the problems

associated with the *Vortex*. Vehicles downstream of the EV return to their original lane once the EV passes. Despite maneuver simplification and headway reduction, there is little difference in the amount of space required by the *Vortex* and *Vortex2*, and there is only slight improvement in maneuver time for the *Vortex2*. Additional performance improvements may be possible with further redesign.

Suggested future work should include integrated testing of the link and coordination layer controllers. Because of computational limits, the microsimulation performed for the *Vortex* and *Vortex2* maneuvers included only the regulation and coordination layer controllers. The computing power needed to microsimulate the large scale AHS for testing of the link layer is currently not possible and is the subject of ongoing PATH research [1]. This particular project intends to develop a simulation package which integrates portions of mesoscopically simulated highway with AHS regions that are microscopically simulated. In this way, a microscopic "window" can be used to observe individual vehicles while evaluating large scale effects on another portion of the AHS. As a result of this project, it will be possible to follow a single vehicle (such as an EV) encompassed inside a microscopically simulated region around a large scale AHS, the remainder of which is mesoscopically simulated. Many mesoscopic traffic effects, such as shockwaves, are caused by the actions of individual vehicles. The link (*Bubble* and *Volcano*) and coordination (*Vortex2*) layer maneuvers work in conjunction with one another to promote high priority EV transit and should be tested together. An EV, which travels to an accident site, should not lead to dangerous traffic conditions in another location.

Work performed in this thesis was supported by the California Partners for Automated

[1] See project MOU-383.

Transit and Highways under MOU 311 and by Caltrans. Their support is gratefully acknowledged.

Bibliography

Alvarez, L. and Horowitz, R. (1997). Traffic flow control in automated highway systems. Technical Report UCB-ITS-PRR-97-47.

Alvarez, L. and Horowitz, R. (1999). Safe platooning in automated highway systems. part I: Safety regions design. *Vehicle System Dynamics*, 32(1):23–56.

Alvarez, L., Horowitz, R., and Li, P. (1996). Link layer vehicle flow controller for the PATH AHS architecture. In *Proceedings of the 1996 IFAC World Congress, San Francisco*, volume Q, pages 207–212.

Alvarez, L., Horowitz, R., and Li, P. (1999). Traffic flow control in automated highway systems. *Control Engineering Practice*, 7(11):1071–1078.

Bana, S. (2000). *to be published*. PhD thesis, University of California at Berkeley.

Bose, A. and Ioannou, P. (1999). Analysis of traffic flow with mixed manual and semi-automated vehicles. Technical report, California PATH Program, Institute of Transportation Studies. UCB-ITS-PRR-99-14.

Broucke, M., Varaiya, P., Kourjankski, M., and Khorramabadi, D. (1996). Smartcap User's

Guide. Technical report, Department of Electrical Engineering and Computer Science, University of California, Berkeley, California.

Carbaugh, J., Godbole, D. N., and Sengupta, R. (1997). Tools for safety analysis of vehicle automation systems. In *Proceedings of the ACC*.

Cremer, M. and Papageorgiou, M. (1981). Parameter identification for a traffic flow model. *Automatica*, 17(6):837–843.

Daganzo, C. F. (1997). *Fundamentals of Transportation and Traffic Operations*. Pergamon, Oxford; New York.

Deshpande, A., Gollu, A., and Semenzato, L. (1998). The SHIFT programming language for dynamic networks of hybrid automata. *IEEE Transactions on Automatic Control*, 43(4):584–7. See `http://www.path.berkeley.edu/shift`.

Eskafi, F. (1996). *Modeling and Simulation of the Automated Highway Systems*. PhD thesis, Department of Electrical Engineering and Computer Sciences, University of California at Berkeley.

Eskafi, F., Khorramabadi, D., and Varaiya, P. (1995). An automated highway system simulator. *Transportation Research C*, 3A(1):1–17.

Godbole, D., Eskafi, F., Singh, E., and Varaiya, P. (1995). Design of entry and exit maneuvers for IVHS. In *Proceedings of the 1995 American Control Conference*, volume 5, pages 3576–80. IEEE. Cat No. 95CH35736.

Gollu, A. and Varaiya, P. (1998). SmartAHS: a simulation framework for automated vehicles and highway systems. *Mathematical and Computer Modelling*, 27(9-11):103–28.

Gomes, G., Alvarez, L., and Horowitz, R. (2000). Traffic flow patterns in AHS: system user optimals. In *American Controls Conference*.

Har'El, Z. and Kurshan, R. (1987). *COSPAN User's Guide*. AT&T Bell Laboratories, Murray Hill, NJ.

Holland, E. and Woods, A. (1995). Continuum models of dispersion in multilane traffic flow. In *IEEE Colloquim Dynamic Control of Strategic Inter-Urban Road Networks*, pages 6/1–2. Digest No. 1995/039.

Holland, E. N. and Woods, A. W. (1997). A continuum model for the dispersion of traffic on two-lane roads. *Transportation Research B*, 31(6):473–485.

Horowitz, R. (1997). Automated Highway Systems: the Smart Way to Go. In *Proceedings of the 8th IFAC Symposium on Transportation Systems (Plenary Presentation)*, Chania, Greece.

Larsen, K., Petterson, P., and Yi, W. (1997). UPPAAL in a nutshell. *International Journal on Software Tools for Technology Transfer*, 1(1-2):134–52. See `http://www.uppaal.com`.

Leung, K. (1994). Emergency vehicle maneuvers for an automated highway system. Master's thesis, University of California at Berkeley.

LeVeque, R. J. (1997). Wave propagation algorithms for multidimensional hyperbolic systems. *Journal of Computational Physics*, 131:327–353.

Li, P., Alvarez, L., and Horowitz, R. (1997a). AHS safe control laws for platoon leaders. *IEEE Transactions on Control Systems and Technology*, 5(6):614–628.

Li, P., Horowitz, R., Alvarez, L., Frankel, J., and Roberston, A. (1997b). An AHS link layer controller for trafic flow stabilization. *Transportation Research, Part C: Emerging Technologies*, 5(1):11–37.

Lighthill, M. and Whitham, G. (1955). On kinematic waves II. a theory of traffic flow on long crowded roads. *Proceedings of the Royal Society, London Series A*, 229:317–345.

Lygeros, J., Godbole, D., and Broucke, M. (1995). Design of an extended architecture for degraded modes of operation for IVHS. In *Proceedings of the 1995 American Control Conference*, volume 5, pages 3592–6. IEEE. Cat No. 95CH35736.

Lygeros, J., Godbole, D., and Broucke, M. (2000). A fault tolerant control archiecture for automated highway systems. *IEEE Transactions on Control Systems Technology*, 8(2):205–219.

Mahal, S. (2000). Effects of communications delays on string stability in an AHS environment. Master's thesis, University of California at Berkeley.

Papageorgiou, M., Blosseville, J.-M., and Hadi-Salem, H. (1990). Modelling and real-time control of traffic flow on the southern part of Boulevard Peripherique in Paris: Part I: Modelling and part II: Coordinated on-ramp metering. *Transportation Research A*, 24A(5):345–370.

Payne, H. J. (1971). Models of freeway traffic and control. In Bekey, G. A., editor, *Mathematical Models of Public Systems*, volume 1 of *Simulation Councils Proceedings*, pages 51–60, La Jolla, CA.

Rao, B. and Varaiya, P. (1993). Roadside intelligence for flow control in IVHS. Technical report, PATH, University of California at Berkeley.

Richards, P. (1956). Shockwaves on highways. *Operations Research*, 4:42–51.

Skabardonis, A., Petty, K., Varaiya, P., and Bertini, R. (1998). Evaluation of the freeway service patrol (fsp) in los angeles. Technical report, California PATH Research Report. UCB-ITS-PRR-98-31.

Strang, G. (1998). On the construction and comparison of difference schemes. *SIAM Journal of Numerical Analysis*, 5(3):506–517. reprint.

Swaroop, D. (1994). *String Stability of Interconnected Systems: An Application to Platooning in Automated Highway Systems*. PhD thesis, Department of Mechanical Engineering, University of California at Berkeley.

Varaiya, P. (1993). Smart cars on smart roads: problems of control. *IEEE Transactions on Automatic Control*, AC-38(2):195–207.

Varaiya, P. and Shladover, S. E. (1991). Sketch of an IVHS systems architecture. Technical Report UCB-ITS-PRR-91-3, Institute of Transportation Studies, University of California, Berkeley.

Appendix A

Non-stationary Velocity Profiles

Non-stationary velocity profiles must be carefully designed to accomodate the capabilities of individual vehicles involved in the maneuvers. The maximum deceleration and acceleration capabilities of a vehicle, $a_{max,decel} < 0 < a_{max,accel}$, should not be exceeded while it is inside a non-stationary velocity profile. Likewise, if a particular region of the profile is intended for lane changing, then the time spent by a vehicle in that region should be greater than the time needed to change lane. In this section, the limitations that a non-stationary velocity profile imposes are discussed.

Consider the non-stationary velocity profile shown in Fig. A.1, which corresponds to lane 1 of the non-stationary profile used to circulate vehicles out the way of an EV in high density traffic (see Fig. 2.10 for both lanes). Vehicles in the lanes decelerate inside the region $x \in [x_5, x_6]$, which decompresses the traffic. In the new coordinate frame (s, τ), the velocity profile is invariant. The traffic flow velocity in lane 1 for $x \in [x_5, x_6]$ obeys

$$V - V_{nom,1} = \frac{V_{nom,1} - V_{low}}{x_6 - x_5} (s - s_6) . \tag{A.1}$$

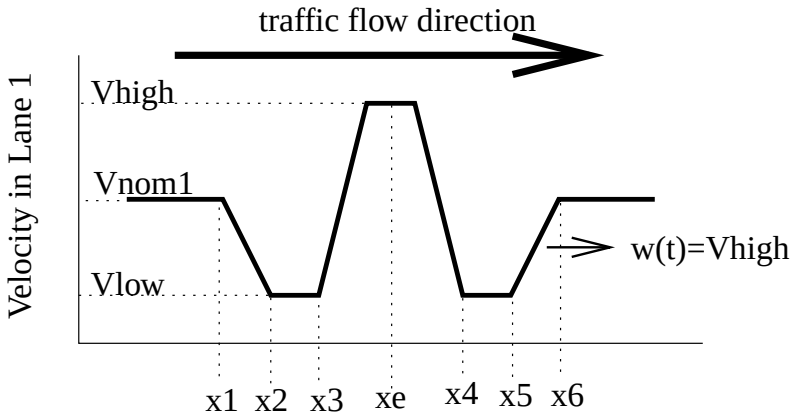

Figure A.1: Non-stationary velocity profile for lane 1 of the Volcano maneuver - This figure matches that shown in Fig. 2.10 and is labeled appropiately for a discussion of limits that individual vehicle capabilities place upon non-stationary velocity profiles.

Combining the above equation with the definition of non-stationary profile as given by

$$s = x - \int_0^t w(\epsilon) d\epsilon, \tag{A.2}$$

a relation for the deceleration experienced on average by vehicles is obtained. Under the assumption that the profile travels faster than the highway, $w(t) > V$, the maximum deceleration capabilities of an AHS vehicle impose restrictions on the shape of the non-stationary velocity profile.

$$0 > a_{max,decel} > a = \frac{dV}{dt} = \frac{V_{nom,1} - V_{low}}{x_6 - x_5} \left(V - w\left(t\right) \right), \tag{A.3}$$

where V is the traffic flow speed in the region $x \in [x_5, x_6]$. In a manner similiar to that of Eq. (A.3), the maximum acceleration capability of an AHS vehicle imposes design requirements on the non-stationary velocity profile.

$$a_{max,accel} > a = \frac{dV}{dt} = \frac{V_{low} - V_{nom,1}}{x_2 - x_1} \left(V - w\left(t\right) \right) > 0 \tag{A.4}$$

Once vehicles have decelerated, they are requested to change lane out of the way of the EV in the region $x \in [x_4, x_5]$. The time spent by a vehicle in this region, t, should be significantly less than the time required for a lane change, t_{LC}.

$$t_{LC} << t = \frac{x_5 - x_4}{w(t) - V_{low}} \tag{A.5}$$

The time needed for a lane change has been determined to be in the range from 3 seconds (under emergency conditions) to 6 seconds (under normal conditions in real-time demonstrations).

Appendix B

Changelane Maneuver

The changelane maneuver is intended for use by a free agent that wishes to change lane, one lane at a time. Moving multiple lanes at a time is not permitted; it is assumed that the side radar of the vehicle with its cone geometry range can only detect vehicles in the immediate adjacent lane. Vehicle markers embedded in the road pavement allow each car to determine its position relative to its neighbors. In addition, this maneuver is restricted to freeagent use because in a multiple car platoon, all vehicles must monitor the safety space in the destination lane and coordinate with the leader to determine safe conditions for a lane change. (Leung, 1994) does present a general *Platoon Lane Change* maneuver, but the protocol does not define safety criteria or a methodology for implementation.

A schematic for the changelane maneuver is shown in Fig. B.1. The vehicle that intends to change lane (the changelane maneuver initiator) is indicated by orange. Upon receiving a successful probability request from the link layer or a request from the EV, the initiator starts the changelane maneuver and determines the nearest platoon in the adjacent lane

(Platoon A or B). If there is no nearby vehicle within the safety range in the adjacent lane, the initiator performs the changelane. The safety range is determined from maximum acceleration/deceleration capabilities of the vehicles.

If platoon B is closer, the initiator sends a **Changelane_decel** message to platoon B. Depending on its busy status (busy if involved in another maneuver), Platoon B sends either an acknowledgement or denial message back to initiator. If not busy, platoon B begins to decelerate to provide space for the initiator. Once platoon B has decelerated a safe distance from the initiator, it sends a **Changelane_decel_completed** message. Then the initiator again tries to determine the nearest platoon in the adjacent lane (platoon A or B). If platoon A is closer, the initiator begins to decelerate to produce space between itself and A. As soon as the initiator gets closer to B than to A, it sends a **Changelane_decel** message to platoon B. If B is not busy, it replies with an acknowledgement message and also begins to decelerate relative to A. Because the initiator and platoon B are in different lanes, safety is maintained even though both are decelerating at the same time. Platoon C is not directly involved in the changelane maneuver, but its leader law requires it to maintain a safe distance from the initiator at all times.

The FSMs for the initiator and responder (Platoon B) are shown in Figs. B.2 and B.3, respectively. One possibility for the changelane maneuver is to also involve Platoon A directly, by requesting it to accelerate to provide space. However, this may not be possible due to downstream traffic. To maintain safety, an AHS vehicle can only control its own headway distance and make similar control requests of other downstream vehicles.

Figure B.1: Changelane Maneuver

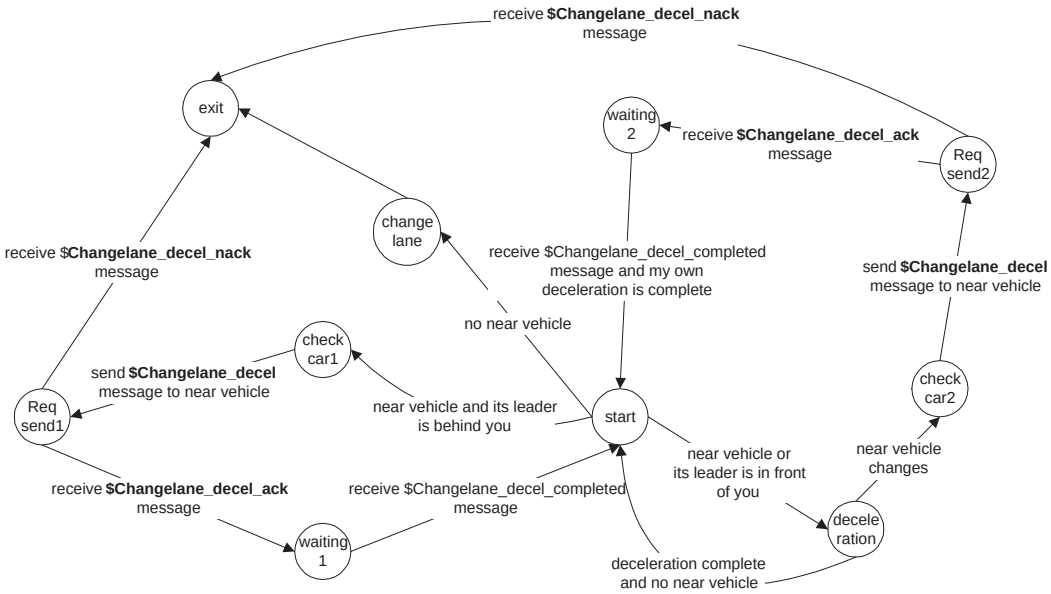

Figure B.2: Changelane Initiator's FSM

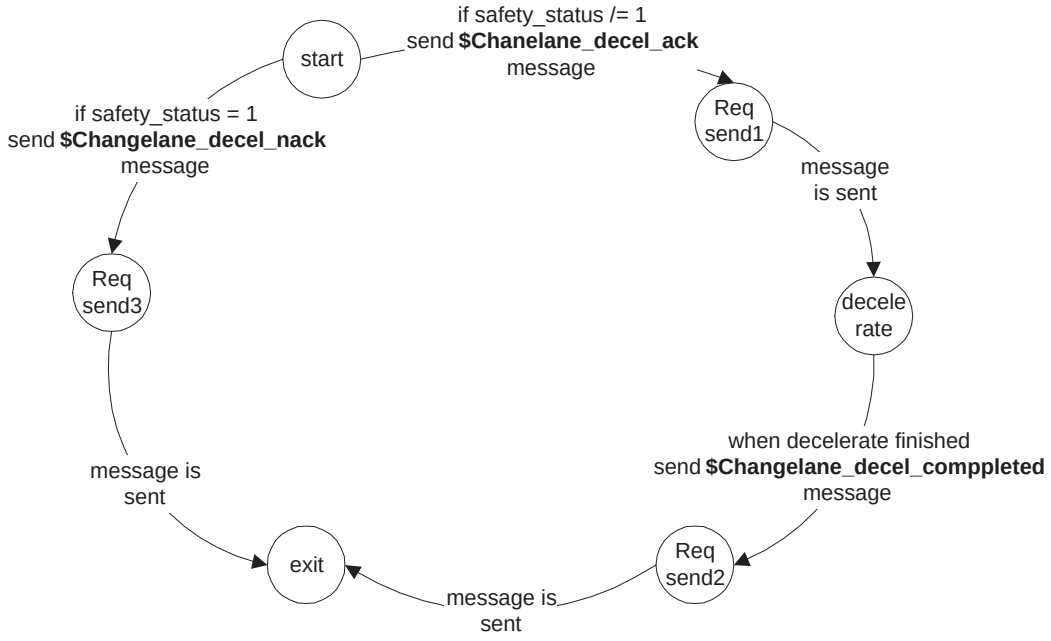

Figure B.3: Changelane Responder's FSM